

# **Integrated Ocean Drilling Program Expedition 339 Preliminary Report**

## **Mediterranean Outflow**

### **Environmental significance of the Mediterranean Outflow Water and its global implications**

16 November 2011–16 January 2012

Expedition 339 Scientists



Published by  
Integrated Ocean Drilling Program Management International, Inc.,  
for the Integrated Ocean Drilling Program

## **Publisher's notes**

Material in this publication may be copied without restraint for library, abstract service, educational, or personal research purposes; however, this source should be appropriately acknowledged. Core samples and the wider set of data from the science program covered in this report are under moratorium and accessible only to Science Party members until 17 June 2013.

### **Citation:**

Expedition 339 Scientists, 2012. Mediterranean outflow: environmental significance of the Mediterranean Outflow Water and its global implications. *IODP Prel. Rept.*, 339. doi:10.2204/iodp.pr.339.2012

### **Distribution:**

Electronic copies of this series may be obtained from the Integrated Ocean Drilling Program (IODP) Scientific Publications homepage on the World Wide Web at [www.iodp.org/scientific-publications/](http://www.iodp.org/scientific-publications/).

This publication was prepared by the Integrated Ocean Drilling Program U.S. Implementing Organization (IODP-USIO): Consortium for Ocean Leadership, Lamont Doherty Earth Observatory of Columbia University, and Texas A&M University, as an account of work performed under the international Integrated Ocean Drilling Program, which is managed by IODP Management International (IODP-MI), Inc. Funding for the program is provided by the following agencies:

National Science Foundation (NSF), United States

Ministry of Education, Culture, Sports, Science and Technology (MEXT), Japan

European Consortium for Ocean Research Drilling (ECORD)

Ministry of Science and Technology (MOST), People's Republic of China

Korea Institute of Geoscience and Mineral Resources (KIGAM)

Australian Research Council (ARC) and GNS Science (New Zealand), Australian/New Zealand Consortium

Ministry of Earth Sciences (MoES), India

## **Disclaimer**

Any opinions, findings, and conclusions or recommendations expressed in this publication are those of the author(s) and do not necessarily reflect the views of the participating agencies, IODP Management International, Inc., Consortium for Ocean Leadership, Lamont-Doherty Earth Observatory of Columbia University, Texas A&M University, or Texas A&M Research Foundation.

## Expedition 339 participants

### Expedition 339 scientists

**Francisco J. Hernández-Molina**  
**Co-Chief Scientist**  
Departamento Geociencias Marinas  
Universidad de Vigo  
Facultad de Ciencias Del Mar  
36310 Vigo  
Spain  
[fjherman@uvigo.es](mailto:fjherman@uvigo.es)

**Dorrik A.V. Stow**  
**Co-Chief Scientist**  
Institute of Petroleum Engineering  
Heriot-Watt University  
Edinburgh  
Scotland EH14-4AS  
United Kingdom  
[dorrik.stow@pet.hw.ac.uk](mailto:dorrik.stow@pet.hw.ac.uk)

**Carlos Alvarez Zarikian**  
**Expedition Project Manager/Staff Scientist**  
Integrated Ocean Drilling Program  
Texas A&M University  
1000 Discovery Drive  
College Station TX 77845-9547  
USA  
[zarikian@iodp.tamu.edu](mailto:zarikian@iodp.tamu.edu)

**Trevor Williams**  
**Logging Staff Scientist**  
Borehole Research Group  
Lamont-Doherty Earth Observatory  
PO Box 1000, Route 9W  
Palisades NY 10964  
USA  
[trevor@ldeo.columbia.edu](mailto:trevor@ldeo.columbia.edu)

**Johanna Lofi**  
**Logging Staff Scientist**  
Géosciences Montpellier  
Université Montpellier II  
CC 60, Place Eugène Bataillon  
34095 Montpellier Cedex 05  
France  
[johanna.lofi@gm.univ-montp2.fr](mailto:johanna.lofi@gm.univ-montp2.fr)

**Gary D. Acton**  
**Stratigraphic Correlator**  
Department of Geology  
University of California, Davis  
One Shields Avenue  
Davis CA 95616  
USA  
[gdacton@ucdavis.edu](mailto:gdacton@ucdavis.edu)

**André Bahr**  
**Physical Properties Specialist**  
Institute of Geosciences  
University of Frankfurt  
Altenhoferallee 1  
60438 Frankfurt  
Germany  
[a.bahr@em.uni-frankfurt.de](mailto:a.bahr@em.uni-frankfurt.de)

**Barbara Balestra**  
**Paleontologist (nannofossils)**  
School of Earth and Environmental Sciences  
Queens College (CUNY)  
60-35 Kissena Boulevard  
Flushing NY 11367  
USA  
[balestrabb@gmail.com](mailto:balestrabb@gmail.com)

**Emmanuelle Ducassou**  
**Sedimentologist**  
EPOC, UMR CNRS 5805  
Université de Bordeaux I  
Avenue des Facultes  
33405 Talence  
France  
[e.ducassou@epoc.u-bordeaux1.fr](mailto:e.ducassou@epoc.u-bordeaux1.fr)

**Roger D. Flood**  
**Sedimentologist**  
Marine Sciences Research Center  
State University of New York, Stony Brook  
Endeavour 145  
Stony Brook NY 11794  
USA  
[roger.flood@sunysb.edu](mailto:roger.flood@sunysb.edu)

**José-Abel Flores**  
**Paleontologist (nannofossils)**

Departamento de Geología  
Universidad de Salamanca  
Facultad De Ciencias  
37008 Salamanca  
Spain  
[flores@usal.es](mailto:flores@usal.es)

**Satoshi Furota**  
**Sedimentologist**

Department of Natural History Sciences  
Hokkaido University  
Kita-ku  
Sapporo 060-0810  
Japan  
[furota@mail.sci.hokudai.ac.jp](mailto:furota@mail.sci.hokudai.ac.jp)

**Patrick Grunert**  
**Paleontologist (foraminifers)**

Institute of Earth Sciences  
University of Graz  
Heinrichstrasse 26  
8010 Graz  
Austria  
[patrick.grunert@uni-graz.at](mailto:patrick.grunert@uni-graz.at)

**David A. Hodell**  
**Inorganic Geochemist**

Department of Earth Sciences  
Godwin Laboratory for Palaeoclimate  
Research  
University of Cambridge  
CB2 3EQ Cambridge  
United Kingdom  
[dah73@cam.ac.uk](mailto:dah73@cam.ac.uk)

**Francisco J. Jimenez-Espejo**  
**Physical Properties Specialist**

Institute of Biogeosciences  
Japan Agency for Marine-Earth Science and  
Technology  
Natsushima-cho 2-15  
Yokosuka 237-0061  
Japan  
[fjjspejo@jamstec.go.jp](mailto:fjjspejo@jamstec.go.jp)

**Jin Kyoung Kim**  
**Inorganic Geochemist**

Research Group for Marine Resources in the  
Korea EEZ  
Korea Ocean Research and Development Insti-  
tute  
1270 Sadong  
Ansan 426-744  
Korea  
[jink92@kordi.re.kr](mailto:jink92@kordi.re.kr)

**Lawrence A. Krissek**  
**Sedimentologist**

School of Earth Sciences  
Ohio State University  
275 Mendenhall Laboratory  
125 South Oval  
Columbus OH 43210-1308  
USA  
[lkrissek@asc.ohio-state.edu](mailto:lkrissek@asc.ohio-state.edu)

**Junichiro Kuroda**  
**Sedimentologist**

Institute for Frontier Research on Earth Evolu-  
tion (IFREE)  
Japan Agency for Marine-Earth Science and  
Technology  
2-15 Natsushima-cho, Yokosuka  
Kanagawa 237-0061  
Japan  
[kurodaj@jamstec.go.jp](mailto:kurodaj@jamstec.go.jp)

**Baohua Li**  
**Paleontologist (foraminifers)**

Department of Micropalaeontology  
Nanjing Institute of Geology and Palaeontol-  
ogy  
Academia Sinica  
39 East Beijing Road  
Nanjing 210008  
China  
[bh-li@nigpas.ac.cn](mailto:bh-li@nigpas.ac.cn)

**Lucas Lourens**  
**Stratigraphic Correlator**

Institute of Earth Sciences  
Utrecht University  
Budapestlaan 4  
3584 Utrecht  
The Netherlands  
[llourens@geo.uu.nl](mailto:llourens@geo.uu.nl)

**Madeline D. Miller**  
**Inorganic Geochemist**  
Department of Mechanical Engineering  
California Institute of Technology  
1200 East California Boulevard  
MC 100-23  
Pasadena CA 91125  
USA  
[madeline@caltech.edu](mailto:madeline@caltech.edu)

**Futoshi Nanayama**  
**Sedimentologist**  
Institute of Geology and Geoinformation  
National Institute of Advanced Industrial Science and Technology  
Geological Survey of Japan (AIST)  
Site 7, Higashi 1-1-1, Tsukuba  
Ibaraki 305-8567  
Japan  
[nanayama-f@aist.go.jp](mailto:nanayama-f@aist.go.jp)

**Naohisa Nishida**  
**Sedimentologist**  
Institute of Geology and Geoinformation  
National Institute of Advanced Industrial Science and Technology  
Geological Survey of Japan (AIST)  
Site 7, Higashi 1-1-1, Tsukuba  
Ibaraki 305-8567  
Japan  
[n.nishida@aist.go.jp](mailto:n.nishida@aist.go.jp)

**Carl Richter**  
**Paleomagnetist**  
Department of Geology and Energy Institute  
University of Louisiana  
PO Box 44530  
Lafayette LA 70504-0002  
USA  
[richter@louisiana.edu](mailto:richter@louisiana.edu)

**Maria F. Sanchez Goni**  
**Palynologist**  
EPOC, UMR CNRS 5805  
Université de Bordeaux I  
Avenue des Facultes  
33405 Talence  
France  
[mf.sanchezgoni@epoc.u-bordeaux1.fr](mailto:mf.sanchezgoni@epoc.u-bordeaux1.fr)

**Francisco J. Sierro Sánchez**  
**Paleontologist (foraminifers)**  
Departamento de Geología  
Universidad de Salamanca  
Facultad de Ciencias  
C/Parque s/n  
37008 Salamanca  
Spain  
[sierro@usal.es](mailto:sierro@usal.es)

**Arun D. Singh**  
**Paleontologist (foraminifers)**  
Department of Geology  
Banaras Hindu University  
Varanasi  
221 005 Uttar Pradesh  
India  
[arundeosingh@yahoo.com](mailto:arundeosingh@yahoo.com)

**Craig R. Sloss**  
**Sedimentologist**  
Department of Biogeosciences  
Queensland University of Technology  
GPO Box 2434  
Brisbane QLD 4001  
Australia  
[c.sloss@qut.edu.au](mailto:c.sloss@qut.edu.au)

**Yasuhiro Takashimizu**  
**Sedimentologist**  
Mathematical and Natural Sciences  
Niigata University  
8050 Ikarashi, 2-no-cho Nishi-ku  
Niigata 950-2181  
Japan  
[takashimi@ed.niigata-u.ac.jp](mailto:takashimi@ed.niigata-u.ac.jp)

**Alexandrina Tzanova**  
**Organic Geochemist**  
Department of Geological Sciences  
Brown University  
324 Brook Street  
Box 1846  
Providence RI 02912  
USA  
[alexandrina\\_tzanova@brown.edu](mailto:alexandrina_tzanova@brown.edu)

**Antje Voelker**  
**Paleontologist (foraminifers)**  
Marine Geology Department  
Geological Survey of Portugal (LNEG)  
Estrada da Portela  
Zambujal  
2610-143 Amadora  
Portugal  
[antje.voelker@lneg.pt](mailto:antje.voelker@lneg.pt)

**Chuang Xuan**  
**Paleomagnetist**  
College of Oceanic and Atmospheric Sciences  
Oregon State University  
104 COAS Administration Building  
Corvallis OR 97331  
USA  
[cxuan@coas.oregonstate.edu](mailto:cxuan@coas.oregonstate.edu)

## Observers

**Estefanía Llave Barranco**  
Geological Survey of Spain  
Instituto Geológico y Minero de España  
(IGME)  
28760 Tres Cantos  
Spain  
[e.llave@igme.es](mailto:e.llave@igme.es)

**Ana Cristina Freixo Roque**  
Instituto Geológico e Mineiro  
Geological Survey of Portugal (LNEG)  
Estrada da Portela  
Apartado 7586  
2721-866 Zambujal  
Portugal  
[cristina.roque@lneg.pt](mailto:cristina.roque@lneg.pt)

## Education and outreach

**Hélder Pereira**  
**Education Officer**  
Grupo de Biologia e Geologia  
Escola Secundária de Loulé  
Avenida Laginha Serafim  
8100-740 Loulé  
Portugal  
[hpereira@es-loule.edu.pt](mailto:hpereira@es-loule.edu.pt)

## Technical support

**Grant Banta**  
**Marine Computer Specialist**

**Heather Barnes**  
**X-ray Laboratory**

**John Beck**  
**Imaging Specialist**

**Christopher Bennight**  
**Chemistry Laboratory**

**Timothy Blaisdell**  
**Applications Developer**

**Chad Broyles**  
**Curatorial Specialist**

**Etienne Claassen**  
**Marine Instrumentation Specialist**

**Trevor Cobine**  
**Paleomagnetism Laboratory**

**Roy Davis**  
**Laboratory Officer**

**Thomas Gorgas**  
**Core Laboratory**

**Ronald Grout**  
**Operations Superintendent**

**Ted Gustafson**  
**Thin Section Laboratory**

**Hillary Hall**  
**Marine Laboratory Specialist (temporary)**

**Sandra Herrmann**  
**Underway Geophysics Laboratory**

**Michael Hodge**  
**Marine Computer Specialist**

**Dwight Hornbacher**  
**Applications Developer**

**Jan Jurie Kotze**  
**Marine Instrumentation Specialist**

**Erik Moortgat**  
**Chemistry Laboratory**

**Chieh Peng**  
**Assistant Laboratory Officer**

**Paul Pleasant**  
**Publications Specialist**

**Steve Prinz**  
**Assistant Laboratory Officer**

**Melissa Rotella**  
**Marine Laboratory Specialist (temporary)**

**Kerry Swain**  
**Logging Engineer**

**Yulia Vasilyeva**  
**Physical Properties Laboratory**

## Abstract

During Integrated Ocean Drilling Program Expedition 339, five sites were drilled in the Gulf of Cádiz and two sites were drilled off the West Iberian margin from November 2011 to January 2012. Total length of recovered core is 5447 m, with an average recovery of 86.4%. The Gulf of Cádiz was targeted for drilling as a key location for the investigation of Mediterranean Outflow Water (MOW) through the Strait of Gibraltar gateway and its influence on global circulation and climate. The gulf is also a prime area for understanding the effects of tectonic activity on evolution of the Strait of Gibraltar gateway and margin sedimentation.

Drilling penetrated into the Miocene at two sites in the Gulf of Cádiz, where sedimentary record showed a strong MOW signal following the opening of the Strait of Gibraltar gateway. Preliminary results indicate contourite deposition from 4.2 to 4.5 Ma, although subsequent research will establish whether this deposition dates from the first onset of MOW. The Pliocene succession, penetrated at four sites, displays characteristics consistent with low bottom-current activity linked with weak MOW. Significant widespread unconformities at 3.0–3.2 and 2.2–2.4 Ma are interpreted as a signal of intensified MOW, especially from ~2.4 Ma. The Quaternary succession displays characteristics consistent with a much more pronounced phase of contourite drift development, with two distinct periods of increased MOW activity separated by a widespread unconformity at ~0.9 Ma related to even higher MOW. Following this unconformity, the final phase of drift evolution established the contourite depositional system architecture we see today.

There is significant climate control on this evolution of MOW and bottom-current activity. However, from the closure of the Atlantic-Mediterranean gateways in Spain and Morocco around 6 Ma to the opening of the Strait of Gibraltar gateway at 5.3 Ma, even stronger tectonic control affected margin development, downslope sediment transport, and contourite drift evolution. Based on the timing of events recorded in the sedimentary record, we propose tectonic pulsing in the region linked with small movements of the African and Iberian plates.

The Gulf of Cádiz is the world's premier contourite laboratory and thus presents an ideal testing ground for the contourite paradigm. Following recovery of >4.5 km of contourite cores, existing models for contourite deposition are found to be sound. Further study of these models will undoubtedly allow us to resolve outstanding issues of depositional processes, drift budgets, and recognition of fossil contourites in the



ancient record onshore. The expedition also verified the presence of a more than expected quantity and extensive distribution of contourite sands that are clean and well sorted. These sands represent a completely new and important exploration target for potential oil and gas reservoirs. Preliminary work has shown a remarkable record of orbital-scale variation in bulk sediment properties of contourites at several of the drift sites and good correlation between all sites. Climate control on contourite sedimentation is clearly significant at this scale; further work will determine the nature of controls at the millennial scale.

## Introduction

Integrated Ocean Drilling Program (IODP) Expedition 339 combined IODP Proposal 644-Full2 and ancillary proposal letter (APL)-763. The expedition was primarily paleo-oceanographic in nature, focusing mainly on the broader significance of Mediterranean Outflow Water (MOW) on North Atlantic Ocean circulation and climate. This expedition offered a rare opportunity to understand the global link between paleo-oceanographic, climatic, and sea level changes from Messinian to recent time and addressed the importance of ocean gateways in regional and global ocean circulation and climate.

Seven sites (U1385–U1391) were cored and, of those seven, five sites were logged during the expedition in the Gulf of Cádiz and on the West Iberian margin (Figs. [F1](#), [F2](#)) to study the contourite depositional system (CDS) generated by MOW influence and its evolution and environmental implications. This CDS has developed at very high rates of sediment accumulation over the past 5 m.y. as the direct result of MOW, providing an expanded sedimentary record that permits detailed examination of paleo-circulation patterns linked to past environmental change. In addition, one of the sites, U1385, was cored to produce a marine reference section of Pleistocene millennial-scale climate variability and changes in surface and deepwater circulation along the Portuguese margin (APL-763). Climate signals from this reference section will constrain the temporal relationships of abrupt climate change recorded in the northeast Atlantic Ocean, the polar ice cores, and European terrestrial records.

The objectives of Expedition 339 address key elements of the IODP Initial Science Plan (ISP) through targeted drilling of a Neogene and Quaternary continental margin sequence in the Gulf of Cádiz and off West Iberia.

## **Oceanic gateways and their influence**

Tectonically induced changes are highlighted in the ISP as one of the principal internal forcing mechanisms for environmental change. By drilling in the Gulf of Cádiz, we seek to document the effects of opening the Strait of Gibraltar gateway at ~5 Ma and therefore initiating the major influx of warm, saline intermediate water into the North Atlantic Ocean.

## **Paleocirculation and climate**

One of the fundamental scientific questions identified in the ISP under Environmental Change, Processes, and Effects is “How did the Earth system respond to climatic change and at what timescales?” A key response of the ocean system to climate forcing is significant reorganization of global circulation and adjustment in the thermohaline conveyor belt model. Hence, the record of paleocirculation and paleoclimate is further identified as a specific target in the ISP. Expedition 339 research will address changes in and effects of MOW as a component of North Atlantic circulation in the post-Miocene time period.

## **Rapid climate change**

Rapid climate change is highlighted as a special initiative in the ISP under Environmental Change, Processes, and Effects. Future advances in our understanding of the causes of abrupt change will rely on our ability to correlate high-resolution sedimentary archives from oceans, ice cores, and terrestrial sequences and to interpret these records in the context of novel Earth system modeling approaches. A challenge for IODP, and the broader drilling community, is to identify sequences from appropriate locations with adequate temporal resolution to study processes of the integrated climate system. Expedition 339 recovered sediment records deposited at high accumulation rates containing high-fidelity signals of Pleistocene climate variability and rapid climate change that can be correlated to polar ice-core and terrestrial archives.

## **Sea level change and sediment architecture**

The response of sediment architecture, especially along continental margins, to sea level change is highlighted in the ISP as the second principal internal forcing mechanism for environmental change. Whereas considerable attention and several past Ocean Drilling Program (ODP) drilling legs have been directed toward placing turbi-

dites and other downslope systems within a sequence stratigraphic context, there is no generally accepted understanding of how and where the alongslope sedimentary system, driven by bottom water circulation, fits within these models. Fundamental questions regarding the timing and extent of hiatuses and condensed sequences and the corollary periods of alongslope deposition, drift development, and paleodepth reconstruction have yet to be answered. The objectives of Expedition 339 address precisely these aspects of sediment architecture within the Gulf of Cádiz and West Iberian marginal sequences in relation to changes in sea level and other forcing mechanisms.

## **Neotectonic activity**

Margin evolution anywhere is controlled by complex interactions of many different forcing variables, most importantly sea level and climate, sediment supply, and tectonics. Results from Expedition 339 will be used to reconstruct the timing of neotectonic activity that had a significant impact on submarine topography and, consequently, controlled the flow path of the two branches of MOW and their influence in the North Atlantic.

Expedition 339 was certainly ambitious in scope and scientifically very exciting. It was carefully crafted by a broad spectrum of scientists over an 8 y gestation period. The expedition reflects intense international interest in the region and its global significance, building on a research database accumulated over 35 y. Furthermore, the study of the CDS should be of great interest to the international community not only because of its stratigraphic, sedimentologic, paleoceanographic, and paleoclimatologic significance but also because of its close relationship with possible specific deep-marine geohabitats and/or mineral and energy resources (Rebesco and Camerlenghi, 2008).

## **Background**

### **Geological and oceanographic setting**

#### **Tectonic framework**

The southwestern margin of the Iberian Peninsula, at the eastern end of the Azores-Gibraltar zone, is the location of the diffuse plate boundary between Eurasia and Africa. The present plate convergence between the African and Eurasian plates in the

Gulf of Cádiz area is ~4 mm/y with a northwest–southeast trend and is accommodated over that broad, diffuse deformation zone (Olivet, 1996; Argus et al., 1989). Distinct periods of crustal deformation, fault reactivation, and halokinesis related to movement between Eurasia and Africa (Malod and Mauffret, 1990; Srivastava et al., 1990; Maldonado et al., 1999; Gutscher et al., 2002; Alves et al., 2003; Gutscher, 2004; Medialdea et al., 2004, 2009; Lopes et al., 2006; Terrinha et al., 2009; Zitellini et al., 2009) are known to have controlled the tectonostratigraphic evolution of this part of the Iberian Peninsula. The tectonic structure of this area is a consequence of the distinct phases of rifting since the Late Triassic to the Early Cretaceous caused by the opening of the central and North Atlantic basin (Murillas et al., 1990; Pinheiro et al., 1996; Wilson et al., 1996; Srivastava et al., 2000; Borges et al., 2001) and its later deformation during the Cenozoic, especially in the Miocene (Ribeiro et al., 1990; Zitellini et al., 2009). Cenozoic evolution in the Gulf of Cádiz was controlled by the Alpine tectonic phases that affected the southern part of Europe. During the Pliocene and Quaternary, glacio-eustatic variations rather overprinted structural effects on the margin and resulted in erosion, sedimentary progradation, and incision of major submarine canyons (Mougenot, 1988; Alves et al., 2003; Terrinha et al., 2003, 2009).

The Gulf of Cádiz straddles this oblique-compressive zone between the Eurasian and African plates, extending from the Gloria transform fault zone to the Gibraltar arc, which marks the western front of the Betic-Rif collisional orogen. Since the late Miocene, the northwest–southeast compressional regime developed simultaneously with the extensional collapse of the Betic-Rif orogenic front by westward emplacement of a giant “olistostrome,” the Cádiz Allochthonous Unit (CAU), and by very high rates of basin subsidence coupled with strong diapiric activity. At the end of the Messinian, a transtensional regime caused reopening of the connection between the Atlantic and the Mediterranean through the Strait of Gibraltar (Maldonado et al., 1999). By the end of the early Pliocene, subsidence decreased and the margin evolved toward its present, more stable condition (Maldonado et al., 1999; Maestro et al., 2003; Medialdea et al., 2004), although the CAU provides an unstable substratum for late Miocene, Pliocene, and Quaternary sedimentation (Medialdea et al., 2004; Zitellini et al., 2009). Some neotectonic reactivation is also evident, as expressed by the occurrence of mud volcanoes, diapiric ridges (Díaz-del-Río et al., 2003; Somoza et al., 2003; Gutscher, 2004; Fernández-Puga et al., 2007; Zitellini et al., 2009), and fault reactivation (Maestro et al., 1998; Gràcia et al., 2003a, 2003b; Lobo et al., 2003; Terrinha et al., 2009). Tectonics represent a key long-term factor in affecting seafloor morphology, which has exerted strong control on the pathways of MOW and, therefore, the architecture of the CDS.

## Oceanographic setting

The present-day circulation pattern is dominated by exchange of water masses through the Strait of Gibraltar (Fig. F3). This exchange is driven by highly saline and warm MOW flowing out of the Mediterranean Sea near the bottom and the turbulent, less saline, cool-water mass of Atlantic water flowing east and into the Mediterranean Sea at the surface. MOW forms a strong bottom current flowing toward the west and northwest above North Atlantic Deep Water (NADW) (Madelain, 1970; Melières, 1974; Zenk, 1975; Thorpe, 1976; Ambar and Howe, 1979).

After it exits through the Strait of Gibraltar gateway, MOW represents an intermediate water mass that is warm and very saline and flows to the northwest along the middle slope (Fig. F3) under Atlantic Inflow and above NADW (Zenk, 1975; Thorpe, 1976; Gardner and Kidd, 1983; Ochoa and Bray, 1991; Baringer and Price, 1999). MOW also represents a flux of  $\sim 1.78$  Sv through the Strait of Gibraltar gateway, composed of both Levantine Intermediate Water (LIW) and Western Mediterranean Deep Water (WMDW) (Bryden and Stommel, 1984; Bryden et al., 1994; Millot, 1999, 2009), and generates important alongslope sedimentary processes along the Atlantic margin (Serra et al., 2010a, 2010b). In the Gulf of Cádiz, MOW flows between 500 and 1400 meters below sea level (mbsl) at a velocity close to 300 cm/s at the Strait of Gibraltar (Ambar and Howe, 1979) and  $\sim 80$ – $100$  cm/s at the latitude of Cape São Vicente (Cherubin et al., 2000). Distribution of MOW is conditioned by the complex morphology of the continental slope, which generates two main cores: between 500 and 700 mbsl (upper core or Mediterranean upper water [MU]) and between 800 and 1400 mbsl (lower core or Mediterranean lower water [ML]). ML is further divided into three branches (Fig. F3) (Madelain, 1970; Zenk, 1975; Ambar and Howe, 1979; Johnson and Stevens, 2000; Borenäs et al., 2002). In the western sectors, the interaction of these branches with the seafloor generates large meddies (Richardson et al., 2000).

After exiting the Gulf of Cádiz, MOW has three principal branches (Fig. F4): the main branch flows to the north, the second to the west, and the third to the south, reaching the Canary Islands and then veering toward the west (Iorga and Lozier, 1999; Slater, 2003). The northern branch flows along the middle slope of the Portuguese margin and is further divided into two branches by the influence of Galicia Bank (Fig. F4). These two branches return to converge and subsequently circulate to the east in the Gulf of Biscay, following the continental slope contour (Fig. F4). MOW reaches Porcupine Bank and partly circulates to the north along Rockall Trough until reaching the Norwegian Sea (Iorga and Lozier, 1999; Slater, 2003).

Between ~500 and 1500 mbsl, the water column along the West Iberian margin is dominated by warm, salty MOW, the two cores of which are centered at ~800 and 1200 mbsl (Ambar and Howe, 1979) and flow as undercurrents northward along the margin and also spread westward. Below MOW at ~1600 mbsl, Labrador Sea Water (LSW) can be found on the margin north of 40.5°N (Fiuza et al., 1998). Below 2000 mbsl, recirculated Northeast Atlantic Deep Water (NEADW) prevails, representing a mixture of LSW, Iceland Scotland Overflow Water (ISOW), Denmark Strait Overflow Water (DSOW), and to a lesser extent MOW and Lower Deep Water (LDW) (van Aken, 2000). Abyssal water in the region consists of a lower fringe of NEADW that obtains an increasing component of southern-sourced LDW with depth until ~4000 mbsl, where LDW dominates.

### **Morphosedimentary and stratigraphic framework**

The major part of the Gulf of Cádiz comprises a pronounced outward bulge sloping to the west with irregular surface relief (Fig. F5). The principal physiographic features of this broad slope are

- A shelf-break located between 100 and 140 mbsl,
- A steeper (2°–3°) upper slope between 150 and 400 mbsl,
- Two gently dipping (>1°) wide terraces at 500–750 and 800–1200 mbsl on the middle slope crossed by channels and ridges that trend northeast, and
- A smooth lower slope (0.5°–1°).

For the most part, this slope lacks submarine canyons, except in the western area of the Algarve margin (Hernández-Molina et al., 2006; Mulder et al., 2006; Marchès et al., 2007). The West Iberian margin is characterized by a steeper slope (~4.5°) that is crossed by several major submarine canyons, but there is also a middle slope terrace (Alves et al., 2003; Terrinha et al., 2003; Llave et al., 2007).

The interaction of MOW with the Gulf of Cádiz margin has resulted in the development of one of the most extensive and complex CDSs ever described. Many authors have highlighted this interaction and have characterized the erosive and depositional features along the middle slope (e.g., Madelain, 1970; Gonthier et al., 1984; Nelson et al., 1993, 1999; Llave et al., 2001, 2006, 2007, 2010, submitted; Habgood et al., 2003; Hernández-Molina et al., 2003, 2006, submitted; Mulder et al., 2003, 2006; Hanquiez et al., 2007; Marchès et al., 2007). This CDS has both large depositional and erosional features (Fig. F2), conditioned by a strong current with speeds reaching nearly 300 cm/s close to the Strait of Gibraltar, slowing to ~80 cm/s at Cape São Vicente (Kenyon

and Belderson, 1973; Ambar and Howe, 1979; Cherubin et al., 2000). The main depositional features are sedimentary wave fields, sedimentary lobes, mixed drifts, plastered drifts, elongated mounded and separated drifts, and sheeted drifts. The main erosional features are contourite channels, furrows, marginal valleys, and moats. All of these features have a specific location along the margin, and their distribution defines five morphosedimentary sectors within the CDS (details can be found in Hernández-Molina et al., 2003, 2006, and Llave et al., 2007). The development of each of these five sectors at any time is related to systematic deceleration of MOW as it flows westward from the Strait of Gibraltar, caused by interaction of MOW with margin bathymetry and the effects of Coriolis force. In general, the drifts are composed mainly of muddy, silty, and sandy sediments with a mixed terrigenous (dominant component) and biogenic composition (Gonthier et al., 1984; Stow et al., 1986, 2002). In contrast, sand and gravel are found in the large contourite channels (Nelson et al., 1993, 1999), as are many erosional features (Hernández-Molina et al., 2006; García et al., 2009). In the proximal sector close to the Strait of Gibraltar, an exceptionally thick (~815 m) sandy-sheeted drift with sand layers averaging 12–15 m thick (minimum thickness = 1.5 m; maximum thickness = 40 m) is present (Buitrago et al., 2001).

Four major depositional sequences that must be related to MOW paleoceanographic changes have been recognized in the large contourite systems of the Pliocene and Quaternary sedimentary record. The depositional sequences are separated by four major regional discontinuities (Fig. F6), which from bottom to top are late Miocene (M), intra-lower Pliocene (LPR), base Quaternary discontinuity (BQD), and mid-Pleistocene revolution (MPR) (Llave et al., 2001, 2007, 2010, submitted; Hernández-Molina et al., 2002, 2009; Stow et al., 2002). Together, these discontinuities constitute an impressive record of changes in water mass circulation and of the tectonic and/or environmental changes that have affected evolution of the margin.

Portuguese margin sediments, by contrast, are dominated by hemipelagic muds, with variable admixtures of terrigenous silt and sand, and biogenic components (Baas et al., 1997). Pelagic sedimentation prevails during interglacial periods. Input of terrigenous material is enhanced during glacial periods because of lowered sea level and input from local sources such as density-driven slope lateral advection and low-concentration turbidity currents, as well as minor influences from bottom currents and ice rafting. High sedimentation rates are typical in this region because of elevated fluxes in both glacial (clay) and interglacial (silt) material; however, distinct climate control results in enhanced sedimentation during colder periods at both orbital and



millennial timescales. This pattern is observed in water depths between 2500 and 4600 m (Hall and McCave, 2000; Lebreiro et al., 2009). Detrital input from rivers (Tagus) channeled by turbidity currents is limited to submarine canyon systems (Lebreiro et al., 2009) and abyssal plains (Lebreiro et al., 1997) and does not affect open slope deposition. Ice-rafted detritus occasionally reached the Iberian margin during the last glacial period, especially during Heinrich events, when sea-surface temperatures were very low (Lebreiro et al., 1996; Baas et al., 1997; Cayre et al., 1999; Thouveny et al., 2000; de Abreu et al., 2003).

### **Neotectonic implications**

Tectonism during the Pliocene and Quaternary caused by the broad northwest–southeast compressional regime determined in the short term the local thickness, geometry, and present position of various depositional bodies and in the long term also contributed to paleoceanographic changes. Several features of the CDS in the Gulf of Cádiz and west of Portugal can be related to this recent tectonic activity, which has involved the reactivation of faults and diapiric structures related to local movements (Maldonado et al., 1999; Medialdea et al., 2004, 2009; Fernández-Puga et al., 2007; Neves et al., 2009; Terrinha et al., 2009; Zitellini et al., 2009). The most recent tectonic activity has directly created the conditions that led to several features (Llave et al., 2001, 2003; Hernández-Molina et al., 2003; García et al., 2009), including

- The recent configuration of the channels and ridges sector,
- The inactivity of several fossil mounded and sheeted drifts identified in Sectors 3 and 4,
- The recent genesis of the Diego Cão Channel, and
- The recent overexcavation and northward migration of the Cádiz Channel.

On the West Iberian margin, recent tectonic activity is variable from north to south. The Lisbon margin in the north has undergone significant subsidence through the Pliocene and Quaternary. The Alentejo margin further south has undergone moderate subsidence during the early Pliocene but evolved to a region of mixed transpression–transtension during the late Pliocene and Quaternary, in association with uplift of Gorringe Bank. Neotectonic activity is recognized in this area at the present time (Alves et al., 2003; Gràcia et al., 2003a, 2003b; Terrinha et al., 2003; Zitellini et al., 2009).



## **Seismic studies/Site survey data**

A broad database of Gulf of Cádiz and West Iberian margin information collected over the past 40 y by many different nations and cruises provides a superb template for drilling. This database is composed of

- Bathymetric data, including swath bathymetry of the middle slope using Simrad EM12S-120 and EM300 multibeam echo-sounder systems;
- Side-scan sonar image data from Seamap, OKEAN, geological long range inclined Asdic (GLORIA), and towed ocean bottom instrument (TOBI) systems;
- An extensive seismic data grid, including low-resolution multichannel seismic profiles from oil companies (mainly REPSOL and TGS-NOPEC); medium-resolution seismic profiles from Sparker, air gun, Geopulse, and Uniboom systems; high-resolution seismic profiles using a 3.5 kHz system; and ultrahigh-resolution seismic profiles using topographic parametric sonar (TOPAS);
- A variety of core data, ranging from box cores and short gravity cores to giant piston cores;
- More than 3000 submarine photographs taken with a BENTHOS-372 camera; and
- Physical oceanographic information.

## **Objectives**

Drilling in the Gulf of Cádiz and off the West Iberian margin offers a unique opportunity to tackle key scientific goals enumerated in the IODP ISP related to

- Oceanic gateways and their global influence,
- Paleocirculation and climate,
- Rapid climate change,
- Sea level and related controls on sediment architecture, and
- Neotectonic activity and controls on continental margin sedimentation.

The extensive CDS that has been developing within the Gulf of Cádiz and extending around the West Iberian margin over the past 5 m.y. is a direct result of MOW (e.g., Madelain, 1970; Gonthier et al., 1984; Faugères et al., 1985; Nelson et al., 1993, 1999; Llave et al., 2001, 2006, 2007, 2010, submitted; Stow et al., 2002; Habgood et al., 2003; Hernández-Molina et al., 2003, 2006, submitted; Mulder et al., 2003, 2006;

Hanquiez et al., 2007; Marchès et al., 2007). The high accumulation rates and expanded sedimentary records of drift deposits permit high-resolution examination of past environmental change (Llave et al., 2005; Voelker et al., 2006). The CDS deposits, therefore, hold the very best signal of MOW flow through the Strait of Gibraltar gateway and a clear record of its influence on the oceanography and climate of the North Atlantic Ocean and on NADW variability (Bigg and Wadley, 2001a, 2001b; Bigg et al., 2003). However, the region had not previously been drilled for scientific purposes, even though the Strait of Gibraltar gateway clearly has major implications for global climate and oceanography. The deeper target off western Portugal (APL-763) lies outside the direct influence of MOW but contains an expanded record of primarily hemipelagic sediment with which we can develop a Pleistocene marine archive of climate change.

We identified five broad scientific objectives for the proposed drilling program.

*1. Understand the opening of the Strait of Gibraltar gateway and onset of MOW.*

Tectonic adjustments along the suture line between the African and Eurasian plates could have lead to the opening of the Strait of Gibraltar gateway at the end of the Miocene at 5.3 Ma (Berggren and Hollister, 1974; Mulder and Parry, 1977; Maldonado et al., 1999; Blanc, 2002; García-Castellanos et al., 2009). Other authors have stressed that the cut into the threshold of Gibraltar was due to regressive erosion of a stream that was flowing toward the desiccated Mediterranean Basin, resulting in the opening of the strait (Blanc, 2002; Loget and Van Den Driessche, 2006). Reopening of the Strait of Gibraltar gateway marked the end of complete isolation of the Mediterranean Sea and the global effects of the Messinian salinity crisis (Ryan et al., 1973; Hsü et al., 1978; Comas et al., 1999; Duggen et al., 2003). Immediately following this initial opening, the gateway depth was most likely insufficient to allow very significant outflow of deep MOW into the Gulf of Cádiz. Therefore, the onset of deep MOW, the initiation of contourite drift sedimentation in the gulf, and the broader influence of warm saltwater influx in the North Atlantic lagged behind gateway opening. However, the actual timing of this event is uncertain.

Our first objective was to drill through the drift succession and into late Miocene sediments at several different sites and therefore date the basal age of drift sedimentation in the Gulf of Cádiz. We also aimed to evaluate the nature of change in the patterns of sedimentation and microfauna/microflora from the end of the Miocene through the early to middle Pliocene, from proximal regions closest to the Strait of Gibraltar gateway to distal regions on the West Iberian margin. This evaluation will allow us to

determine any downstream variation in the onset of contourite deposition and of MOW bottom water signature.

*2. Determine MOW paleocirculation and global climate significance.*

The present-day flux of MOW through the Strait of Gibraltar gateway is nearly 2 Sv (i.e.,  $2 \times 10^6 \text{ m}^3/\text{s}$ ), carrying warmer waters and more than 300,000 tons of excess salt into the North Atlantic every second. The consequent increase in density of NADW may stabilize, or in cases of decreased MOW flux, destabilize thermohaline circulation and therefore trigger climate change (Johnson, 1997; Rahmstorf, 1998; Bigg and Wadley, 2001a; Bigg et al., 2003). The importance of MOW in North Atlantic Ocean circulation and climate is now widely recognized. MOW millennial to long-term variability and its effects on thermohaline circulation is an active and prolific line of research at present. It has been inferred that the rate of deepwater formation reached its highest level in the Mediterranean during glacial stages, when contribution of NADW was at a minimum and Antarctic Bottom Water (AABW) at a maximum, but there are still many questions to resolve in this regard (e.g., Duplessy et al., 1988; Abrantes, 1988; Caralp, 1988, 1992; Sarnthein et al., 1994; Schönfeld, 1997, 2002; Cayre et al., 1999; Flower et al., 2000; Sierro et al., 2000, 2005; Shackleton et al., 2000; Schönfeld and Zahn, 2000; Cacho et al., 2000, 2001; Moreno et al., 2002; de Abreu et al., 2003; Schönfeld et al., 2003; Slater, 2003; Löwemark et al., 2004; Raymo et al., 2004; Voelker et al., 2006; Llave et al., 2006; Lebreiro et al., 2009; Lebreiro, 2010; Voelker and Lebreiro, 2010; among others).

Our second objective was to date the principal unconformities and minor discontinuities identified on seismic records, thereby calibrating the seismic stratigraphic framework. We can therefore assess their link to paleocirculation variation and events and evaluate their global correlation and significance. Detailed reconstruction of paleo-oceanographic conditions over centennial, millennial, and longer timescales at high resolution will disclose their evolution through time and help elucidate the background driving forces.

*3. Establish a marine reference section of Pleistocene climate (rapid climate change).*

Few marine sediment cores have played such a pivotal role in paleoclimate research as those from the Portuguese margin Shackleton sites, so-called to honor Nick Shackleton's seminal work in highlighting the global importance of these sections (Shackleton et al., 2000). These cores preserve a high-fidelity record of millennial-scale climate variability for the last glacial cycle that can be correlated precisely to polar ice

cores in both hemispheres (Fig. F7). Moreover, the narrow continental shelf off Portugal results in rapid delivery of terrestrial material (e.g., pollen) to the deep-sea environment, thereby permitting correlation of marine and ice-core records to European terrestrial sequences. IODP drilling at Site U1385 (proposed Site Shack-04 and location of piston Core MD01-2444) on the Iberian margin during Expedition 339 provided a rare opportunity to recover a marine reference section of Pleistocene climate variability that can be correlated confidently to polar ice cores and terrestrial archives.

Our third objective (and the principal objective of Site U1385 [APL-763]) was to recover a Pleistocene sediment archive offshore Portugal that will greatly improve the precision with which marine sediment records of climate change are correlated to and compared with ice-core and terrestrial records. By yielding multiproxy records that can be placed on an integrated stratigraphy, drilling of proposed Site Shack-04 resulted in major advances in our ability to reconstruct millennial-scale climate variability during the Pleistocene and understand its underlying causes.

#### *4. Identify external controls on sediment architecture of the Gulf of Cádiz CDS and West Iberian margin.*

The effects of sea level change on Pliocene–Quaternary sedimentary architecture in the Gulf of Cádiz and along the West Iberian margin have been considerably amplified by the direct influence of the Strait of Gibraltar gateway cross-sectional area (see above). Detailed analysis of the sedimentary architecture of CDS drift deposits is essential to distinguishing between climate and sea level change and to the further development of the global sequence stratigraphic model. In particular, the global role of bottom currents and evolution of alongslope depositional systems has not been adequately considered as a major component of the generalized sequence stratigraphic framework for continental margins. Furthermore, the cyclicity of MOW flux and resultant deposits has a relationship to eustatic influences on the Gibraltar sill that needs to be defined as a control on circulation of the entire North Atlantic.

Our fourth objective was to establish the nature of sedimentation and the timing of associated hiatuses by first-order drilling, dating, facies analysis, and correlation between all drill sites. This will further allow us to determine the stacking pattern and evolution of the Pliocene–Quaternary drift deposits and evaluate contourite cyclicity at seismic to sediment scales. Combining facies analysis and sedimentation rates with detailed compositional studies allows a more complete understanding of sediment supply and remobilization within the bottom-current system and quantification of a sedimentary budget and flux for the CDS in the gulf.

### 5. Ascertain synsedimentary neotectonic control on architecture and evolution of the CDS.

Charting the chronology of neotectonic activity that has had significant effect on development and architecture of the CDS is essential to a more complete understanding of the margin system in this region. Margin evolution anywhere is controlled by complex interaction of many different forcing variables, most importantly sea level and climate, sediment supply, and tectonics. The Gulf of Cádiz provides an excellent example of how recent tectonic activity has markedly affected submarine topography (Medialdea et al., 2004; Hernández-Molina et al., 2006; Fernández-Puga et al., 2007; Llave et al., 2007; García et al., 2009; Terrinha et al., 2009; Zitellini et al., 2009) and, consequently, controlled changes in the distribution of branches of MOW and their influence in the North Atlantic (Llave et al., 2007). The initiation and early history of MOW with regard to timing and tectonic control of the Strait of Gibraltar gateway is the focus of Objective 1 (above).

Our fifth objective was to chart the chronology of neotectonic activity that has had significant effect on development and architecture of the CDS and to identify the principal morphological changes that have resulted from this tectonic activity. We will thus be able to evaluate the direct influence of recent diapiric activity on the evolution of the CDS, particularly with regard to the erosion of channels and moats through the softer cores of diapir strings. There is also an excellent opportunity to determine the rate of diapiric movement and its change through time.

## Site summaries

### Site U1385

#### Background and objectives

Site U1385 is located at 2585 mbsl on the southwestern Iberian margin (37°34.285'N; 10°7.562'W) near the position of Core MD01-2444 (Fig. F8), which contains a detailed record of millennial-scale variability for the last 190 ka (Fig. F9). The overall objective of this site is to recover a late Pleistocene sediment record needed to extend this remarkable record to 1.4 Ma. The acquired record will greatly improve the precision with which marine sediment records of climate change can be correlated to and compared with polar ice cores and European terrestrial records.

Site U1385 was occupied on 25 November 2011. Five holes were cored at this site using the APC and nonmagnetic core barrels (Fig. F10). Four holes were cored to ~150

mbsf and one (Hole U1385C) to just 9.5 mbsf (1 core). A total of 67 cores were collected to obtain 622 m of sediment (103% recovery). The APCT-3 was deployed 12 times.

## Main results

The sediments at Site U1385 are defined as a single lithologic unit (Unit I). Unit I is a very uniform lithology composed of a Holocene–Pleistocene sequence dominated by bioturbated calcareous muds and calcareous clays that vary in the relative proportion of biogenic carbonate material (23%–39%), as shown by color variation from lighter (i.e., more calcareous) to darker (i.e., more terrigenous) sediment (Fig. F11). Relatively more terrigenous-dominated sediments are present in the upper quarter of Unit I, but their occurrence does not warrant the definition of any additional lithologic units or subunits. No primary sedimentary structures were observed; however, bioturbation is the most obvious secondary sedimentary structure and ranges from sparse to moderate. Other features, such as small-scale subvertical microfaults and contoured beds, are present at several depth intervals. These features are local and of minor importance and do not seriously disrupt the continuity of the stratigraphic section. The entire section cored at this site is therefore considered to be typical hemipelagic deposits with average sedimentation rates of ~10 cm/k.y.

The five holes cored at Site U1385 provided ample sediment for constructing a complete spliced stratigraphic section containing no notable gaps or disturbed intervals. A primary splice was constructed using all holes and provides an optimal composite section for all physical and magnetic properties measured using pass-through multi-sensor tracks (Figs. F10, F11). Two nearly complete secondary splices were also constructed, one using intervals from Holes U1385A and U1385B and the other using intervals from Holes U1385D and U1385E. These alternate splices will maximize the core material available for sampling while adhering to IODP sampling policy.

Biostratigraphy at Site U1385 is based on the shipboard study of calcareous nannofossils and planktonic and benthic foraminifers in core catcher samples from Holes U1385A–U1385D and the five lowermost core catcher samples of Hole U1385E. Nannofossils and planktonic foraminifers were very abundant and relatively well preserved in all samples. Benthic foraminifers were also relatively abundant and diverse; however, ostracods were rare and pteropods were not observed in any samples down-hole with the exception of the mudline sample. Pollen and spores were generally abundant and moderately well preserved, providing an excellent opportunity for marine-terrestrial correlations. The chronological framework for Site U1385 was mainly

based on calcareous nannofossil and planktonic foraminifer events as well as one benthic foraminifer datum, suggesting a continuous Pleistocene record with a nearly uniform sedimentation rate of  $\sim 10$  cm/k.y. The age of the base of the section is estimated to be  $\sim 1.4$  Ma.

Natural remanent magnetization (NRM) intensity ranges from  $\sim 10^{-5}$  to  $\sim 10^{-3}$  A/m. Within the uppermost 50 m the intensity is on the order of  $10^{-2}$  A/m, but below  $\sim 60$  mbsf the intensity decreases to  $\sim 10^{-3}$  to  $\sim 10^{-5}$ . The correlation between remanent intensity and magnetic susceptibility suggests that the magnetic minerals that carry the NRM are the same grains that dominate the magnetic susceptibility. Magnetic susceptibility generally varies between  $10 \times 10^{-5}$  and  $50 \times 10^{-5}$  SI (Fig. F10). The Brunhes–Matuyama polarity transition (0.781 Ma) as well as the termination and beginning of the Jaramillo Subchron (C1r.1n; 0.988 and 1.072 Ma, respectively) are identified at Site U1385. In addition, a brief normal polarity interval is tentatively interpreted to represent the Cobb Mountain Subchron (C1r.2n; 1.173–1.185 Ma). Postcruise paleomagnetic analysis of samples from Site U1385 will provide a reliable record of variations in relative paleointensity of Earth’s geomagnetic field.

The most remarkable aspect of all physical property records at Site U1385 is a gradual reduction of magnetic susceptibility values beginning at  $\sim 30$  mbsf (Fig. F10). Despite the reduction in intensity, magnetic susceptibility displays distinct high-amplitude variability until 50 mbsf, being comparatively low and less variable downhole. This main change between 30 and 60 mbsf seems to correspond to a general change in lithology and/or diagenetic overprint (e.g., mirrored in low natural gamma ray [NGR] counts and high  $L^*$  values) (Figs. F10, F11). A likely cause for the overall decrease of magnetic susceptibility is the reduction of fine-grained magnetite to iron sulfides within the sulfate reduction zone. High-frequency variations show a close correlation to gamma ray attenuation (GRA) densities, likely reflecting varying relative amounts of clay and carbonate. There is also a notable positive correlation between NGR and magnetic susceptibility below 40 mbsf that is not apparent above this depth, hinting at a change in the factors influencing the sedimentary composition during this interval.

Organic carbon is generally low ( $<1$  wt%) and the C/N ratio indicates that the organic carbon is mainly of marine origin. Diagenesis of organic matter has led to depletion of dissolved sulfate in interstitial waters. In this process, sulfate is consumed and alkalinity, ammonium, and phosphate are produced as by-products. The increase in alkalinity promotes authigenic precipitation of carbonate minerals (e.g., calcite and



dolomite), consistent with decreases in magnesium and calcium concentrations in the sulfate reduction zone. Hydrogen sulfide ions produced by sulfate reduction and anaerobic methane oxidation can react with iron to form iron sulfide minerals, which are paramagnetic and have lower susceptibility than magnetite. This process may explain the decrease in magnetic susceptibility observed below ~40 mbsf. Oxygen and hydrogen isotope values of interstitial water show considerable variability in the uppermost 30 m, which is unexpected from a profile that should be dominated by diffusion.

The measured geothermal gradient at Site U1385 is ~39.2°C/km, and the estimated heat flow is 47.5 mW/m<sup>2</sup>, which is in the lower half of the normal range for heat flow on the Portuguese margin.

## Highlights

Exactly as predicted, drilling at Site U1385 recovered a continuous 1.4 Ma record (lithologic Unit I) of hemipelagic deposits with an average sedimentation rate of ~10 cm/k.y. The multiple spliced records recovered in five holes provide essential material needed for postcruise studies of millennial-scale climate variability through the Mid-Pleistocene Transition (MPT). Variations in physical properties and color display cyclic changes that reflect cyclic changes in the proportion of biogenic carbonate and detrital material delivered to the site. These variations will prove useful to orbitally tune the record at Site U1385, serve as a marine reference section of Pleistocene climate variability, and significantly improve the precision with which marine climate records can be correlated to polar ice cores and terrestrial sequences.

## Site U1386

### Background and objectives

Site U1386 is located on the southern Iberian margin (36°49.685'N; 7°45.321'W) ~25 km south-southeast of the Portuguese city of Faro, in a water depth of 561 mbsl (Fig. [F1](#)). It is the most distal of our sites from the Strait of Gibraltar gateway, within the depositional sector of the Cádiz CDS. The site targets the eastern end of an elongated mounded and separated drift (the Faro Drift) that has a total length of 100 km, a width up to 20 km, and a maximum thickness of ~700 m.

The Faro Drift represents a classic example of middle-slope contourite deposits, which shows a well-layered internal acoustic structure with laterally extensive, aggradational to progradational seismic depositional units and widespread discontinuities



(Fig. F12). Faro Drift has been developing along the middle slope over the past 4–5 m.y. under the direct influence of MOW. It therefore holds a clear signal of MOW through the Strait of Gibraltar gateway, which reopened following tectonic adjustments at the end of the Messinian salinity crisis.

Our primary objective was to recover a key Pleistocene and Holocene sedimentary succession formed under the influence of MU, and hence a clear record of MOW influence on the North Atlantic Ocean. The high rates of accumulation and expanded sedimentary record of this drift site should permit high-resolution examination of past environmental change (climatic and eustatic). This site is complementary to Site U1387, located ~4.1 km southeast, which will target a Pliocene and lower Pleistocene sedimentary record also influenced by MU.

Site U1386 was occupied on 30 November. Three holes were drilled and cored using the APC, XCB, and RCB, achieving the target depth of 526 mbsf in Hole U1386C. Downhole logging was carried out in Hole U1386C using the triple combo, FMS-sonic, and VSI tool strings. Overall recovery at Site U1386 was 351 m (102%) with the APC, 417.6 m (89%) with the XCB, and 82 m (58.5%) with the RCB. The total cored interval at Site U1386 was 954.4 m, and total recovery was 850.6 m (89%).

## Main results

The sedimentary succession at Site U1386 extends from the latest Miocene to Holocene (Fig. F13). It is divided into two lithologic units (Units I and II), distinguished on the basis of inferred depositional process. Unit I is a Pleistocene–Holocene sequence dominated by classic contourite deposition, including nannofossil mud, calcareous silty mud, and silty bioclastic sand lithologies. These three lithologies are generally organized as bi-gradational sequences, the most complete of which coarsen upward from nannofossil mud to calcareous silty mud to silty bioclastic sand, and then fine upward through calcareous silty mud into nannofossil mud. Unit I is divided into three subunits (IA, IB, and IC) based on the relative importance of the silty muds and silty sands. Thin turbidite intercalations occur very rarely in the uppermost part of Subunit IA and more commonly in the lowermost 30 m of Subunit IC.

Unit II is a late Miocene–Pleistocene sequence characterized by the deposits of downslope processes interbedded with contouritic and hemipelagic nannofossil muds. The downslope facies include medium- and thick-bedded disorganized turbidites and thick- to very thick-bedded chaotic debrites. Quartz-lithic-rich turbidites are more

common in the uppermost part, whereas debrites and bioclastic (shelly) turbidites are typical of the lowermost part.

Calcareous microfossils (nannofossils, planktonic and benthic foraminifers, and ostracods) are mostly common to abundant with moderate to good preservation through lithologic Unit I but occur more sporadically and with poorer preservation through Unit II. The sedimentary record is continuous for the most part in the Holocene and Pleistocene to ~1.9 Ma, with an average sedimentation rate of 35 cm/k.y. between 0 and 384 mbsf (contourite dominated) decreasing to 15 cm/k.y. between 384 and 453 mbsf (turbidite dominated). Preliminary shipboard dating suggests the presence of a major hiatus before 1.9 Ma, which cuts out much of the early Pleistocene and late Pliocene, and a somewhat discontinuous record through the debrite-dominated section. The lowermost 15 m of the record is most likely of Messinian age (<5.8 Ma).

The observed variability in both benthic foraminifer and ostracod distribution seems to reveal significant changes in depositional processes and bottom water environmental conditions over the last ~5 m.y. In general, there is marked mixing with shelf-derived taxa in the lower part of the succession as a result of direct input from down-slope processes and progressive upward increase in cold-water taxa. Periodic increases in bottom-current energy and ventilation are indicated by both lithologic changes and benthic faunas. Pollen and spores are abundant in all the samples analyzed, along with microcharcoal and dinocysts. Together, these indicate significant changes in terrestrial climate and vegetation comparable with the marine record.

Paleomagnetic measurements identified the Brunhes–Matuyama polarity transition (0.781 Ma) as well as the termination and beginning (0.988 and 1.072 Ma, respectively) of the Jaramillo Subchron (C1r.1n). These give reliable confirmation of biostratigraphic dating for Site U1386 and confirm the relatively high rates of sedimentation through the contourite succession.

Based on the physical property data, distinct changes have been identified that are commonly related to boundaries between defined lithologic units. In addition, cyclic variation in NGR and magnetic susceptibility values and persistent covariation of both parameters with sediment color appear to track decimeter-scale cyclicity noted in lithologic character. Especially high magnetic susceptibilities correspond to the turbidite-dominated section between 420 and 445 mbsf. Below 445 mbsf, low values in

NGR and magnetic susceptibility conform with a shift in the lithology to debrites and turbidites below a major hiatus.

The pore water profile at Site U1386 is dominated by organic matter diagenesis with a shallow sulfate reduction zone in the uppermost 12.5 m and methanogenesis below. High alkalinity associated with sulfate reduction and anaerobic methane oxidation has resulted in authigenic calcite and dolomite formation. Iron sulfide minerals formed as a consequence of sulfate reduction. A maximum in  $\delta^{18}\text{O}$  and  $\delta\text{D}$  coincident with a minimum of chloride in interstitial water suggests the influence of gas hydrates that dissociated upon core recovery.

Downhole measurements were made in Hole U1386C to a total depth of 526 mbsf. Despite a certain degree of borehole rugosity, the combination of logs used closely reflects both lithologic changes and cementation recorded in the recovered cores. This allowed us to infer lithologies from some of the gaps in core recovery. Preliminary inspection also revealed a marked cyclicity from 102 to 346 mbsf through the contourite section, which seems to relate to Milankovitch precession cycles of ~20 k.y. These data will be carefully scrutinized together with cycles observed in both the lithologic and physical property records.

The measured geothermal gradient at Site U1386 is ~34.3°C/km, and the estimated heat flow is 42.1 mW/m<sup>2</sup>.

## Highlights

Coring at Site U1386 on the Faro Drift recovered a thick Pleistocene–Holocene succession of mud/silt contourites, as anticipated. These successions showed a continuous record of drift sedimentation over the past 1.9 m.y. at an average sedimentation rate of 35 cm/k.y. for the past 1 m.y. What was not expected was to reach into the latest Miocene at ~515 mbsf.

We confirmed the classic contourite model of meter-scale bi-gradational cyclicity with apparent millennial-scale forcing. There was also evidence of a strong lateral supply of terrigenous material to the bottom currents. We also recognized decimeter-scale cycles characterized by relative abundance and thickness of silty contourites. These are provisionally related to seismic cycles with Milankovitch-scale forcing.

At the base of the main constructional drift, interbedded turbidites and contourites are underlain by a 40 m thick unit of early Pleistocene turbidite sandstones, which probably represent deposition during sea level lowstand. These directly overlie a ma-

major hiatus of 0.3–2.2 m.y. duration, which we provisionally relate to aggressive erosion by bottom currents sometime after the onset of MOW. The early Pliocene succession comprises bioclastic debrites and turbidites, most likely the result of widespread tectonic activity and slope instability. These events at the very beginning of the Pliocene might be related to the final stages in the opening of the Strait of Gibraltar gateway.

## Site U1387

Site U1387 is located on the southern Iberian margin (36°48.321'N; 7°43.1321'W) about 29 km south-southeast of the Portuguese city of Faro in a water depth of 559.1 mbsl (Fig. F1). This site is a close companion to Site U1386 at the eastern end of the Faro Drift and part of the larger Cádiz CDS. Although lying only 4 km southeast of Site U1386, interpretation of the seismic records indicates a slightly reduced Pleistocene section and an expanded Pliocene succession.

The Faro Drift represents a classic example of middle-slope contourite deposits, showing a well-layered internal acoustic structure with laterally extensive aggradational to progradational seismic depositional units and widespread discontinuities (Fig. F6). Faro Drift has been developing along the middle slope over the past 4–5 m.y., under the direct influence of MOW. It therefore holds a clear signal of MOW through the Strait of Gibraltar gateway, which reopened following tectonic adjustments at the end of the Messinian salinity crisis.

Our primary objective at this site was to recover a full Pliocene, Pleistocene, and Holocene sedimentary succession formed under the influence of MU and also to penetrate the Miocene/Pliocene boundary. As at its companion site, the high rates of accumulation and expanded sedimentary record of this site should permit high-resolution examination of past environmental change (climatic and eustatic).

Site U1387 was occupied on 8 December. Three holes were drilled and cored using the APC, XCB, and RCB, achieving the target depth of 870 mbsf in Hole U1387C. Down-hole logging was carried out in Hole U1387C using the triple combo, FMS-sonic, and VSI tool strings. Overall recovery at Site U1387 was 97 m (103%) with the APC, 578.4 m (97%) with the XCB, and 409.5 m (70.6%) with the RCB. The total cored interval at Site U1387 was 1270.7 m, and total recovery was 1084.95 m (85%).

## Main results

The sedimentary succession at Site U1387 extends for 870 m from the latest Miocene to Holocene (Fig. F14) and is divided into four lithologic units (I–IV) distinguished on the basis of lithologic character and inferred depositional process. Unit I is a Pleistocene–Holocene sequence dominated by classic contourite deposition, including nannofossil mud, calcareous silty mud, and silty bioclastic sand lithologies generally organized as bi-gradational sequences. Thin turbidite intercalations occur more commonly than at Site U1386 and are especially noted in the lowermost 100–150 m of the unit.

Below a more significant unconformity, Unit II is capped by two well-cemented dolomite horizons. For the most part the unit represents Pliocene sedimentation characterized by a clear cyclic arrangement of lighter colored facies having turbidite and/or contourite affinity and darker colored facies of pelagite affinity (Fig. F14). There is close interaction between processes and more or less continuous bioturbation throughout. In Unit III the evidence of downslope resedimentation is still more evident, including poorly sorted turbidite sandstones, a chaotic debrites, and slump units as thick as 5 m. Shallow-water bioclastic debris is common together with resedimented lignitic material in places. Below ~680 mbsf, a 50 m thick section includes hard calcite-cemented sandstone turbidites and poor core recovery. This unit is mainly early Pliocene in age, but may start in the latest Miocene.

Unit IV is a relatively thinner basal unit of late Miocene age with a very different character (Fig. F14) dominated by middle-slope hemipelagic sediments to nannofossil muds and muddy oozes.

Calcareous microfossils (nannofossils, planktonic and benthic foraminifers, and ostracods) are mostly common to abundant with moderate to good preservation through lithologic Units I and IV and relatively poorer preservation through Units II and III, where considerable reworking is also apparent. The sedimentary record is continuous for the most part in the Holocene and Pleistocene to about 1.8 Ma, with an average sedimentation rate of 25 cm/k.y. Below the Pliocene–Pleistocene hiatus (1.8–3.2 Ma) at 450 mbsf (Fig. F14), the mean sedimentation rate is ~15 cm/k.y., although a significant proportion of this section comprises instantaneous event beds. The lowermost unit is most likely of Messinian age (<5.8 Ma).

The observed variability in both benthic foraminifer and ostracod distribution reveals significant environmental changes over the last ~5 m.y., closely comparable with

those observed at Site U1386. In general, the Pleistocene succession shows typical upper bathyal assemblages indicative of increased organic matter input and reduced ventilation. There is marked mixing with shelf-derived taxa in the Pliocene part of the succession as a result of direct input from downslope processes and progressive upward increase in cold-water taxa, as noted also by planktonic assemblages. Periodic increases in bottom-current energy and ventilation are indicated by both lithologic changes and benthic faunas. Pollen and spores are abundant in most of the samples analyzed, along with microcharcoal and dinocysts. Together, these indicate normal (fresh) supply from Mediterranean forests and grasslands for the Pleistocene, a transitional zone mixed with corroded, reworked forms, and then a Pliocene succession with a notable absence of freshly derived pollen.

Paleomagnetic measurements identified the Brunhes–Matuyama polarity transition (0.781 Ma) but no clear Jaramillo Subchron. Measurements also identified a reliable Matuyama–Olduvai transition (1.778 Ma) toward the base of Unit I. These measurements give reliable confirmation of the biostratigraphic dating for Site U1387 and confirm the relatively high rates of sedimentation through the contourite succession. Cyclic variation in the intensity of NRM and magnetic susceptibility requires further study.

Physical property data show generally high values of NGR, magnetic susceptibility, and bulk density within the uppermost 50 m of lithologic Unit I, with lower values downhole. Cyclic variation in values and the presence or absence of covariation between different parameters (and with sediment color) show a complex track of decimeter-scale cyclicity noted in lithologic character. In some cases, high magnetic susceptibility values correspond to individual turbidites within the Pleistocene section but not those in the Pliocene.

The pore water profile at Site U1387 shows a similar shallow sulfate reduction zone to that found at Site U1386, followed by transition to methanogenesis. This is assumed to be related to high rates of organic matter accumulation. High alkalinity associated with sulfate reduction and anaerobic methane oxidation has resulted in authigenic calcite and dolomite formation. Iron sulfide minerals also formed as a consequence of sulfate reduction.

Downhole measurements were made in Hole U1387C to a bridged-hole depth of 649 mbsf with the first tool string. There was further bridging at shallower depths for subsequent tool strings. Moderately severe borehole rugosity severely hampered ship-

board interpretation, although the combination of logs used generally reflects both lithologic changes and cementation recorded in the recovered cores. Apparent cyclicity in some parts of the section will require further study following an attempt to correct for variation in borehole diameter. The sonic log and vertical seismic profile will be useful in refining our interpretation of key reflectors on seismic profiles at this site. Only one downhole temperature measurement was achieved at the site because of the shallow change to XCB drilling at ~47 mbsf.

## Highlights

Although only 4 km apart, Sites U1386 and U1387 on the Faro Drift showed some interesting and significant differences, as well as similarities. There was the same thick Pleistocene–Holocene succession of mud/silt contourites at Site U1387, indicating a continuous record of mounded drift construction over the past 1.8 m.y., at an average sedimentation rate of 25 cm/k.y. Meter-scale bi-gradational contourite cyclicity was common, with evidence of a strong lateral supply of terrigenous material to the bottom currents, especially before ~1.8 Ma. Decimeter-scale cycles characterized by relative abundance and thickness of silty contourites are most evident on physical property and downhole logs. These correlate well between sites and with Milankovitch-scale forcing. The same extended Pliocene–Pleistocene hiatus (~1.4 m.y.) is recognized as being related to a phase of highly active MOW but within drift rather than at the floor of a channel, which was the case at Site U1386.

Interbedded contourites and turbidites characterize the later Pliocene phase of sheeted drift construction with clear evidence of process interaction. The early Pliocene is dominated by resedimented facies, including debrites, slump deposits, and channel-fill turbidite sandstones. This is further evidence of widespread tectonic activity and slope instability at a time close to the opening of the Strait of Gibraltar gateway.

## Site U1388

Site U1388 is located on the southern Iberian margin (36°16.142'N; 6°47.647'W) about 50 km southwest of the Spanish city of Cádiz, in a water depth of 663 mbsl (Fig. F1). This lies within the extensive Cádiz sand sheet, which is in the proximal part of the larger Cádiz CDS. This site is the site closest to the Strait of Gibraltar gateway drilled during Expedition 339.

The Cádiz sand sheet represents an important example of very poorly studied sandy contourite deposits on a middle-slope terrace. The seismic profiles show a well-layered internal acoustic structure with laterally extensive, aggradational to seismic depositional units, some thin intervals of lateral progradation, and inferred section discontinuities (Fig. F15). This sand sheet has accumulated on a middle-slope terrace over the past 4–5 m.y. under the direct influence of MOW.

Our primary objective at this site was to recover a full Pliocene, Pleistocene, and Holocene sedimentary succession formed under the influence of MOW close to its exit from the Strait of Gibraltar gateway and to penetrate the Miocene/Pliocene boundary. Site U1388 was intended as our deepest penetration site (1550 mbsf).

Site U1388 was occupied on 18 December. Three holes were drilled and cored using the APC, XCB, and RCB, but a depth of only 226 mbsf was achieved in the third hole (U1388C). The site was terminated prematurely as a result of hole instability; down-hole logging was considered unwise. Overall recovery for Site U1388 was 3.6 m (107%) with the APC, 107 m (47%) with the XCB, and 10.4 m (43%) with the RCB. The total cored interval for Site U1388 was 253 m and total recovery was 121 m (47.8%), which was significantly lower than at the other expedition sites.

## **Main results**

The sedimentary succession at Site U1388 extends 226 m from the mid-Pleistocene to Holocene (Fig. F16) and comprises a single lithologic unit notable for its distinctly sandy nature and consequent low core recovery. The principal lithologies include sand, silty sand, and silty mud, all calcareous in nature with 10%–25% carbonate content, which is part bioclastic and part detrital in origin. On the assumption that much of the missing material is unconsolidated sand, the upper 100 m is sandier than the underlying 50 m. The remainder of the unit comprises alternating 20–30 m thick units of sand-rich and mud-rich material. A range of bi-gradational normally graded and reverse-graded sequences occur, which are interpreted as mainly contouritic in nature, although further work is required to improve our understanding of the depositional process.

Calcareous microfossils (nannofossils, planktonic and benthic foraminifers, ostracods, and rare pteropods) are much less abundant than at other sites but generally show good to very good preservation. The section is inferred to reach an age of <0.56–0.7 Ma, with a sedimentation rate of 60 cm/k.y. Temperate to subtropical conditions are indicated by the planktonic foraminifer assemblages. Benthic foraminifers show



typical upper bathyal assemblages, some mixing with shelf-derived taxa, and variation in ventilation and/or MOW intensity.

Paleomagnetic measurements from all three holes indicate that only the Brunhes normal polarity chron (C1n) is recorded in these sediments, which confirms the biostratigraphic dating. Neither the intensity of NMR nor magnetic susceptibility values are especially high. Physical property data show a correspondence between higher magnetic susceptibility and sandier layers within the more mud-prone sections; otherwise, the data are relatively poor.

The pore water profile at Site U1388 shows a relatively deep sulfate reduction zone in which sulfate reduces to zero levels at ~50 mbsf followed by transition to methanogenesis. This corresponds to a level of increased authigenic dolomite recorded in the cores. An anomalous increase in both Na and Cl is apparent downhole, indicating mixing with deeper saline waters. Total organic carbon values of 0.2–0.8 wt% are relatively lower than at other sites

## Highlights

Although drilling was difficult, recovery was generally poor, and the site was terminated early because of hole instability, the sediments recovered form a very important part of the MOW story. High rates of sedimentation and a generally sand-rich section testify to intensified MOW flow coupled with abundant sediment supply. These sandy contourites represent the best record we have to date of this facies type, which appears to be significantly different from the downflow counterparts at other drilled sites. Also, the presence of thick mud-rich intervals records variable MOW intensity over the past ~0.6 m.y. during construction of a sand-prone sheeted contourite drift.

## Site U1389

Site U1389 is located on the southern Iberian margin (36°25.515'N; 7°16.683'W) ~90 km west of the Spanish city of Cádiz, in a water depth of 644 mbsl (Fig. F1). This site is one of two sites in the “channels and ridges” sector of the larger Cádiz CDS and is perched on a relative topographic high, which is currently elevated 50–250 m above the flanking contourite channels and lies ~4 km northwest of the Guadalquivir diapiric ridge.

We designate this as the Huelva sheeted/patch drift, which is in fact a small remnant of a much larger middle-slope sheeted drift system that has been dissected by several

contourite channels. Huelva Channel lies along the northern flank and Guadalquivir Channel along the southern flank of Huelva Drift. Seismic profiles show a well-layered internal acoustic structure with laterally extensive, mainly aggradational seismic depositional units and widespread discontinuities (Fig. F17). There is a complex erosional-depositional relationship between drift and flanking channel. Huelva Drift has been developing in this region over the past 4 m.y., at least, and is presently under the influence of the ML.

Our primary objective at this site was to recover a Pliocene, Pleistocene, and Holocene sedimentary succession formed under the influence of ML and to compare this record with that found at Sites U1386 and U1387, which formed under MU.

Site U1389 was occupied on 21 December. Five holes were drilled and cored using the APC, XCB, and RCB, achieving the target depth of 990 mbsf in the fifth hole (U1389E). Downhole logging was carried out in Holes U1389A and U1389E using the triple combo, FMS-sonic, and VSI tool strings. Overall recovery for Site U1389 was 307 m (104%) with the APC, 464 m (90.5%) with the XCB, and 352 m (54%) with the RCB. The total cored interval for Site U1389 was 1463.4 m, and total recovery was 1123.5 m (77%).

## Main results

The sedimentary succession at Site U1389 extends for 990 m from the early Pliocene to Holocene (Fig. F18) and is represented by a thick, rapidly accumulated, and very uniform series of contouritic sediment, which has been divided into a single lithostratigraphic unit and five subunits (IA–IE). Unit I is dominated by classic contourite deposition, including calcareous mud, silty mud, sandy mud, and silty bioclastic sand lithologies. These are generally organized as bi-gradational sequences and partial sequences, of which base-cutout, normally graded sequences are more common than top-cutout, inversely graded sequences. Carbonate content ranges from 21–35 wt%, and total organic carbon ranges from 0.3–1.8 wt%. The division of Unit I into five subunits is based on subtle changes in the relative abundance of the different lithologies and silt/sand intervals.

Calcareous microfossils (nannofossils, planktonic and benthic foraminifers, and ostracods) are mostly common to abundant with moderate to good preservation throughout. Pteropod fragments are more common at this site than at any of the other sites, mainly within the uppermost 30 m. The sedimentary record is continuous through the Holocene and Pleistocene to ~2.1 Ma, with a sedimentation rate between

30 and 40 cm/k.y. A relatively short hiatus (2.1–2.4 Ma) occurs at ~640 mbsf, below which the average sedimentation rate is 25 cm/k.y. There is some evidence from lithologic, physical property, and downhole logging data for two other minor hiatuses at ~0.4 and 0.9 Ma. The deepest part of the section is younger than 3.7 Ma.

Distinctive variability in benthic foraminifer assemblages reveals significant environmental changes through the Pliocene–Holocene succession closely comparable with that observed at other sites. The upper 0.9 m.y. of the Quaternary shows typical upper bathyal assemblages indicative of increased organic matter input and reduced ventilation. The remainder of the Pleistocene shows lower nutrient supply, greater influence of MOW, and significant mixing with shelf-derived taxa. Pliocene assemblages suggest high-nutrient, low-oxygen conditions and generally warmer waters. Pollen and spores are abundant in most of the samples analyzed, along with microcharcoal and dinocysts. Together, these indicate normal (fresh) supply from Mediterranean forests and grasslands for the late Pleistocene, a transitional zone mixed with corroded, reworked forms and no pines, and then a Pliocene succession with mostly corroded conifers.

Paleomagnetic measurements identified the Brunhes–Matuyama polarity transition (0.781 Ma), the top and bottom of the Olduvai Subchron (1.778 and 1.945 Ma, respectively), the Matuyama–Gauss transition (2.581 Ma), the Gauss–Gilbert transition, and potentially three minor excursions. These give reliable confirmation of the biostratigraphic dating for Site U1389, although some of the inferred polarity boundaries need further confirmation.

Physical property data show relatively close tracking of magnetic susceptibility and bulk density with more sand-/silt-rich intervals within the Pleistocene succession but a much more complex pattern within the Pliocene. The downhole distribution of porosities shows higher values in an interval of high interstitial water chlorinity, arguing in favor of lateral advection of brine-related fluids through more permeable strata.

The pore water profiles at Site U1389 show distinct maxima in several elements at ~530 mbsf, with relatively sharp transitions above and below. This suggests either a barrier to vertical diffusion or enhanced lateral fluid flux. The increase in concentrations is likely due to dissolution of minerals, most likely carbonates. A strong negative correlation also exists between  $\delta^{18}\text{O}$  and  $\delta\text{D}$ , which is characteristic of clay mineral dehydration reactions that take place at temperatures  $>50^\circ\text{C}$ . This requires that the fresh signal is a result of fluid migration from a deeper, higher temperature source.

Downhole measurements were made in Hole U1389A to 355 mbsf and in Hole U1389E to a bridged-hole depth of 568 mbsf. A good suite of FMS image logs was obtained in Hole U1389A. There is a distinct change in log characteristics at ~320 mbsf, which correlates closely with a lithostratigraphic boundary and a zone of poor core recovery. This zone appears to be more sand rich on the basis of borehole logs, although no sands were recovered by coring. Distinct cyclicity is apparent in some parts of the section, corresponding to both lithologic and physical property data. This will require further study. Nine downhole temperature measurements were made in the uppermost 100 m of section, indicating a geothermal gradient of 20.9°C/km, relatively lower than at other sites of this expedition.

## Highlights

We recovered core to a total depth of 990 mbsf at Site U1389, the deepest penetration of the expedition. The site lies under the influence of ML and is perched on a topographic high between contourite channels. For much of its Pleistocene history, it has only received sediment from either bottom current or hemipelagic processes. Especially notable is the extreme uniformity of the succession and its rapid accumulation at rates of 25–40 cm/k.y. The sediments are distinctively contouritic in character throughout, with mixed terrigenous-biogenic composition and characteristic bi-gradational or partial contourite sequences. Significantly, the long-duration hiatus observed at both Sites U1386 and U1387 on the Faro Drift under MU, and related to a phase of highly active MOW, are reduced at Site U1389 to 2.1–2.4 Ma. Two other minor hiatuses are inferred at around 0.4 and 0.9 Ma, and are also indicative of enhanced MOW at these times.

## Site U1390

Site U1390 is located on the southern Iberian margin (36°19.110'N; 7°43.078'W) ~130 km west of the Spanish city of Cádiz in a water depth of 992 mbsl (Fig. [F1](#)). This site is the second of two sites drilled in the channels and ridges sector of the larger Cádiz CDS and is near the western end of a sheeted drift adjacent to the Guadalquivir contourite channel at 300 m above the channel floor and ~20 km northwest of the of the Guadalquivir diapiric ridge.

This sheeted drift is known as the Guadalquivir drift, which is part of a much larger middle-slope sheeted drift system that has been dissected by several contourite channels. Site U1389 lies on the Huelva drift, which is another dissected portion of this same system also under the influence of ML (see “[Site U1389](#)” in “Site summaries”).

On seismic profiles the Huelva drift displays a well-layered internal acoustic structure with laterally extensive, mainly aggradational seismic depositional units (Fig. F19) and lies unconformably above two earlier buried drifts that have been differentially tilted up toward the north adjacent to the tectonically elevated Guadalquivir bank.

Our primary objective at this site was to recover the Pliocene–Quaternary sedimentary succession close to and affected by tectonic uplift of the Guadalquivir bank. By penetrating the unconformities between the surface and buried drifts we have been able to evaluate the timing of this tectonic activity and its effects on drift sedimentation. The secondary objective at this site was to further assess drift sedimentation under the influence of the ML.

Site U1390 was occupied on 2 January 2012. Three holes were drilled and cored using the APC and XCB systems, achieving the target depth of 350 mbsf in the first hole (U1390A). The second and third holes were piston cored to refusal. Downhole logging was carried out in Hole U1390A using the triple combo and FMS-Sonic tool strings. Overall recovery for Site U1390 was 438 m (98%) with APC and 248 m (91%) with XCB. The total cored interval for Site U1390 was 719.5 m and total recovery was 686.3 m (95%).

## Main results

Whereas our predrilling interpretation had assumed a relatively low rate of sedimentation above base-Quaternary and mid-Pliocene unconformities, instead we found very high rates of sedimentation under the influence of an active ML. The unconformities noted on seismic records, therefore, are much younger than expected. The basal unconformity of Guadalquivir Drift is 0.9–1.2 Ma, and the bottom of the hole reached to about 1.3 Ma.

The sedimentary succession at Site U1390 extends for 350 m from the mid-Pleistocene to Holocene (Fig. F20). It is represented by a very rapidly accumulated and uniform series of contouritic sediment, which has been divided into a single lithologic unit and two subunits (IA and IB). Unit I is dominated by classic contourite deposition, including calcareous mud, silty mud, sandy mud, and silty bioclastic sand lithologies. These are generally organized as bi-gradational sequences and partial sequences, of which base-cutout, normally graded sequences are more common than top-cutout, inversely graded sequences in Subunit IA. Whereas top-cutout, inversely graded sequences are more common in Subunit IB. Carbonate content ranges from 21–35 wt%, and total organic carbon ranges from 0.4–1.1 wt%. The division of Unit

I into two subunits is based on a marked change at 290 mbsf in the relative abundance and thickness of the silt/sand intervals. These are more prominent in Subunit IB, where the sandy facies makes up ~50% of the total.

Calcareous microfossils (nannofossils, planktonic and benthic foraminifers, and ostracods) are mostly common to abundant with moderate to good preservation throughout. Pteropod fragments are present sporadically. There are two relatively short hiatuses in the sedimentary record at 0.3–0.6 Ma and 0.9–1.2 Ma, separating intervals with rapid rates of sedimentation, averaging 75 cm/k.y. above the upper hiatus and 85 cm/k.y. below. Holocene sedimentation rates are also very high, around 80 cm/k.y. Although age constraints are not yet refined, it appears that the rate below the lower hiatus exceeds 100 cm/k.y. This is the highest rate we know of for any contourite drift site.

Distinctive variability in benthic foraminifer assemblages is apparent and reveals significant long-term trends as well as short-term cycles of environmental change. Comparable with other sites, the upper 0.9 m.y. of the Quaternary shows typical upper bathyal assemblages indicative of increased organic matter input and reduced ventilation. The remainder of the Pleistocene shows lower nutrient supply and greater ventilation. The direct role and influence of MOW at this site requires further study. The shipboard palynological study was carried out at a very coarse resolution but, as for other sites drilled, shows dominance of the four main plant ecological groups that characterize this region, *Pinus*, Mediterranean forest, semidesert, and grasslands.

Magnetostratigraphy proved difficult to resolve closely, in part because of coring disturbance and in part because of the presence of hiatuses at or near critical polarity transitions. The upper 230 m of section is within the Brunhes Chron, but the deeper section requires more detailed shore-based study to resolve. Strong peaks in magnetic susceptibility in these cores appear to correlate with large amounts of diagenetic iron sulfides (presumably including greigite and pyrrhotite).

As was observed at the other sites drilled during Expedition 339, physical property data show relatively close tracking of magnetic susceptibility and bulk density in much but not all of the section. These may correlate or anticorrelate with NGR values and color reflectance ( $L^*$  and  $a^*$  values). Both larger scale trends and smaller scale cycles are evident, with some correlation at the small scale with lithology.

The pore water profiles at Site U1390 show significantly higher concentrations of many elements, including Na, Cl, Ca, Mg, Sr, and  $\text{NH}_4$ , than at any of the other sites

drilled to this point, including Site U1389, where the values reached a distinct maximum at ~530 mbsf. However, the high chloride and sodium concentrations are associated with low  $\delta D$  values, which indicates that high salinity may not be the result of in situ salt dissolution. Instead, we suggest that salts were dissolved at depth by pore waters that had been altered by clay mineral dehydration reactions, which can also affect water sodium concentration.

Downhole measurements were made in Hole U1390A to 350 mbsf with good quality data obtained as a result of good hole conditions, especially in the upper 270 m. There is a distinct change in log characteristics at ~290 mbsf, which correlates closely with the lithologic boundary between subunits and the change downhole to a more sand-rich lithology. Distinct cyclicity is apparent in some parts of the section, corresponding with both lithologic and physical property data. This will require further study to unravel. Nine downhole temperature measurements were made in the uppermost 110 m of section, indicating a geothermal gradient of 32.0°C/km.

## Highlights

At Site U1390, we penetrated a short but very interesting section to a total depth of 350 mbsf. The site lies under the influence of ML close to the Guadalquivir contourite channel and shows very high rates of sedimentation in both the sand-rich and mud-rich sections. With maximum rates of 85 cm/k.y., and perhaps in excess of 100 cm/k.y., these are the highest known rates for contourite drifts anywhere. As a result, some of the contourite muds retain a distinctive lamination, albeit discontinuous in character, whereas the thicker sands are especially clean and well sorted. Two important hiatuses at ~0.4 and ~0.9 Ma reflect episodes of enhanced bottom-current flow, in part related to tectonic adjustment of the local topography. Significantly, these hiatuses are correlative across the Cádiz CDS on the basis of seismic stratigraphy and are recognized as more minor events at the other sites.

## Site U1391

Site U1391 is located on the southwest Iberian margin (37°21.532'N; 9°24.656'W) ~50 km northwest of Cape São Vicente in a water depth of 1085 mbsl (Fig. F1). This site is the most distal of the drilled sites under the influence of MOW and lies on the broad, gently inclined middle-slope region of the southwest Portuguese margin, on which the seismic data indicate an extensive plastered drift that stretches alongslope for ~90 km between the São Vicente and Setubal downslope-oriented submarine canyons.



We consider this plastered drift as part of the larger Cádiz CDS. On seismic profiles it shows a well-layered internal acoustic structure with laterally extensive, mainly aggradational seismic depositional units and gentle thickening of the Quaternary succession toward the axial region of the drift (Fig. F21). Deeper within the section is one or more unconformities apparent in the seismic profiles and potentially related to recent tectonic activity. There is no separate designation of MU and ML along the Portuguese margin, although in terms of water depth, Site U1391 would be closer to ML.

Our primary objective at this site was to recover a Pliocene, Pleistocene, and Holocene sedimentary succession formed under the influence of MOW and to compare this record with that found at sites within the Gulf of Cádiz that are closer to the Strait of Gibraltar gateway. Very little is known about contourite deposition along this margin, so all data will be new and significant in this regard. The record at this site will also provide a direct comparison with hemipelagic sedimentation at Site U1385, which is removed from contourite input and under the influence of NADW.

Site U1391 was occupied on 8 January. Three holes were drilled and cored using the APC, XCB, and RCB systems, achieving a total depth of 672 mbsf in the third hole (U1391C). Downhole logging was carried out in Hole U1391C using the triple combo and FMS-sonic tool strings. Overall recovery for Site U1391 was 359 m (105%) with the APC, 331 m (91%) with the XCB, and 269 m (81%) with the RCB. The total cored interval for Site U1391 was 1038.1 m and total recovery was 958.6 m (92%).

## Main results

The sedimentary succession at Site U1391 extends for 672 m from the mid-Pliocene to Holocene (Fig. F22) and is represented by a thick, very uniform series of mud-rich contouritic sediment, with rapid rates of sedimentation through the later Quaternary. The succession has been divided into two lithologic units (I and II), both of which are dominated by calcareous mud-rich contourite deposition with more minor lithologies including silty mud, sandy mud, nannofossil mud, and biosiliceous mud. Bioclastic silty sand is rare. These lithologies are generally organized as bi-gradational sequences and partial sequences with bioturbated and gradational upper and lower contacts. Carbonate content ranges from 17.5 to 48 wt%, and total organic carbon ranges from 0.5 to 1.8 wt%.

Unit I is divided into Subunit IA, which has a greater number of silty (and sandy) intervals as well as distinct alternation of greenish and reddish units. Subunit IB is even more mud rich with mainly greenish gray to dark greenish gray color cyclicity. The



Unit I/II boundary occurs at a possible minor hiatus, below which there is a slightly more mixed system, including the base of a debrite, some minor faulting (slump unit?), more biosiliceous material, and a 50 cm thick well-cemented dolomitic mudstone below a probable second minor unconformity. The mud-rich sediments in Unit II have an intermediate contourite-hemipelagite aspect.

Calcareous microfossils (nannofossils, planktonic and benthic foraminifers, and ostracods) are mostly common to abundant with moderate to good preservation throughout. The sedimentary record appears to be relatively continuous through the Quaternary period, with an average sedimentation rate of 27 cm/k.y. for the later Pleistocene and 17 cm/k.y. for the early Pleistocene. However, there may be minor hiatuses present at ~0.7–0.9 and 2.41–2.5 Ma. The average sedimentation rate for the Pliocene section recovered is 13 cm/k.y., although there is also evidence for a minor hiatus at 3.0–3.19 Ma or, alternatively, for much reduced rates of sedimentation at this time.

As found at the other CDS sites, distinctive variability in benthic foraminifer assemblages reveals significant environmental changes through the Pliocene–Holocene succession. In general, the later Quaternary shows typical upper bathyal assemblages that are indicative of increased organic matter input and reduced ventilation. This signature is also evident during some earlier intervals. The remainder of the Quaternary and Pliocene succession shows lower nutrient supply and improved or variable ventilation. Certain signature taxa show somewhat lesser influence of MOW on the Portuguese margin than in the Gulf of Cádiz. Although nannofossils show common reworking in parts of the succession, it is less evident in general than at the Cádiz sites, and there is no evident reworking of planktonic foraminifers. Pollen and spores are abundant in most of the samples analyzed, together with microcharcoal and dinocysts. They show a similar assemblage and pattern to that found at the other drilled sites.

Paleomagnetic measurements indicate that the Brunhes–Matuyama polarity transition (0.781 Ma) occurs below 175 mbsf but is not clear, perhaps because of the inferred hiatus across this boundary. Specific identification of the top and bottom of the Olduvai Subchron (1.778 and 1.945 Ma, respectively) and the Matuyama–Gauss transition (2.581 Ma) was made. These give reliable confirmation of the biostratigraphic dating for Site U1391, although some of the inferred polarity boundaries need further confirmation.

As observed at the other drilled sites, physical property data show relatively close tracking of magnetic susceptibility and bulk density in much but not all of the section. These may correlate or anticorrelate with NGR values and color reflectance ( $L^*$  and  $a^*$  values). Both larger scale trends and smaller scale cycles are evident, with some correlation at the small scale with lithology. In lithologic Unit II, much lower NGR variability and very low magnetic susceptibility values are apparent.

The pore water profile at Site U1391 shows some significant distinction from that of Site U1385, commensurate with the deposition under MOW rather than NADW. Rates of sedimentation and hence of organic matter accumulation are greater at Site U1391, which makes for a shallower zone of sulfate reduction.

Downhole measurements were made in Hole U1391C to 668 mbsf, almost the bottom of the hole. The borehole was very rugose with many narrow washouts that affected log quality. Minor changes in log characteristics occur at ~562 mbsf, which correlates closely with a lithologic boundary. The deeper interval has generally lower NGR values and includes two zones with poor core recovery that may be more sand rich on the basis of borehole logs, although no sands were recovered by coring. Distinct cyclicity is apparent in some parts of the section, corresponding to both lithologic and physical property data. Ten downhole temperature measurements were made in the uppermost 146 m of the hole, indicating a geothermal gradient of 14.2°C/km, the lowest of this expedition.

The three holes cored provide a complete composite stratigraphic section to the base of the APC interval at 171 mbsf and a virtually complete section all the way to 354 mbsf. The section below this was cored only in Hole U1391C to a total depth of 671.5 mbsf, with some short gaps between cores and larger gaps in the few instances where core recovery was low. This will be very beneficial for all subsequent paleoceanographic studies.

## Highlights

We recovered core to a total depth of 672 mbsf at Site U1391 on the southwest Portuguese margin. The site lies under the influence of ML and penetrates through a relatively complete Quaternary and late Pliocene section of a plastered contourite drift. This is the most distal of our MOW sites and is distinctly more mud rich throughout than those in the Gulf of Cádiz. Nevertheless, sedimentation rates (27 cm/k.y.) for the later Quaternary are as high as those of the Faro Drift, and the contouritic signature of uniformity and bi-gradational sequences is ever present. Important similarities

with other sites include an uphole increase in sedimentation rate, the number of silt/sand intervals, and organic matter supply, as well as reduced ventilation uphole. These all support enhanced MOW influence through the Quaternary. Hiatuses, possible hiatuses, or much reduced sedimentation rates are noted at ~0.7–0.9, 2.4–2.5, and 3.0–3.2 Ma, all of which are recognized at one or more of the Cádiz sites. These are interpreted as episodes of enhanced MOW and bottom-current activity.

## **Expedition synthesis**

Expedition 339 drilled five sites in the Gulf of Cádiz and two sites off the west Iberian margin from November 2011 to January 2012 (Fig. [F23](#)). In total, we recovered nearly 5.5 km of core, with an average recovery of 86.4%, from a region never before drilled for scientific purposes. The Gulf of Cádiz represents a key location for the investigation of MOW through the Strait of Gibraltar gateway and its influence on global circulation and climate and is a prime area for understanding the effects of tectonic activity on evolution of the Strait of Gibraltar gateway and on margin sedimentation. The Gulf of Cádiz has also become known as the world's premier contourite laboratory in which to thoroughly investigate and challenge existing models of contourite sedimentation.

Extensive previous work, both onshore and offshore and including seismic surveys for oil company exploration, has allowed us to develop a good regional understanding. Most importantly, we have been able to establish a firm seismic stratigraphic framework into which we could fit the ages of key seismic reflectors as determined by the drilling results from this expedition.

The principal results of Expedition 339 can be summarized as follows.

## **Mediterranean Outflow Water onset and evolution**

We penetrated the Miocene at two different sites and established the strong signal of MOW in the sedimentary record of the Gulf of Cádiz following opening of the Strait of Gibraltar gateway at 5.3 Ma. Our present documentation shows clear contourites in the record from ~4.2 to 4.5 Ma. However, MOW was not well developed at this stage and the signal is relatively weak. Additional seismic evidence for sheeted drift development exists in the early Pliocene. The contourite signal is also mixed with considerable downslope resedimentation and hiatuses in the record. Further work

will establish how far back in time we can extend the onset of contourite sedimentation.

The Pliocene succession was penetrated at four sites, all of which show relatively low bottom-current activity linked with a generally weak MOW, with some evidence for a slow increase in activity through the later Pliocene. Significant unconformities are apparent at ~3.0–3.2 and 2.1–2.4 Ma to a variable extent at different sites. We interpret these as indicative of enhanced bottom currents related to intensified MOW, the principal phase occurring from ~2.4 Ma.

In general, the Quaternary succession shows a much more pronounced phase of contourite deposition and drift development throughout the region. Although there is some variation between sites, we recognize two periods of current intensification, noted by increased sandy and silty contourites in the sedimentary record. The first is from ~2.0 to 0.9 Ma and culminates in a regional hiatus of variable duration (~0.7–0.9 m.y.). The second is from 0.9 Ma to the present; this also includes a more locally developed hiatus at ~0.4 Ma.

In part, there is an important climate control on this long-period cyclicity in the development of MOW and bottom-current activity. Another part is tectonic (see below).

## **Tectonic pulse at a plate boundary**

Regionally, there appears to be very strong tectonic control on margin development, downslope sediment transport, and contourite drift evolution. From the occurrence, nature, and disposition of the sedimentary record, as well as from the known timing of closure and opening of the Atlantic-Mediterranean gateways, we recognize a clear signal of this tectonic activity.

We have established a clear signal of tectonic pulsing over the past 6 m.y. in this region that has controlled

1. Closure of Atlantic-Mediterranean connections in Spain and Morocco,
2. Initial opening of the Strait of Gibraltar gateway and probable subsequent deepening,
3. Continental margin instability and episodes of active downslope resedimentation,
4. Basin subsidence in the Gulf of Cádiz,
5. Local uplift and diapiric intrusion within the basin, and

6. Constriction of MOW and development of narrow core bottom currents instead of a broad tabular.

According to the timing of these different events, we propose an ~1 m.y. duration of tectonic pulsing with an overprint of larger 2.5 m.y. cycles. We further relate this tectonic pulsing to regional asthenosphere activity that is especially apparent at the plate boundary between the African and European tectonic plates.

## **Testing the contourite paradigm**

Of the 5.5 km of core recovered, at least 4.5 km is from the Cádiz CDS in the world's premier contourite laboratory. This was the ultimate testing ground for the contourite paradigm. In general, we have found the models for contourite deposition to be in very good order, contrary to recent doubts expressed in the literature. Sedimentation rates ranged from moderate (~20 cm/k.y.) to extremely high (>100 cm/k.y.).

The contourites recovered are remarkably uniform in composition and textural attributes. They have a noted absence of primary sedimentary structures and an intense continuous bioturbation throughout. They are particularly characterized by bi-gradational sequences from inverse to normal grading with a range of partial sequence types, as predicted by the models.

However, very interesting modifications are required, for example, to the detail of the sand-silt contributions and the role of sediment supply. These are very significant for future use of contourite systems in paleoceanographic studies and in hydrocarbon exploration. We have documented very interesting interactions between contourite and turbidite processes that are completely new and different from the current models.

## **Paradigm shift for oil exploration**

We have verified an enormous quantity and extensive distribution of contourite sands (and bottom-current-modified turbidite sands), and have begun to establish their detailed characteristics. Drilling at the proximal site (U1388) managed to penetrate only the uppermost 220 m of what we had interpreted as a very thick sandy contourite drift. Hole instability and collapse of these unconsolidated sands prevented further penetration. At other proximal sites (U1389 and U1390), we also encountered thick contourite sands (as thick as 10 m) within the muddy contourite drifts.

These are completely different deepwater sands than the turbidite sands that are currently dominant as deepwater oil and gas plays and are formed in different depositional settings, have different depositional architectures, and are clean and well sorted. These characteristics would provide good quality potential reservoirs when buried deeply.

In addition, the associated contourite muds are very thick, rapidly deposited, and moderately rich in organic carbon (up to 2 wt%). These could provide potential source rocks in the subsurface, as well as suitable seals in stratigraphic traps.

These new findings could herald a paradigm shift in exploration targets in deepwater settings.

## **Cracking the climate code**

At the Shackleton site (U1385), we succeeded in recovering multiple sets of a pristine Quaternary record over the past 1.4 m.y. These sets will form the basis of a detailed shore-based scientific collaboration to establish a marine reference section of Quaternary climate change for comparison with ice-core and terrestrial records. There are many years of research ahead to decode the full climatic signal from these cores.

However, we have also shown that exactly the same climate signal is evident in all the contourite drift sites at which the sedimentation rate is 3–10 times as high. This will allow even more detailed sampling, a possibly better marine archive, and a hugely important comparison with the Shackleton site for documenting the nature and variation of MOW. The comparison between the influence and effects of MOW compared with NADW (above the Shackleton site) will also be of great interest. We can be confident of identifying hiatuses where these occur in the contourite records and therefore can avoid this problem in their interpretation. At the most distal site on the Portuguese margin, for example, hiatuses were minimal, although sedimentation rates for the last 1.5 m.y. were about three times as high as those of the Shackleton site.

Preliminary work has shown a remarkable record of orbital-scale variation in bulk sediment properties at several of the drift sites, a good correlation between sites, and, significantly, a very close correlation with the same records at the Shackleton site. The climate control on contourite sedimentation is clearly significant at this scale. Further work will determine the nature of controls at the millennial scale.

## Preliminary scientific assessment

There can be no doubt that the expedition results have more than met our scientific objectives at the outset. The results are both expected in that they confirm many of our pre-expedition hypotheses and also unexpected in the wealth of new ideas and data that have arisen. We set out with five broad objectives. They have been addressed and met as follows.

*1. Understand the opening of the Strait of Gibraltar gateway and onset of MOW.*

We drilled to the Miocene at two sites, assessed the basal age of drift sedimentation caused by MOW, and evaluated the nature and effects of climate change in the patterns of drift sedimentation. We recognize clear evolution from proximal to distal sites.

*2. Determine MOW paleocirculation and global climate significance.*

We penetrated most key Miocene to recent reflectors at one or several sites and therefore have been able to date these reflectors and confirm or refine our seismic stratigraphic framework accordingly. We have been able to understand and evaluate their link to paleocirculation variation and events with respect to MOW, as well as to the sedimentary and tectonic evolution of the whole region. We recognized orbital- and millennial-scale signals in the sedimentary record, which will be evaluated through subsequent work.

*3. Establish a marine reference section of Quaternary climate change.*

We recovered a very complete record of sedimentation at the Shackleton site (U1385) dating back to ~1.4 Ma. Four holes were drilled and cored to 150 meters below seafloor (mbsf), allowing construction of two complete spliced records. Detailed sampling and subsequent study of this material will certainly increase the precision with which marine sediment records of climate change are correlated and compared with ice-core and other terrestrial records. It will also support and refine the proposals for further drilling on this margin.

*4. Identify external controls on sediment architecture of the Gulf of Cádiz and Iberian margin.*

We have established the nature of sedimentation and timing of associated hiatuses by drilling and correlation between sites. This correlation has enabled us to further refine our understanding of the stacking pattern and evolution of the Quaternary drift de-

posits and to evaluate the nature of contourite cyclicity at different scales. Further detailed work on the contourite sediments will allow us to better understand the nature of bottom current processes and contourite deposition and gain better insight into the sedimentary budget for contourite drifts. We have already established the key sources of sediment and their controls.

*5. Ascertain synsedimentary tectonic control on architecture and evolution of the CDS.*

We have been able to accurately chart the chronology of neotectonic activity in the Gulf of Cádiz and to clearly see evidence of the varied effects of this activity, both on the alongslope (contourite) depositional system and on the downslope component. The timing and local effects of diapiric activity have been established; further work will allow closer refinement and understanding of these effects and of rates of movement.

## Operations

### Port call

Expedition 339 began with the first line ashore at 0830 h, 16 November 2011, to Berth 12 in Ponta Delgada harbor on the island of São Miguel, Azores. The IODP technical crew change occurred as scheduled on 17 November, although a group of IODP personnel arrived on 18 November because of weather-related travel problems. The scientific complement joined the vessel on 18 November. Education and public relation activities were carried out on Friday and Saturday, 18–19 November, and included tours of the R/V *JOIDES Resolution* for 175 students and 15 teachers from 4 local high schools (Escola Secundária Antero de Quental-Ponta Delgada, Escola Secundária das Laranjeiras-Ponta Delgada, Escola Secundária de Lagoa-Lagoa, and Escola Secundária da Ribeira Grande-Ribeira Grande), 12 students and professors from the Universidade dos Açores, 25 students and researchers from the Centro de Vulcanologia e Avaliação de Riscos Geológicos, 20 local visitors, 9 local government representatives, the Portuguese European Consortium for Ocean Research Drilling delegate, and 6 local journalists (press).

In addition to routine resupply of consumables and offloading of returning freight, the ship was loaded with ~600 MT of marine gasoil 60 ST of sepiolite, and 20 ST of barite drilling mud. Just prior to concluding the port call in Ponta Delgada, the home port of registry for the *JOIDES Resolution* was changed from Monrovia, Liberia, to Li-



massol, Cyprus. The port call concluded when the last line was released at 0800 h, 22 November.

## Site U1385

We arrived at Site U1385 (proposed Site SHACK-04A) at 0400 h Universal Time Coordinated (UTC), 25 November 2011, after a 68 h, 741 nmi journey from Ponta Delgada. Five holes were cored at this site using the advanced piston corer (APC) system and nonmagnetic core barrels (Table T1). Four holes were cored to ~150 mbsf and one to just 9.5 mbsf (1 core). A total of 67 cores were required to obtain 621.8 m of sediment (103.2% recovery). The advanced piston corer temperature tool (APCT-3) was deployed 12 times.

### Hole U1385A

The initial pipe trip was extended by routine measuring and “rabbiting” that occurs on the first deployment of the drill string. Following a 3 h survey of the seabed using the underwater camera system, during which no obstructions were observed, Hole U1385A was spudded with the APC at 2300 h, 25 November. Recovery of the first core established the seafloor depth at 2598 meters below rig floor (mbrf) (2587 mbsl). Piston coring with nonmagnetic core barrels advanced to a total depth of 151.1 mbsf (17 cores), which was the depth objective of the site. Total recovery in Hole U1385A was 155.9 m (103%). Cores 339-U1385A-4H through 17H were oriented with the Flexit tool. The APCT-3 was deployed to take temperature measurements at 30 (Core 4H), 58.5 (Core 7H), 87 (Core 10H), and 115.5 (Core 13H) mbsf. The APC experienced partial strokes on Cores 14H and 17H. The last core advanced only 7.7 m when the formation became firm and abruptly stopped the APC. The drill crew experienced difficulty extracting the sinker bars from the drill string prior to pulling out of the hole, requiring 4.5 h of IODP rig time to remove a deformed section of coring line before operations could resume. This involved the removal of 100 m of coring line, reheading the line, and redressing the oil saver.

### Hole U1385B

Following a vessel offset of 20 m east of Hole U1385A, operations in Hole U1385B began at 0030 h, 27 November. The water depth calculated from the recovery of the first core was 2598 mbrf (2587 mbsl). Piston coring using nonmagnetic core barrels continued to a total depth of 147.9 mbsf (16 cores). Total recovery in Hole U1385B was

150.7 m (103%). APCT-3 measurements were made at 34.6 (Core 4H), 63.1 (Core 7H), 91.6 (Core 10H), and 120.1 (Core 13H) mbsf.

### **Hole U1385C**

Hole U1385C was spudded at 1830 h, 27 November. Because the core barrel was retrieved full of sediment (9.87 m), a mudline depth could not be determined and another hole was required to obtain a good mudline core. Total recovery in Hole U1385C was 9.9 m (104%).

### **Hole U1385D**

Following a vessel offset of 20 m south, Hole U1385D was spudded at 2045 h. The first core established a seafloor depth at 2595 mbsf (2584 mbsl). Piston coring advanced without incident to a final depth of 146.4 mbsf (16 cores) with an average recovery of 105.2%. Cores were oriented starting with Core 4H. The APCT-3 was deployed at 35.4 (Core 4H), 60.9 (Core 7H), 89.4 (Core 10H), and 117.9 (Core 13H) mbsf. Cores 15H and 16H were partial strokes and advanced by recovery. All cores were obtained with nonmagnetic core barrels. The bit cleared the seafloor at 1255 h, 28 November.

### **Hole U1385E**

After a vessel offset of 20 m west of Hole U1385D, piston coring in the last hole at Site U1385 began at 1520 h, 28 November, using nonmagnetic core barrels. Seventeen cores were taken to the total depth of 148.7 mbsf by 0730 h, 29 November. We recovered 151.3 m of sediment (102%). Cores were oriented starting with Core 5H. The last three cores (Cores 15H through 17H) were partial strokes and advanced by recovery. Two cores were intentionally repositioned (Core 8H and 10H) to maintain an offset relative to the previous holes on this site. All cores were obtained with nonmagnetic core barrels. This hole concluded operations at this site.

The drill string was recovered and the bit cleared the seafloor at 0850 h. Once the drilling equipment was secured and the beacon recovered, the vessel departed for the next site at 1515 h, 29 November. Total time on site was 4.5 days.

## **Site U1386**

After a 150 nmi transit from Site U1385, the *JOIDES Resolution*, arrived at Site U1386 (proposed Site GC-01A; 560.4 mbsl) at 0415 h, 30 November 2011. We deployed the camera system and conducted a ~2 h survey of the seabed on a 30 m grid pattern to ensure that the seafloor was free of man-made obstructions. No obstructions were ob-

served on the seafloor, but many shallow linear furrows were seen that were assumed to be the result of fishing trawls.

Three holes were drilled at Site U1386 (Table T1). Hole U1386A was cored using the APC system to 183.1 mbsf and then cored with the extended core barrel (XCB) system to 349.3 mbsf. Similarly, Hole U1386B was cored with the APC to 162.3 mbsf and then with the XCB to 464.9 mbsf. Hole U1386C was drilled to 405 mbsf and then cored using the rotary core barrel (RCB) system to the target depth of 526 mbsf. Two cores were taken in the initial drilled interval (Core 339-U1386C-2R, 165–174.6 mbsf, 40% recovery; Core 4R, 205–214.6 mbsf, 93% recovery) to try to fill in short gaps in APC cores recovered from Holes U1386A and U1386B. Downhole logging was carried out in Hole U1386C using the triple combination (triple combo), Formation MicroScanner (FMS)-sonic, and Versatile Sonic Imager (VSI) tool strings (see “[Downhole logging at Site U1386](#)”). Overall recovery at Site U1386 was 351 m (101.62%) with the APC, 417.63 m (89.1%) with the XCB, and 82 m (58.5%) with the RCB. The total cored interval for Site U1386 was 954.4 m, and total recovery was 850.64 m (89.1%).

### Hole U1386A

Once the camera system was recovered at 1255 h, 30 November, we began piston coring in Hole U1386A. APC coring continued to refusal at 183.1 mbsf (Cores 1H through 21H). Recovery for this interval was 101%. Temperature measurements were obtained at 32.3 (Core 4H), 60.8 (Core 7H), 89.3 (Core 10H), 117.8 (Core 13H), 114.0 (Core 16H), and 167.2 (Core 19H) mbsf. Cores were oriented starting with Core 4H. The corer was advanced by recovery on Cores 16H to 19H and 21H. Nonmagnetic hardware was used on all cores. At 183.1 mbsf, the coring system was switched to the XCB and coring continued to a total depth of 349.3 mbsf (Cores 22X through 39X) by 0415 h, 2 December. The 166.2 m interval was cored with a recovery of 97%. The total recovery in Hole U1386A was 346.2 m, which represented 99% of the cored interval. The bit cleared the seafloor at 0620 h, 2 December, and the vessel offset 20 m east of Hole U1386A.

### Hole U1386B

Piston coring in Hole U1386B began at 0825 h, 2 December, and advanced to an APC refusal depth of 162.3 mbsf (Cores 1H through 18H). Recovery for the APC interval was 100%. The calculated water depth from the recovery of the first core was 562 mbsl. Temperature measurements using the APCT-3 were taken at 16.8 (Core 2H), 45.3 (Core 5H), 73.8 (Core 8H), 102.8 (Core 11H), 130.8 (Core 14H), and 157.6 (Core

17H) mbsf. The cores were oriented starting with Core 3H. There were partial strokes with Cores 15H, 16H, and 18H. Nonmagnetic hardware was used to obtain all cores. At 2200 h, 2 December, the coring system was switched to XCB and coring continued to 455.4 mbsf (Cores 19X through 49X), where XCB refusal was reached. Recovery for the XCB interval was 293.5 m (100%).

### **Hole U1386C**

The third hole of Site U1386 was offset 20 m south of Hole U1386B and spudded with the RCB at 0345 h, 5 December. This hole was drilled with a wash barrel to 405 mbsf, except for RCB coring of two intervals that eluded recovery in the two previous XCB holes (Cores 2R and 4R from 165.0–174.6 and 205.0–214.6 mbsf, respectively). Continuous RCB coring started at 405 mbsf at 0545 h, 6 December, and reached the depth objective of 526 mbsf by 0200 h, 7 December. The RCB interval (140 m) recovered 59%. The drilled interval was 386 m. The total cored interval for all holes at this site was 954 m with a recovery of 89% (104 cores).

### **Downhole logging at Site U1386**

Following a wiper trip and hole conditioning, Hole U1386C was displaced with 172 bbl of 10.5 ppg mud to prepare the hole for downhole logging. The open end of the pipe was placed at a logging depth of 102.4 mbsf. During rig up of the wireline cable, the cable jumped from the lower left most sheave wheel in the wireline heave compensator and became jammed between the wheel and the frame. Because of the possibility of damage to the cable, it was cut above the crimped section.

The triple combo tool string descended through the seafloor at 2003 h and was successful in reaching the bottom of the hole (526 mbsf). The tool string was back on deck by 0100 h, 8 December. Subsequently, the FMS-sonic tool suite was run into the hole at 0410 h. The tool suite was blocked from further downhole progress by a bridge at 948 mbrf (375 mbsf), the lowermost of the tight sections observed in the triple combo run. Rig down of the FMS-sonic tool string was completed by 0930 h, 8 December.

The marine mammal watch for conducting the vertical seismic profile (VSP) experiment started at 0800 h, 8 December. The VSI tool started its descent in Hole U1386C at ~1030 h and reached a bridge at 940 mbrf (367 mbsf) at 1105 h. The slightly shallower penetration for this tool run indicated that the hole was closing with time. The seismic source (two-gun cluster; 7 mbsl on the port side) had been ramped up in soft start mode. It was difficult to get a good clamp with the VSI, and consequently noisy

waveforms were obtained that were attributed to the rugose borehole and soft formation. Only a fraction of the shots produced clean first arrivals, but there were enough at most stations to stack. The upper part of the hole was especially difficult. The tool was back on deck at 1440 h and rigged down by 1530 h, 8 December. The drill string was recovered and the vessel departed for the next site at 1730 h, 8 December. Total time at Site U1386 was 8.6 days.

## Site U1387

The vessel was offset in dynamic position mode 2.2 nmi on a bearing of 128° to Site U1387 (proposed Site GC-09A). During this move, accomplished in 3 h, maintenance was performed on the 480 V switchboard, which required shutting down the regulated power from 1800 to 1845 h. The vessel was positioning on Site U1387 at 2030 h, 8 December 2011.

Three holes were drilled at Site U1387 (Table [T1](#)). Hole U1387A was cored using the APC to 47.7 mbsf and then with the XCB to 352.4 mbsf. Hole U1387B was cored with the APC to 46.9 mbsf and then with the XCB to 338.3 mbsf. Hole U1387C was drilled without coring to 290 mbsf and then cored using the RCB to the target depth of 870 mbsf. Downhole logging was carried out in Hole U1387C using the triple combo, FMS-sonic, and VSI tool strings (see [“Downhole logging at Site U1387”](#)). Overall recovery at Site U1387 was 97.03 m (102.6% recovery) with the APC, 578.42 m (97% recovery) with the XCB, and 409.5 m (70.6% recovery) with the RCB. The total cored interval at Site U1387 was 1270.7 m, and total recovery was 1084.95 m (85.4%).

### Hole U1387A

Prior to spudding Hole U1387A, a 2 h underwater camera survey of the seafloor was made during which many linear furrows on the seabed were observed. These furrows were presumed to be the result of fishing bottom trawls. The vessel had to be offset 10 m from the original position to avoid spudding into what appeared to be man-made debris (a spiral of loose wire or cable). Hole U1387A was spudded with the APC at 0325 h, 9 December. Seafloor depth calculated from the recovery of the first core was established at 570.5 mbrf (559.1 mbsl). APC coring advanced to 47.7 mbsf, where very sticky, firm clay prevented further progress. The APC cored 47.7 m and recovered 48.83 m (102.4% recovery). Cores 339-U1387A-4H through 6H were oriented. The APCT-3 tool was deployed on Core 4H (33.9 mbsf). Nonmagnetic core barrels were used to obtain all piston cores. XCB coring was initiated at 0915 h, 9 December, and deepened Hole U1387A from 47.7 mbsf to a final depth of 352.4 mbsf by 0545 h, 10

December. The XCB system cored 304.7 m with a 98.1% recovery. The total cored interval in Hole U1387A was 352.4 m, with a recovery of 98.7%.

### **Hole U1387B**

The bit was pulled clear of the seafloor at 0715 h, 10 December, and the vessel offset 20 m east of Hole U1387A. The underwater camera was deployed to ensure no man-made debris was present on the seafloor prior to coring. Hole U1387B was spudded with the APC at 1050 h and established a water depth of 569.6 mbrf (558.2 mbsl). Piston coring advanced to 46.9 mbsf (102.8% recovery) before switching to the XCB. Cores 3H through 5H were oriented. All cores were obtained with nonmagnetic core barrels.

XCB coring deepened Hole U1387B to a final depth of 338.3 mbsf. The average recovery for the XCB cored interval of 291.4 m was 95.9%. APC/XCB coring recovered 96.8% of the cored interval in Hole U1387B (338.3 m). Coring was terminated prior to the depth objective of 350 mbsf because the quality of the cores was compromised because of biscuiting disturbance, discovered when the deeper cores in Hole U1387A were examined in the ship's core laboratory.

### **Hole U1387C**

The drill string was recovered with the bit clearing the rotary table at 1305 h, 11 December. After the nonmagnetic drill collar and seal bore drill collar were laid out along with the APC/XCB polycrystalline diamond bit, a four-stand RCB bottom-hole assembly (BHA) with a new CC-3 Rock Bit International bit was made up and deployed along with the underwater camera. Once the video images provided by the underwater camera confirmed that the seafloor was clear of obstructions, the driller tagged the seabed with the RCB bit at 569.8 mbrf (558.4 mbsl) at 1640 h, 11 December. Following retrieval of the camera, Hole U1387C was spudded with the RCB at 1850 h. The hole was drilled with a wash barrel in place to 290.0 mbsf, where continuous RCB coring was initiated.

Rotary coring proceeded without incident to a final depth of 870 mbsf by 0930 h, 16 December. A total of 580 m was cored in Hole U1387C with an average recovery of 70.6%. The average rate of penetration for the cored interval was 11.6 m/h. The drilled portion of the hole was 290 m and the total penetration (cored plus drilled) was 870 m. While penetrating the cored interval, the drillers pumped eleven 20 bbl and two 30 bbl high-viscosity mud flushes to keep the hole clean of cuttings.

## Downhole logging at Site U1387

After a wiper trip and hole conditioning, the bit was dropped at the bottom of Hole U1387C and the hole was displaced with 290 bbl of 10.5 ppg mud. The end of the pipe was positioned at 103.8 mbsf. During the wiper trip, the driller had to pick up the top drive and wash and ream a tight portion of the hole (ledge or bridge) from 649.0 to 653.0 mbsf. There was 28 m of soft fill at the bottom of the hole that was flushed clean with a 50 bbl Hi-Vis sweep.

The triple combo tool string was made up and deployed at 0230 h, 17 December. The tool could not advance past 650 mbsf; therefore, the hole was logged from that point. The triple combo tool string was recovered at 0835 h. The VSI tool was run in the pipe at 1105 h. This tool could not be lowered deeper than 254 mbsf. The Marine Mammal Protocol was observed while conducting the VSP experiment. The VSI tool was recovered at 1420 h. The last log was made with the FMS-sonic tool string, which was deployed at 1610 h and could not go deeper than 334 mbsf. The FMS-sonic tool string was recovered and disassembled by 2300 h. The end of the pipe was pulled clear of the seafloor at 2355 h, and the drill string was recovered. The drilling equipment was secured and the vessel departed for Site U1388 at 0230 h, 18 December. Total time on site was 9.3 days.

## Site U1388

The 55 nmi transit from Site U1387 to Site U1388 (proposed Site GC-04D) was accomplished in ~5 h at an average speed of 11 kt. At 0745 h, 18 December 2011, the vessel was positioned on the new location.

The operations plan for Site U1388 called for APC/XCB/RCB coring in three holes and conducting downhole logging operations in Holes U1388B and U1388C. The first two holes were to be cored with the APC to refusal and then with the XCB to ~350 mbsf. The third hole was to be cored with the RCB from 350 to 1300 mbsf. Ultimately, three holes were drilled (Table T1), but the coring objectives were not achieved because of hardware failure caused by a difficult sandy formation. In Hole U1388A, APC Core 339-U1388A-1H advanced only 3.4 m (recovery of 107.6%) because a thick sand layer at the sediment surface prevented the core from penetrating any further. Hole U1388B was cored using the XCB to 225.7 mbsf with recovery of 47.2%. Hole U1388C was drilled without coring to 205 mbsf and then cored using the RCB to 229 mbsf. Overall recovery at Site U1388 was 120.54 m (47.6%): 3.64 m (107.6% recovery) with



the APC, 106.54 m (97% recovery) with the XCB, and 10.36 m (43.17% recovery) with the RCB. The site was terminated earlier than planned because of formation instability.

### **Hole U1388A**

An APC/XCB BHA with a 9 $\frac{7}{8}$  inch polycrystalline diamond bit, lockable float valve, seal bore drill collar, and nonmagnetic drill collar was assembled and deployed. Following a 1.3 h underwater camera survey of the seafloor over a 30 m grid pattern, Hole U1388A was spudded with the APC at 1500 h. The calculated seafloor depth from the recovery of the first core was 675.1 mbrf (663.6 mbsl), which was 0.7 m deeper than the corrected depth given by the precision depth recorder. The second attempt at a piston core appeared to be an incomplete stroke. The core winch operator spent ~3 h attempting to recover the stuck core barrel. The Kinley cutter was deployed to cut the coring line above the sinker bars when it was not possible to jar off the core barrel. The only course of action remaining was to recover the drill string and extricate the core barrel on the surface. The drill string was retrieved by 2400 h, 18 December. The reason why the core barrel couldn't be recovered was obvious. Most of the BHA was full of sand that apparently "U-tubed" when the driller advanced into the formation to position the bit for the next piston core (2H).

### **Hole U1388B**

The BHA was cleared of sand and deployed to 669.9 mbrf. The vessel offset 20 m east of the previous hole. The underwater camera displayed what appeared to be man-made debris on the seafloor and precipitated another 10 m offset to the east. The strategy for the second hole of the site was to core an XCB hole to depth and use the information acquired from that pilot hole to assess if and where the APC could be deployed in subsequent holes. The driller tagged seafloor at 674.4 mbrf (662.9 mbsl) at 0645 h. The camera system was recovered, and the top drive was picked up. Hole U1388B was spudded with the XCB at 0835 h, 19 December, and advanced to 225.7 mbsf by 0745 h, 20 December. While coring this interval, there was extensive cutting shoe damage suggesting that the distribution of fluid flow between the cutting shoe and the polycrystalline diamond bit was not optimum for this formation. Rather than continue coring in this fashion and considering that the objectives of this site were deeper in the formation, XCB coring was terminated at 225.7 mbsf. The average recovery for this hole was 47.2%. The driller pumped a 5 bbl slug of heavy mud prior to making a connection for Cores 1X through 12X (110.9 mbsf) to avoid a recurrence of the sand backflowing into the BHA. A 20 bbl sepiolite flush was made at



216.1 mbsf. The drill string was pulled clear of the seafloor at 0925 h and on deck at 1155 h, 20 December.

### Hole U1388C

A four-stand RCB BHA with a new CC-4 Rock Bit International bit and mechanical bit release was made up and run in to 668.0 mbrf. After a short underwater camera survey confirmed that the location of the hole was clear of debris, the driller tagged the seafloor at 674.0 mbrf (662.5 mbsl). The underwater camera was recovered, the top drive was picked up, and Hole U1388C was spudded with the RCB at 1915 h, 20 December. The hole was washed to 205.0 mbsf, where rotary coring was initiated. At 119.8 and 167.6 mbsf, 20 bbl Hi-Vis mud sweeps were circulated. Rotary coring advanced from 205.0 to 229.0 mbsf, where the drill string became firmly stuck in the formation. There was no rotation and limited circulation. It required 1.5 h to free the pipe utilizing overpulls of as much as 120,000 lb and adjusting rotary current limits as high as 1050 A. Once the pipe came free, more mud (both Hi-Vis and 10.5 ppg) was pumped to clear out some of the sand that had collapsed on the BHA. The drill string was pulled free of the seafloor at 1330 h and on deck by 1725 h, 21 December. The formation was considered too unstable to safely core and the decision was made to move on to the next planned site of the expedition. Total time at Site U1388 was 3.2 days, which was 10 days less than the allotted time. The vessel departed for Site U1389 at 1730 h, 21 December.

### Site U1389

The vessel departed for Site U1389 (proposed Site GC-11A) at 1730 h, 21 December 2011. The 25 nmi journey from Site U1388 was accomplished in 2.5 h, and the *JOIDES Resolution* was positioned on the new site by 2000 h, 21 December.

Four holes were drilled at Site U1389 (Table [T1](#)). Hole U1389A was cored using the APC to 97.2 mbsf and then with the XCB to 354.9 mbsf. Only one piston core (9.5 m) was taken in Hole U1389B. Hole U1389C was cored with the APC to 95 mbsf and then with the XCB to 350 mbsf. Hole U1389D was cored with the APC to 94 mbsf to provide an additional record of the upper section at the site. Hole U1389E was drilled without coring to 335 mbsf and then cored using the RCB to the depth objective of 990 mbsf. Downhole logging was carried out in Holes U1389A and U1389E using the triple combo and FMS-sonic tool strings (see [“Downhole logging at Site U1389”](#)). Overall recovery at Site U1389 was 307.28 m (103.55%) with the APC, 463.93 m (90.49% recovery) with the XCB, and 352.28 m (53.78% recovery) with the RCB. The

total cored interval at Site U1389 was 1463.4 m and total recovery was 1123.49 m (76.8%).

### **Hole U1389A**

The APC/XCB BHA was assembled and deployed to 651.7 mbrf. Subsequent to a 1.3 h survey of the seafloor, Hole U1389A was spudded with the APC at 0240 h, 22 December. The water depth calculated from the recovery of the first core established the seafloor at 656.2 mbrf (644.7 mbsl). This was 1.3 m shallower than the corrected precision depth recorder depth.

Piston coring advanced Hole U1389A to the refusal depth of 99 mbsf. The average recovery for this interval was 103%. Core orientation started with Core 339-U1389A-4H. Three APCT-3 measurements were made at 33 (Core 4H), 61 (Core 7H), and 90 (Core 10H) mbsf. Nonmagnetic core barrels were utilized on all cores. XCB coring deepened the hole to a final depth of 357 mbsf by 1415 h, 23 December. The average recovery for the 258 m XCB interval of the hole was 91%. The total average recovery for the entire hole was 94%.

### **Holes U1389B and U1389C**

Hole U1389B was spudded at 2010 h, but the full core barrel could not be used to ascertain the seafloor depth. Hole U1389C was spudded with the APC at 2025 h and established the seafloor depth at 654.5 mbrf (643 mbsl). Piston coring advanced to 95 mbsf. Cores were oriented starting with Core 3H. The APCT-3 was deployed at 19 (Core 2H), 47.5 (Core 5H), and 76 (Core 8H) mbsf. All cores were obtained with non-magnetic core barrels. Coring continued in Hole U1389C with the XCB, which reached the depth objective of 350 mbsf at 0815 h, 26 December. Recovery for the 255 m XCB interval of the hole was 90%. The total recovery for both coring systems for Hole U1389C was 94%. The bit was pulled free of the seafloor at 1000 h, 26 December, and the vessel offset 20 m south of the previous hole.

### **Holes U1389D**

An additional hole was piston cored to obtain a complete section of the uppermost ~100 m portion of the sedimentary record at Site U1389. Hole U1389D was spudded with the APC at 1120 h, and the water depth was established at 655.5 mbrf (644 mbsl). Piston coring advanced without incident to the depth objective of 94 mbsf by 1845 h. Recovery was 104%. The cores were oriented starting with Core 3H. Three

APCT-3 measurements were made at 24.5 (Core 3H), 53 (Core 6H), and 75 (Core 9H) mbsf. All cores were obtained with the nonmagnetic core barrels.

### **Holes U1389E**

The drill string was recovered, and the bit cleared the rotary table at 2220 h, 26 December. The vessel offset 20 m west. A four-stand RCB BHA was made up and deployed. After the driller tagged the seafloor at 655 mbrf (643.5 mbsl), Hole U1389E was spudded with the RCB at 0240 h, 27 December. We drilled without coring to 355 mbsf, where continuous rotary coring was initiated at 1830 h, 27 December. Rotary coring continued until 0845 h, 1 January 2012, when the hole was terminated at the depth objective of 989.9 mbsf. A total of 654.9 m was cored with a recovery of 54%.

### **Downhole logging at Site U1389**

On 23 and 24 December, we carried out downhole logging operations in Hole U1389A. During preparations for logging, the wiper trip found only 1 m of soft fill at the bottom of the hole, and the hole was filled with 112 bbl of 10.5 ppg mud. The open end of the pipe was placed at a logging depth of 85.7 mbsf. The triple combo tool string, composed of the natural gamma radiation, density, and resistivity tools, descended through the seafloor at 2300 h, 23 December, and was run to the bottom of the hole at 1011 mbrf (355 mbsf). A short pass of 75 m was followed by a main pass up to the seabed. Sand-rich layers are apparent by their low gamma radiation signature. The hole was mostly in gauge but had several meter-scale washouts. The tool string was back on deck by 0140 h.

The FMS-sonic reached the bottom of the hole and made two passes, recording resistivity images of the borehole, sonic velocities, and natural gamma radiation data over the entire interval. The tool string was back on deck at 0950 h. The VSI tool was run to conduct the VSP experiment. Marine mammal watch started at ~1100 h, 24 December. The air guns (two-gun cluster, 7 mbsl on the port side) were ramped up in a soft start procedure. The VSI tool started its descent in Hole U1389A at 1145 h and reached the bottom of the hole. Ten out of eleven stations recorded good sonic waveforms. Stations were spaced at ~25 m intervals, and the survey itself lasted from 1300 to 1500 h. The tool string was back on deck at 1630 h, and logging equipment was rigged down by 1715 h. At 1755 h, 24 December, the bit cleared the seafloor and the vessel offset 20 m east of Hole U1389A.

After coring operations had finalized at Hole U1389E, a wiper trip was conducted to condition the hole in preparation for downhole logging. After concluding the wiper

trip, the bit was released and the hole displaced with 375 bbl of 10.5 ppg logging mud. The end of pipe was positioned at 102.2 mbsf. The first log was made with the triple combo tool string, which was deployed shortly after 2400 h, 1 January. The tool was not able to pass a bridge or ledge at 567 mbsf. The tool was recovered at 0610 h after logging the hole up from 567 mbsf. The second logging experiment was made with the FMS-sonic tool string, which was also unable to penetrate deeper than 567 mbsf. The FMS-sonic was recovered at 1425 h after logging the upper portion of the hole.

The VSP experiment was canceled. Shortly after arriving at Site U1389, maintenance was carried out in the vessel's sea chest and bilge spaces. As part of this routine, ultrasonic thickness readings were taken on the steel plating. Evaluation of the readings indicated that some of the sea chest plating had wastage beyond acceptable limits and that several frames on the starboard side required immediate attention. Although repairs were in progress, it was felt that the sound pressure generated by the air gun during seismic profiling could subject the deteriorated sea chest to sufficiently high levels of vibration that would present a potential risk to the vessel. Therefore, VSP measurements planned for the last three sites of the expedition were canceled. The logging equipment was rigged down, the drill string was recovered, and the beacon was recalled. The vessel departed for the sixth site of the expedition at 1930 h, 2 January. Total time at Site U1389 was 12 days.

## Site U1390

The vessel departed for Site U1390, the sixth site of the expedition, at 1930 h, 2 January 2012. The 22 nmi transit from Site U1389 was covered in just over 2 h. The vessel was positioned on the new coordinates at 2145 h.

Three holes were drilled at Site U1390 (Table T1). Hole U1390A was cored using the APC to 76.7 mbsf and then with the XCB to 350 mbsf. Hole U1390B was cored with the APC to 194.1 mbsf. Hole U1390C was cored with the APC to 175.4 mbsf. Downhole logging was carried out in Hole U1390A using the triple combo and FMS-sonic tool strings (see [“Downhole logging at Site U1390”](#)). Overall recovery at Site U1390 was 437.95 m (98.2%) with the APC and 248.32 m (90.9%) with the XCB. Total cored interval at Site U1390 was 719.5 m and total recovery was 686.27 m (95.4%).

### Hole U1390A

The APC/XCB BHA and the drill string were deployed with the underwater camera. A survey of the seafloor was conducted using a 30 m grid pattern. Other than one large

rock, no significant obstructions were observed. Hole U1390A was spudded with the APC at 0520 h, 3 January. Seafloor depth was established at 1005.1 mbrf (993.4 mbsl), which was 3.1 m deeper than the corrected precision depth recorder value of 1002 mbrf. Piston coring was only able to advance to 76.7 mbsf. The decision was made to switch to the XCB when the last APC core (339-U1390A-9H) required ~3 h to extract from the core barrel. Recovery for the piston cored interval was 102%. Cores were oriented starting with Core 4H. The APCT-3 was deployed to measure temperature at 32.1 (Core 4H) and 60.6 (Core 7H) mbsf. XCB coring deepened the hole to the depth objective of 350 mbsf by 1700 h, 4 January. Recovery for the 273.3 m XCB interval was 91%. The overall recovery in Hole U1390A was 93%.

### **Hole U1390B**

With the scientific objective of “chasing” a contour line on the seismic record at the site, the vessel was offset 200 m north of Hole U1390A. The underwater camera was deployed and the seafloor monitored during the movement of the vessel. Once the vessel was on position, Hole U1390B was spudded with the APC from 1002 mbrf at 1700 h. The calculated seafloor depth was 1002.4 mbrf (990.7 mbsl). Piston coring advanced to 194.1 mbsf, where Core 21H could not be recovered with the coring line. When the orientation tool was retrieved to the surface using the coring line, it was discovered that the bulkhead lock pin between the male and female sections that connect the nonmagnetic sinker bars to the core barrel had parted in two places (possible metal fatigue). After several fishing attempts failed to grasp the female section that remained downhole with the core barrel, the BHA was recovered and the core barrel extracted at the surface. The bit was at the rotary table at 2120 h, 6 January. Piston coring recovered 189.9 m, which represented 98% of the cored interval. Cores were oriented starting with Core 3H. Temperature measurements were obtained with the APCT-3 at 18.6 (Core 2H), 47.1 (Core 5H), and 75.6 (Core 8H) mbsf. All cores were obtained with nonmagnetic core barrels.

### **Hole U1390C**

The drill string was redeployed for the second time on site and the vessel offset 20 m east of Hole U1390B. Hole U1390C was spudded with the APC at 0240 h, 7 January, and established seafloor depth at 1004.1 mbrf (992.4 mbsl). Piston coring proceeded to the depth objective of 174.5 mbsf by 2200 h, 7 January. Stuck core barrels on Cores 2H through 4H required an extra coring line round trip to pull the orientation tool before it was possible to recover the core barrel. Cores were oriented starting with Core 4H and then followed by Cores 9H through 19H (last core). APCT-3 measure-

ments were obtained at 23.4 (Core 3H), 51.9 (Core 6H), 80.4 (Core 9H), and 108.9 (Core 12H) mbsf. Nonmagnetic core barrels were used to obtain all cores. The bit was pulled free of the seafloor at 2300 h and cleared the rotary table at 0115 h, 8 January, ending operations at Site U1390. The vessel departed for the last site of the expedition at 0230 h that morning. Total time on site was 5.2 days.

### **Downhole logging at Site U1390**

Instead of logging the third hole at the site, it was decided to log Hole U1390A. The hole was subjected to the routine conditioning procedures, including a wiper trip, mud flushes, and displacement with 124 bbl of 10.5 ppg mud before the bit was placed at 96.6 mbsf. The logging program consisted of the triple combo and FMS-sonic tool strings. The triple combo tool string was deployed at 2400 h, 4 January, and recovered at 0330 h. The FMS-sonic tool string was run in at 0600 h and recovered at 1000 h, 5 January. Both tools successfully covered the open hole to 350 mbsf. After the FMS-sonic tool string was rigged down, the bit was pulled clear of the seafloor at 1155 h, 5 January.

## **Site U1391**

The 115 nmi voyage to Site U1391 (proposed Site WI-01B) was made at an average speed of 11.5 kt. The vessel was positioned on the last site of the expedition at 1230 h, 8 January 2012.

Three holes were drilled at Site U1391 (Table [T1](#)). Hole U1391A was cored using the APC to 171.1 mbsf and then with the XCB to 353.1 mbsf. Hole U1391B was cored using the APC to 171 mbsf and then with the XCB to 353.5 mbsf. Hole U1391C was drilled without recovery to 340 mbsf and then cored using the RCB to 671.5 mbsf. Downhole logging was carried out in Hole U1391C using the triple combo and FMS-sonic tool strings (see [“Downhole logging at Site U1391”](#)). Overall recovery at Site U1391 was 342.1 m (104.7% recovery) with the APC, 230.7 m (90.7% recovery) with the XCB, and 269.02 m (81.15% recovery) with the RCB. The total cored interval at Site U1391 was 1038.1 m and total recovery was 958.57 m (92.3%).

### **Hole U1391A**

The APC/XCB BHA was made up, and a routine survey of the seafloor was conducted using a 30 m grid pattern. No significant obstructions were observed. Hole U1391A was spudded with the APC at 1080.0 mbrf at 2035 h, 8 January. Seafloor depth was established at 1085.4 mbrf (1073.7 mbsl). Piston coring advanced to final depth of

171.1 mbsf with a recovery of 106%. Cores were oriented starting with Core 339-U1391A-4H. Temperature measurements were made at 32.6 (Core 4H), 61.1 (Core 7H), 89.6 (Core 10H), 118.1 (Core 13H), and 146.6 (Core 16H) mbsf. Nonmagnetic core barrels were used to obtain all piston cores. XCB coring deepened the hole to the depth objective of 353.1 mbsf by 0345 h, 10 January. Average recovery for the 182 m XCB interval was 88.8%. Combined recovery in Hole U1391A was 97%. The drill string was pulled out of the hole, clearing the seafloor at 0520 h, 10 January. The vessel was offset 20 m south of Hole U1391A.

### **Hole U1391B**

Hole U1391B was spudded with the APC at 1085 mbrf at 0815 h, 10 January. Although the mudline core was 9.65 m, the desired vertical offset (5 m deeper) with the previous hole was maintained and piston coring continued to a final depth of 171 mbsf with a recovery of 104%. Cores were oriented starting with Core 3H. Temperature measurements were made at 19 (Core 2H), 47.5 (Core 5H), 76 (Core 8H), 104.5 (Core 11H), and 133 (Core 14H) mbsf. All cores were obtained with nonmagnetic core barrels. XCB coring deepened the hole to the depth objective of 353.5 mbsf. Average recovery for the XCB interval of 182.5 m was 93%. Combined recovery for Hole U1391B was 98%. The drill string was recovered with the bit clearing the seafloor at 1350 h and the rotary table at 1850 h, 11 January. The trip out of the hole was suspended 1.5 h for the routine maintenance procedure of slipping and cutting the drilling line.

### **Hole U1391C**

A four-stand RCB BHA was made up with a new CC-4 Rock Bit International bit and mechanical bit release and deployed. After the driller tagged the seafloor at 1085 mbrf (1073.3 mbsl), Hole U1391C was spudded with the RCB at 2345 h, 11 January. The hole was drilled with a wash barrel to 340 mbsf by 1400 h, 12 January. The empty wash barrel was recovered and a fresh core barrel dropped at 1430 h when rotary coring was initiated. Rotary coring advanced to a final depth of 671.5 mbsf by 1645 h, 14 January. Recovery for the 331.5 m cored interval in Hole U1391C was 81%. Recovery percentage was adversely affected by the absence of recovery in Cores 26R, 29R, and 35R, which was assumed to be formation related. The average rate of penetration for the 331.5 m cored interval was 14.2 m/h.

### **Downhole logging at Site U1391**

Following the wiper trip, Hole U1391C was flushed with sepiolite mud and the bit was released at the bottom. The hole was displaced with 248 bbl of 10.5 ppg heavy



mud, and the end of pipe was placed at the logging depth of 98.9 mbsf. The first log of the hole was made with the triple combo tool string, which was made up of the natural gamma radiation, density, and resistivity tools and deployed at 0330 h, 15 January. The tool string succeeded in reaching 668 mbsf. The tool string was recovered and rigged down by 0815 h. The second and final log was made with the FMS-sonic tool string. The tool string reached 666 mbsf and recorded resistivity images of the borehole, sonic velocities, and natural gamma radiation data. The hole contained many thin washouts. As at previous sites, all the logs have medium-amplitude alternations on the several-meter scale. Sonic velocity, density, and resistivity all show a downhole compaction trend. Logging equipment was rigged down by 1915 h, concluding all science operations of the expedition. We departed Site U1391 at 0200 h, 16 January. Expedition 339 ended at 1342 h, 16 January, with the first line ashore in Lisbon, Portugal.



## References

- Abrantes, F., 1988. Diatom productivity peak and increased circulation during the latest Quaternary: Alboran Basin (western Mediterranean). *Mar. Micropaleontol.*, 13(1):79–96. doi:10.1016/0377-8398(88)90013-8
- Alves, T.M., Gawthorpe, R.L., Hunt, D.W., and Monteiro, J.H., 2003. Cenozoic tectono-sedimentary evolution of the western Iberian margin. *Mar. Geol.*, 195(1–4):75–108. doi:10.1016/S0025-3227(02)00683-7
- Ambar, I., and Howe, M.R., 1979. Observations of the Mediterranean Outflow—II. The deep circulation in the vicinity of the Gulf of Cádiz. *Deep-Sea Res., Part A*, 26(5):555–568. doi:10.1016/0198-0149(79)90096-7
- Argus, D.F., Gordon, R.G., DeMets, C., and Stein, S., 1989. Closure of Africa-Eurasia-North America plate motion circuit and tectonics of the Gloria fault. *J. Geophys. Res., [Solid Earth]*, 94(B5):5585–5602. doi:10.1029/JB094iB05p05585
- Baas, J.H., Mienert, J., Abrantes, F., and Prins, M.A., 1997. Late Quaternary sedimentation on the Portuguese continental margin: climate-related processes and products. *Palaeogeogr., Palaeoclimatol., Palaeoecol.*, 130(1–4):1–23. doi:10.1016/S0031-0182(96)00135-6
- Baringer, M.O., and Price, J.F., 1999. A review of the physical oceanography of the Mediterranean Outflow. *Mar. Geol.*, 155(1–2):63–82. doi:10.1016/S0025-3227(98)00141-8
- Berggren, W.A., and Hollister, C.D., 1974. Paleogeography, paleobiogeography and the history of circulation of the Atlantic Ocean. In Hay, W.W. (Ed.), *Studies in Paleooceanography*. Spec. Publ.—Soc. Econ. Paleontol. Mineral., 20:126–186.
- Bigg, G.R., Jickells, T.D., Liss, P.S., and Osborn, T.J., 2003. The role of the oceans in climate. *Int. J. Climatol.*, 23(10):1127–1159. doi:10.1002/joc.926
- Bigg, G.R., and Wadley, M.R., 2001a. Millennial-scale variability in the oceans: an ocean modelling view. *J. Quat. Sci.*, 16(4):309–319. doi:10.1002/jqs.599
- Bigg, G.R., and Wadley, M.R., 2001b. The origin and flux of icebergs released into the Last Glacial Maximum Northern Hemisphere oceans: the impact of ice-sheet topography. *J. Quat. Sci.*, 16(6):565–573. doi:10.1002/jqs.628
- Blanc, P.-L., 2002. The opening of the Plio-Quaternary Gibraltar Strait: assessing the size of a cataclysm. *Geodin. Acta*, 15(5–6):303–317. doi:10.1016/S0985-3111(02)01095-1
- Borenäs, K.M., Wåhlin, A.K., Ambar, I., and Serra, N., 2002. The Mediterranean Outflow splitting—a comparison between theoretical models and CANIGO data. *Deep-Sea Res., Part II*, 49(19):4195–4205. doi:10.1016/S0967-0645(02)00150-9
- Borges, J.F., Fitas, A.J.S., Bezzeghoud, M., and Teves-Costa, P., 2001. Seismotectonics of Portugal and its adjacent Atlantic area. *Tectonophysics*, 331(4):373–387. doi:10.1016/S0040-1951(00)00291-2
- Bryden, H.L., Candela, J., and Kinder, T.H., 1994. Exchange through the Strait of Gibraltar. *Prog. Oceanogr.*, 33(3):201–248. doi:10.1016/0079-6611(94)90028-0
- Bryden, H.L., and Stommel, H.M., 1984. Limiting processes that determine basic features of the circulation in the Mediterranean Sea. *Oceanol. Acta*, 7:289–296.
- Buitrago, J., García, C., Cajebread-Brow, J., Jiménez, A., and Martínez del Olmo, W., 2001. Contouritas: Un Excelente Almacén Casi Desconocido (Golfo de Cádiz, SO de España) [Congreso Técnico Exploración y Producción REPSOL-YPF, Madrid, 24–27 September 2001].

- Cacho, I., Grimalt, J.O., Canals, M., Sbaiffi, L., Shackleton, N.J., Schönfeld, J., and Zahn, R., 2001. Variability of the western Mediterranean Sea surface temperature during the last 25,000 years and its connection with the Northern Hemisphere climatic changes. *Paleoceanography*, 16(1):40–52. doi:10.1029/2000PA000502
- Cacho, I., Grimalt, J.O., Sierro, F.J., Shackleton, N., and Canals, M., 2000. Evidence for enhanced Mediterranean thermohaline circulation during rapid climatic coolings. *Earth Planet. Sci. Lett.*, 183(3–4):417–429. doi:10.1016/S0012-821X(00)00296-X
- Caralp, M., 1992. Paléohydrologie des bassins profonds nord-marocain (Est et Ouest Gibraltar) au Quaternaire terminal: apport des foraminifères benthiques. *Bull. Soc. Geol. Fr.*, 163(2):169–178.
- Caralp, M.-H., 1988. Late glacial to recent deep-sea benthic foraminifera from the northeastern Atlantic (Cadiz Gulf) and western Mediterranean (Alboran Sea): paleoceanographic results. *Mar. Micropaleontol.*, 13(3):265–289. doi:10.1016/0377-8398(88)90006-0
- Cayre, O., Lancelot, Y., Vincent, E., and Hall, M.A., 1999. Paleoceanographic reconstructions from planktonic foraminifera off the Iberian margin: temperature, salinity, and Heinrich events. *Paleoceanography*, 14(3):384–396. doi:10.1029/1998PA900027
- Cherubin, L., Carton, X., Paillet, J., Morel, Y., and Serpette, A., 2000. Instability of the Mediterranean Water undercurrents southwest of Portugal: effects of baroclinicity and of topography. *Oceanol. Acta*, 23(5):551–573 doi:10.1016/S0399-1784(00)01105-1
- Comas, M.C., Platt, J.P., Soto, J.I., and Watts, A.B., 1999. The origin and tectonic history of the Alboran Basin: insights from Leg 161 results. In Zahn, R., Comas, M.C., and Klaus, A. (Eds.), *Proc. ODP, Sci. Results*, 161: College Station, TX (Ocean Drilling Program), 555–579. doi:10.2973/odp.proc.sr.161.262.1999
- de Abreu, L., Shackleton, N.J., Schönfeld, J., Hall, M., and Chapman, M., 2003. Millennial-scale oceanic climate variability off the western Iberian margin during the last two glacial periods. *Mar. Geol.*, 196(1–2):1–20. doi:10.1016/S0025-3227(03)00046-X
- Díaz-del-Río, V., Somoza, L., Martínez-Frias, J., Mata, M.P., Delgado, A., Hernandez-Molina, F.J., Lunar, R., Martín-Rubí, J.A., Maestro, A., Fernández-Puga, M.C., León, R., Llave E., Medialdea, T., and Vázquez, J.T., 2003. Vast fields of hydrocarbon-derived carbonate chimneys related to the accretionary wedge/olistostrome of the Gulf of Cádiz. *Mar. Geol.*, 195(1–4):177–200. doi:10.1016/S0025-3227(02)00687-4
- Duggen, S., Hoernle, K., van den Bogaard, P., Rüpke, L., and Morgan, J.P., 2003. Deep roots of the Messinian salinity crisis. *Nature (London, U. K.)*, 422(6932):602–606. doi:10.1038/nature01553
- Duplessy, J.-C., Shackleton, N.J., Fairbanks, R.G., Labeyrie, L., Oppo, D., and Kallel, N., 1988. Deepwater source variations during the last climatic cycle and their impact on the global deepwater circulation. *Paleoceanography*, 3(3):343–360. doi:10.1029/PA003i003p00343
- Faugères, J.-C., Frappa, M., Gonthier, E., de Resseguier, A., and Stow, D., 1985. Modelé et facies de type contourite à la surface d'une ride sédimentaire édifiée par des courants issus de la veine d'eau méditerranéenne (ride du Faro, Golfe de Cadix). *Bull. Soc. Geol. Fr.*, 1(1):35–47.
- Fernández-Puga, M.C., Vázquez, J.T., Somoza, L., Díaz del Río, V., Medialdea, T., Mata, M.P., and León, R., 2007. Gas-related morphologies and diapirism in the Gulf of Cádiz. *Geo-Mar. Lett.*, 27(2–4):213–221. doi:10.1007/s00367-007-0076-0
- Fiúza, A.F.G., Hamann, M., Ambar, I., Díaz del Río, G., González, N., and Cabanas, J.M., 1998. Water masses and their circulation off western Iberia during May 1993. *Deep-Sea Res., Part I*, 45(7):1127–1160. doi:10.1016/S0967-0637(98)00008-9

- Flower, B.P., Oppo, D.W., McManus, J.F., Venz, K.A., Hodell, D.A., and Cullen, J.L., 2000. North Atlantic Intermediate to Deep Water circulation and chemical stratification during the past 1 Myr. *Paleoceanography*, 15(4):388–403. doi:10.1029/1999PA000430
- García, M., Hernández-Molina, F.J., Llave, E., Stow, D.A.V., León, R., Fernández-Puga, M.C., Díaz del Río, V., and Somoza, L., 2009. Contourite erosive features caused by the Mediterranean Outflow Water in the Gulf of Cádiz: Quaternary tectonic and oceanographic implications. *Mar. Geol.*, 257(1–4):24–40 doi:10.1016/j.margeo.2008.10.009
- García-Castellanos, D., Estrada, F., Jiménez-Munt, I., Gorini, C., Fernández, M., Vergés, J., and De Vicente, R., 2009. Catastrophic flood of the Mediterranean after the Messinian salinity crisis. *Nature (London, U. K.)*, 462(7274):778–781. doi:10.1038/nature08555
- Gardner, J.V., and Kidd, R.B., 1987. Sedimentary processes on the northwestern Iberian continental margin viewed by long-range side-scan sonar and seismic data. *J. Sediment. Res.*, 57(3):397–407. doi:10.1306/212F8B43-2B24-11D7-8648000102C1865D
- Gonthier, E.G., Faugeres, J.C., and Stow, D.A.V., 1984. Contourite facies of the Faro Drift, Gulf of Cádiz. In Stow, D.A.V., and Piper, D.J.W. (Eds.), *Fine-Grained Sediments: Deep Water Processes and Facies*. Geol. Soc. Spec. Publ., 15:275–292. doi:10.1144/GSL.SP.1984.015.01.18
- Gràcia, E., Dañobeitia, J., Vergés, J., Bartolomé, R., and Córdoba, D., 2003a. Crustal architecture and tectonic evolution of the Gulf of Cádiz (SW Iberian margin) at the convergence of the Eurasian and African plates. *Tectonics*, 22(4):1033–1051. doi:10.1029/2001TC901045
- Gràcia, E., Dañobeitia, J., Vergés, J., and PARSIFAL Team, 2003b. Mapping active faults offshore Portugal (36°N–38°N): implications for seismic hazard assessment along the southwest Iberian margin. *Geology*, 31(1):83–86. doi:10.1130/0091-7613(2003)031<0083:MAFOPN>2.0.CO;2
- Gutscher, M.-A., 2004. What caused the Great Lisbon Earthquake? *Science*, 305(5688):1247–1248. doi:10.1126/science.1101351
- Gutscher, M.-A., Malod, J., Rehault, J.-P., Contrucci, I., Klingelhoefer, F., Mendes-Victor, L., and Spakman, W., 2002. Evidence for active subduction beneath Gibraltar. *Geology*, 30(12):1071–1074. doi:10.1130/0091-7613(2002)030<1071:EFASBG>2.0.CO;2
- Habgood, E.L., Kenyon, N.H., Masson, D.G., Akhmetzhanov, A., Weaver, P.P.E., Gardner, J., and Mulder, T., 2003. Deep-water sediment wave fields, bottom current sand channels, and gravity flow channel-lobe systems: Gulf of Cádiz, NE Atlantic. *Sedimentology*, 50(3):483–510. doi:10.1046/j.1365-3091.2003.00561.x
- Hall, I.R., and McCave, I.N., 2000. Palaeocurrent reconstruction, sediment, and thorium focussing on the Iberian margin over the last 140 ka. *Earth Planet. Sci. Lett.*, 178(1–2):151–164. doi:10.1016/S0012-821X(00)00068-6
- Hanquiez, V., Mulder, T., Lecroart, P., Gonthier, E., Marchès, E., and Voisset, M., 2007. High resolution seafloor images in the Gulf of Cádiz, Iberian margin. *Mar. Geol.*, 246(1):42–59. doi:10.1016/j.margeo.2007.08.002
- Hernández-Molina, J., Llave, E., Somoza, L., Fernández-Puga, M.C., Maestro, A., León, R., Medialdea, T., Barnolas, A., García, M., Díaz del Río, V., Fernández-Salas, L.M., Vázquez, J.T., Lobo, F., Alveirinho Dias, J.M., Rodero, J., and Gardner, J., 2003. Looking for clues to paleoceanographic imprints: a diagnosis of the Gulf of Cádiz contourite depositional systems. *Geology*, 31(1):19–22. doi:10.1130/0091-7613(2003)031<0019:LFCTPI>2.0.CO;2
- Hernández-Molina, F.J., Llave, E., Stow, D.A.V., García, M., Somoza, L., Vázquez, J.T., Lobo, F.J., Maestro, A., Díaz del Río, V., León, R., Medialdea, T., and Gardner, J., 2006. The contourite depositional system of the Gulf of Cádiz: a sedimentary model related to the bot-

- tom current activity of the Mediterranean Outflow Water and its interaction with the continental margin. *Deep-Sea Res., Part II*, 53(11–13):1420–1463. doi:10.1016/j.dsr2.2006.04.016
- Hernández-Molina, F.J., Matias, H., Llave, E., and Stow, D.A.V., 2009. Onset of contourite deposition in the Gulf of Cádiz: preliminary results [6th Symposium on the Iberian Atlantic Margin (MIA 09), 1–5 December 2009, Oviedo, Spain].
- Hernández-Molina, F.J., Serra, N., Stow, D.A.V., Llave, E., Ercilla, G., and Van Rooij, D., 2011. Along-slope oceanographic processes and sedimentary products around the Iberian margin. *Geo-Mar. Lett.*, 31(5–6):315–341. doi:10.1007/s00367-011-0242-2
- Hernández-Molina, F.J., Somoza, L., Vazquez, J.T., Lobo, F., Fernández-Puga, M.C., Llave, E., and Díaz-del Río, V., 2002. Quaternary stratigraphic stacking patterns on the continental shelves of the southern Iberian Peninsula: their relationship with global climate and paleoceanographic changes. *Quat. Int.*, 92(1):5–23. doi:10.1016/S1040-6182(01)00111-2
- Hsü, K.J., Montadert, L., Bernoulli, D., Cita, M.B., Erickson, A., Garrison, R.E., Kidd, R.B., Melières, F., Müller, C., and Wright, R., 1978. History of the Mediterranean salinity crisis. In Hsü, K.J., Montadert, L., et al., *Init. Repts. DSDP*, 42 (Pt. 1): Washington, DC (U.S. Govt. Printing Office), 1053–1078. doi:10.2973/dsdp.proc.42-1.155.1978
- Iorga, M.C., and Lozier, M.S., 1999. Signatures of the Mediterranean Outflow from a North Atlantic climatology—1. Salinity and density fields. *J. Geophys. Res., [Oceans]*, 104(C11):25985–26029. doi:10.1029/1999JC900115
- Johnson, J., and Stevens, I., 2000. A fine resolution model of the eastern North Atlantic between the Azores, the Canary Islands, and the Gibraltar Strait. *Deep-Sea Res., Part I*, 47(5):875–899. doi:10.1016/S0967-0637(99)00073-4
- Johnson, R.G., 1997. Climate control requires a dam at the Strait of Gibraltar. *Eos, Trans. Am. Geophys. Union*, 78(27):277–281. doi:10.1029/97EO00180
- Kenyon, N.H., and Belderson, R.H., 1973. Bed forms of the Mediterranean undercurrent observed with side-scan sonar. *Sediment. Geol.*, 9(2):77–99. doi:10.1016/0037-0738(73)90027-4
- Lebreiro, S.M., 2010. Circum-Iberia turbidites and contourites: enhancement of processes by AMOC millennial-scale climate changes. *Geo-Temas*, 11:93–94.
- Lebreiro, S.M., McCave, I.N., and Weaver, P.P.E., 1997. Late Quaternary turbidite emplacement on the Horseshoe Abyssal Plain (Iberian margin). *J. Sediment. Res.*, 67(5):856–870. DOI:10.1306/D4268658-2B26-11D7-8648000102C1865D
- Lebreiro, S.M., Moreno, J.C., McCave, I.N., and Weaver, P.P.E., 1996. Evidence for Heinrich layers off Portugal (Tore Seamount: 39°N, 12°W). *Mar. Geol.*, 131(1–2):47–56. doi:10.1016/0025-3227(95)00142-5
- Lebreiro, S.M., Voelker, A.H.L., Vizcaino, A., Abrantes, F.G., Alt-Epping, U., Jung, S., Thouveny, N., and Gràcia, E., 2009. Sediment instability on the Portuguese continental margin under abrupt glacial climate changes (last 60 kyr). *Quat. Sci. Rev.*, 28(27–28):3211–3223. doi:10.1016/j.quascirev.2009.08.007
- Llave, E., Hernández-Molina, F.J., Somoza, L., Díaz del Río, V., Stow, D.A.V., Maestro, A., and Alveirinho Dias, J.M., 2001. Seismic stacking pattern of the Faro-Albufeira contourite system (Gulf of Cádiz): a Quaternary record of paleoceanographic and tectonic influences. *Mar. Geophys. Res.*, 22(5–6):487–508. doi:10.1023/A:1016355801344
- Llave, E., Hernández-Molina, F.J., Somoza, L., Stow, D.A.V., and Díaz Del Río, V., 2007. Quaternary evolution of the contourite depositional system in the Gulf of Cádiz. *Geol. Soc. Spec. Publ.*, 276:49–79. doi:10.1144/GSL.SP.2007.276.01.03

- Llave, E., Matias, H., Hernández-Molina, F.J., Ercilla, G., Stow, D.A.V., and Medialdea, T., 2010. Pliocene and Quaternary seismic stacking pattern and distribution of contourites in the Algarve margin (northern Gulf of Cádiz, Spain). *Geo-Temas*, 11:103–104.
- Llave, E., Matias, H., Hernández-Molina, F.J., Ercilla, G., Stow, D.A.V., and Medialdea, T., 2011. Pliocene–Quaternary contourites along the northern Gulf of Cadiz margin: sedimentary stacking pattern and regional distribution. *Geo-Mar. Lett.*, 31(5–6):377–390. doi:10.1007/s00367-011-0241-3
- Llave, E., Schönfeld, J., Hernández-Molina, F.J., Mulder, T., Somoza, L., Díaz del Río, V., and Sánchez-Almazo, I., 2006. High-resolution stratigraphy of the Mediterranean Outflow contourite system in the Gulf of Cádiz during the late Pleistocene: the impact of Heinrich events. *Mar. Geol.*, 227(3–4):241–262. doi:10.1016/j.margeo.2005.11.015
- Loget, N., and Van Den Driessche, J., 2006. On the origin of the Strait of Gibraltar. *Sediment. Geol.*, 188–189:341–356. doi:10.1016/j.sedgeo.2006.03.012
- Lobo, F.J., Dias, J.M.A., Vázquez, J.T., Díaz del Río, V., González, R., and Fernández-Puga, M.C., 2003. New data about neotectonic activity in the eastern Algarve shelf, Gulf of Cádiz, SW Iberian Peninsula. *Thalassas*, 19(2):63–64.
- Lopes, F.C., Cunha, P.P., and Le Gall, B., 2006. Cenozoic seismic stratigraphy and tectonic evolution of the Algarve margin (offshore Portugal, southwestern Iberian Peninsula). *Mar. Geol.*, 231(1–4):1–36. doi:10.1016/j.margeo.2006.05.007
- Löwemark, L., Schönfeld, J., Werner, F., and Schäfer, P., 2004. Trace fossils as a paleoceanographic tool: evidence from late Quaternary sediments of the southwestern Iberian margin. *Mar. Geol.*, 204(1–2):27–41. doi:10.1016/S0025-3227(03)00351-7
- Madelain, F., 1970. Influence de la topographie du fond sur l'écoulement méditerranéen entre le Détroit de Gibraltar et le Cap Saint-Vincent. *Cah. Oceanogr.*, 22:43–61.
- Maestro, A., Somoza, L., Díaz del Río, V., Vázquez, J.T., Martín-Alfageme, S., Alveirinho, J.M., Barnolas, A., and Vegas, R., 1998. Neotectónica transpresiva en la plataforma continental Suribérica Atlántica. *Geogaceta*, 24:203–206.
- Maestro, A., Somoza, L., Medialdea, T., Talbot, C.J., Lowrie, A., Vázquez, J.T., and Díaz del Río, V., 2003. Large-scale slope failure involving Triassic and middle Miocene salt and shale in the Gulf of Cádiz (Atlantic Iberian margin). *Terra Nova*, 15(6):380–391. doi:10.1046/j.1365-3121.2003.00513.x
- Maldonado, A., Somoza, L., and Pallarés, L., 1999. The Betic orogen and the Iberian–African boundary in the Gulf of Cádiz: geological evolution (central North Atlantic). *Mar. Geol.*, 155(1–2):9–43. doi:10.1016/S0025-3227(98)00139-X
- Malod, J.A., and Mauffret, A., 1990. Iberian plate motions during the Mesozoic. In Boillot, G., and Fontbote, J.M. (Eds.), *Alpine Evolution of Iberia and its Continental Margins*. Tectonophysics, 184(3–4):261–278. doi:10.1016/0040-1951(90)90443-C
- Marchès, E., Mulder, T., Cremer, M., Bonnel, C., Hanquiez, V., Gonthier, E., and Lecroart, P., 2007. Contourite drift construction influenced by capture of Mediterranean Outflow Water deep-sea current by the Portimão submarine canyon (Gulf of Cádiz, South Portugal). *Mar. Geol.*, 242(4):247–260. doi:10.1016/j.margeo.2007.03.013
- Medialdea, T., Somoza, L., Pinheiro, L.M., Fernández-Puga, M.C., Vázquez, J.T., León, R., Ivanov, M.K., Magalhaes, V., Díaz del Río, V., and Vegas, R., 2009. Tectonics and mud volcano development in the Gulf of Cádiz. *Mar. Geol.*, 261(1–4):48–63. doi:10.1016/j.margeo.2008.10.007
- Medialdea, T., Vegas, R., Somoza, L., Vázquez, J.T., Maldonado, A., Díaz-del-Río, V., Maestro, A., Córdoba, D., and Fernández-Puga, M.C., 2004. Structure and evolution of the “Olisto-



- stromes" complex of the Gibraltar arc in the Gulf of Cádiz (eastern Central Atlantic): evidence from two long seismic cross-sections. *Mar. Geol.*, 209(1–4):173–198. doi:10.1016/j.margeo.2004.05.029
- Melières, F., 1974. Recherches sur la dynamique sédimentaire du golfe de Cádiz (Espagne) [Thèse Doctorat d'Etat]. Univ. Paris.
- Millot, C., 1999. Circulation in the western Mediterranean Sea. *J. Mar. Syst.*, 20(1–4):423–442. doi:10.1016/S0924-7963(98)00078-5
- Millot, C., 2009. Another description of the Mediterranean Sea Outflow. *Prog. Oceanogr.*, 82(2):101–124. doi:10.1016/j.pocean.2009.04.016
- Moreno, E., Thouveny, N., Delanghe, D., McCave, I.N., and Shackleton, N.J., 2002. Climatic and oceanographic changes in the northeast Atlantic reflected by magnetic properties of sediments deposited on the Portuguese margin during the last 340 ka. *Earth Planet. Sci. Lett.*, 202(2):465–480. doi:10.1016/S0012-821X(02)00787-2
- Mougenot, D., 1988. Géologie de la Marge Portugaise [Thèse Doctorat d'Etat des Sciences Naturelles]. Univ. Pierre et Marie Curie, Paris.
- Mulder, C.J., and Parry, G.R., 1977. Late Tertiary evolution of the Alboran Sea at the eastern entrance of the Strait of Gibraltar. In Biju-Duval, B., and Montadert, L. (Eds.), *Structural History of the Mediterranean Basins*: Paris (Ed. Technip), 401–410.
- Mulder, T., Lecroart, P., Hanquiez, V., Marches, E., Gonthier, E., Guedes, J.-C., Thiébot, E., Jaaidi, B., Kenyon, N., Voisset, M., Perez, C., Sayago, M., Fuchey, Y., and Bujan, S., 2006. The western part of the Gulf of Cádiz: contour currents and turbidity currents interactions. *Geo-Mar. Lett.*, 26(1):31–41. doi:10.1007/s00367-005-0013-z
- Mulder, T., Voisset, M., Lecroart, P., Le Drezen, E., Gonthier, E., Hanquiez, V., Faugères, J.-C., Habgood, E., Hernandez-Molina, F.J., Estrada, F., Llave-Barranco, E., Poirier, D., Gorini, C., Fuchey, Y., Volker, A., Freitas, P., Lobo Sanchez, F., Fernandez, L.M., and Morel, J., 2003. The Gulf of Cádiz: an unstable giant contouritic levee. *Geo-Mar. Lett.*, 23(1):7–18. doi:10.1007/s00367-003-0119-0
- Murillas, J., Mougenot, D., Boillot, G., Comas, M.C., Banda, E., and Mauffret, A., 1990. Structure and evolution of the Galicia Interior Basin (Atlantic western Iberian continental margin). *Tectonophysics*, 184(3–4):297–319. doi:10.1016/0040-1951(90)90445-E
- Nelson, C.H., Baraza, J., and Maldonado, A., 1993. Mediterranean undercurrent sandy contourites, Gulf of Cádiz, Spain. *Sediment. Geol.*, 82(1–4):103–131. doi:10.1016/0037-0738(93)90116-M
- Nelson, C.H., Baraza, J., Maldonado, A., Rodero, J., Escutia, C., and Barber, J.H., Jr., 1999. Influence of the Atlantic inflow and Mediterranean outflow currents on late Quaternary sedimentary facies of Gulf of Cádiz continental margin. *Mar. Geol.*, 155(1–2):99–129. doi:10.1016/S0025-3227(98)00143-1
- Neves, M.C., Terrinha, P., Afilhado, A., Moulin, M., Matias, L., and Rosas, F., 2009. Response of a multi-domain continental margin to compression: study from seismic reflection–refraction and numerical modelling in the Tagus Abyssal Plain. *Tectonophysics*, 468(1–4):113–130. doi:10.1016/j.tecto.2008.05.008
- Ochoa, J., and Bray, N.A., 1991. Water mass exchange in the Gulf of Cádiz. *Deep-Sea Res., Part A*, 38(S1):S465–S503.
- Olivet, J.L., 1996. La cinématique de la plaque ibérique. *Bull. Cent. Rech. Explor.–Prod. Elf-Aquitaine*, 20:131–195.
- Pinheiro, L.M., Wilson, R.C.L., Pena dos Reis, R., Whitmarsh, R.B., and Ribeiro, A., 1996. The Western Iberia margin: a geophysical and geological overview. In Whitmarsh, R.B., Saw-

- yer, D.S., Klaus, A., and Masson, D.G. (Eds.), *Proc. ODP, Sci. Results*, 149: College Station, TX (Ocean Drilling Program), 3–23. doi:10.2973/odp.proc.sr.149.246.1996
- Rahmstorf, S., 1998. Influence of Mediterranean Outflow on climate. *Eos, Trans. Am. Geophys. Union*, 79(24):281–282. doi:10.1029/98EO00208
- Raymo, M.E., Oppo, D.W., Flower, B.P., Hodell, D.A., McManus, J.F., Venz, K.A., Kleiven, K.F., and McIntyre, K., 2004. Stability of North Atlantic water masses in face of pronounced climate variability during the Pleistocene. *Paleoceanography*, 19:PA2008. doi:10.1029/2003PA000921
- Rebesco, M., and Camerlenghi, A. (Eds.), 2008. *Contourites*. Dev. Sedimentol., 60.
- Ribeiro, A., Kullberg, M.C., Kullberg, J.C., Manuppella, G., and Phipps, S., 1990. A review of Alpine tectonics in Portugal: foreland detachment in basement and cover rocks. *Tectonophysics*, 184(3–4):357–366. doi:10.1016/0040-1951(90)90448-H
- Richardson, P.L., Bower, A.S., and Zenk, W., 2000. A census of meddies tracked by floats. *Progr. Oceanogr.*, 45(2):209–250. doi:10.1016/S0079-6611(99)00053-1
- Ryan, W.B.F., Hsü, K.J., Cita, M.B., Dumitrica, P., Lort, J., Maync, W., Nesteroff, W.D., Pautot, G., Stradner, H., and Wezel, F.C., 1973. Western Alboran Basin—Site 121. In Ryan, W.B.F., Hsü, K.J., et al., *Init. Repts. DSDP*, 13: Washington, DC (U.S. Govt. Printing Office), 43–89. doi:10.2973/dsdp.proc.13.103.1973
- Sarnthein, M., Winn, K., Jung, S.J.A., Duplessy, J.-C., Labeyrie, L., Erlenkeuser, H., and Ganssen, G., 1994. Changes in East Atlantic deepwater circulation over the last 30,000 years: eight time slice reconstructions. *Paleoceanography*, 9(2):209–267. doi:10.1029/93PA03301
- Schönfeld, J., 1997. The impact of the Mediterranean Outflow Water (MOW) on benthic foraminiferal assemblages and surface sediments at the southern Portuguese continental margin. *Mar. Micropaleontol.*, 29(3–4):211–236. doi:10.1016/S0377-8398(96)00050-3
- Schönfeld, J., 2002. Recent benthic foraminiferal assemblages in deep high-energy environments from the Gulf of Cádiz (Spain). *Mar. Micropaleontol.*, 44(3–4):141–162. doi:10.1016/S0377-8398(01)00039-1
- Schönfeld, J., and Zahn, R., 2000. Late glacial to Holocene history of the Mediterranean Outflow. Evidence from benthic foraminiferal assemblages and stable isotopes at the Portuguese margin. *Palaeogeogr., Palaeoclimatol., Palaeoecol.*, 159(1–2):85–111. doi:10.1016/S0031-0182(00)00035-3
- Schönfeld, J., Zahn, R., and de Abreu, L., 2003. Surface and deep water response to rapid climate changes at the western Iberian margin. *Global Planet. Change*, 36(4):237–264. doi:10.1016/S0921-8181(02)00197-2
- Serra, N., Ambar, I., and Boutov, D., 2010a. Surface expression of Mediterranean water dipoles and their contribution to the shelf/slope–open ocean exchange. *Ocean Sci.*, 6(1):191–209. doi:10.5194/os-6-191-2010
- Serra, N., Käse, R.H., Köhl, A., Stammer, D., and Quadfasel, D. 2010b. On the low-frequency phase relation between the Denmark Strait and the Faroe-Bank Channel overflows. *Tellus, Ser. A*, 62(4):530–550. doi:10.1111/j.1600-0870.2010.00445.x
- Shackleton, N.J., Fairbanks, R.G., Chiu, T.-C., and Parrenin, F., 2004. Absolute calibration of the Greenland time scale: implications for Antarctic time scales and for  $\Delta^{14}\text{C}$ . *Quat. Sci. Rev.*, 23(14–15):1513–1522. doi:10.1016/j.quascirev.2004.03.006
- Shackleton, N.J., Hall, M.A., and Vincent, E., 2000. Phase relationships between millennial-scale events 64,000–24,000 years ago. *Paleoceanography*, 15(6):565–569. doi:10.1029/2000PA000513

- Sierro, F.J., Hodell, D.A., Curtis, J.H., Flores, J.A., Reguera, I., Colmenero-Hidalgo, E., Bárcena, M.A., Grimalt, J.O., Cacho, I., Frigola, J., and Canals, M., 2005. Impact of iceberg melting on Mediterranean thermohaline circulation during Heinrich events. *Paleoceanography*, 20(2):PA2019. doi:10.1029/2004PA001051
- Sierro, F.J., Ledesma, S., Flores, J.-A., Torrecusa, S., and Martínez del Olmo, W., 2000. Sonic and gamma-ray astrochronology: cycle to cycle calibration of Atlantic climatic to Mediterranean sapropels and astronomical oscillations. *Geology*, 28(8):695–698. doi:10.1130/0091-7613(2000)28<695:SAGACT>2.0.CO;2
- Slater, D.R., 2003. The transport of Mediterranean water in the north Atlantic Ocean [Ph.D. dissert.]. Univ. Southampton.
- Smith, W.H.F., and Sandwell, D.T., 1997. Global sea floor topography from satellite altimetry and ship depth soundings. *Science*, 277(5334):1956–1962. doi:10.1126/science.277.5334.1956
- Somoza, L., Díaz-del-Río, V., León, R., Ivanov, M., Fernández-Puga, M.C., Gardner, J.M., Hernández-Molina, F.J., Pinheiro, L.M., Rodero, J., Lobato, A., Maestro, A., Vázquez, J.T., Medialdea, T., and Fernández-Salas, L.M., 2003. Seabed morphology and hydrocarbon seepage in the Gulf of Cádiz mud volcano area: acoustic imagery, multibeam and ultra-high resolution seismic data. *Mar. Geol.*, 195(1–4):153–176. doi:10.1016/S0025-3227(02)00686-2
- Srivastava, S.P., Schouten, H., Roest, W.R., Klitgord, K.D., Kovacs, L.C., Verhoef, J., and Macnab, R., 1990. Iberian plate kinematics: a jumping plate boundary between Eurasia and Africa. *Nature (London, U. K.)*, 344(6268):756–759. doi:10.1038/344756a0
- Srivastava, S.P., Sibuet, J.-C., Cande, S., Roest, W.R., and Reid, I.D., 2000. Magnetic evidence for slow seafloor spreading during the formation of the Newfoundland and Iberian margins. *Earth Planet. Sci. Lett.*, 182(1):61–76. doi:10.1016/S0012-821X(00)00231-4
- Stow, D.A.V., Faugères, J.-C., and Gonthier, E., 1986. Facies distribution and textural variation in Faro Drift contourites: velocity fluctuation and drift growth. *Mar. Geol.*, 72(1–2):71–100. doi:10.1016/0025-3227(86)90100-3
- Stow, D.A.V., Faugères, J.-C., Gonthier, E., Cremer, M., Llave, E., Hernández-Molina, F.J., Somoza, L., and Díaz del Río, V., 2002. Faro-Albufeira drift complex, northern Gulf of Cádiz. *Mem.—Geol. Soc. London*, 22(1):137–154. doi:10.1144/GSL.MEM.2002.022.01.11
- Terrinha, P., Matias, L., Vicente, J., Duarte, J., Luís, J., Pinheiro, L., Lourenço, N., Diez, S., Rosas, F., Magalhães, V., Valadares, V., Zitellini, N., Roque, C., Mendes Víctor, L., and MATESPRO Team, 2009. Morphotectonics and strain partitioning at the Iberia-Africa plate boundary from multibeam and seismic reflection data. *Mar. Geol.*, 267(3–4):156–174. doi:10.1016/j.margeo.2009.09.012
- Terrinha, P., Pinheiro, L.M., Henriot, J.-P., Matias, L., Ivanov, M.K., Monteiro, J.H., Akhmetzh-anov, A., Volkonskaya, A., Cunha, T., Shaskin, P., and Rovere, M., 2003. Tsunamigenic-seismogenic structures, neotectonics, sedimentary processes, and slope stability on the southwest Portuguese margin. *Mar. Geol.*, 195(1–4):55–73. doi:10.1016/S0025-3227(02)00682-5
- Thorpe, S.A., 1976. Variability of the Mediterranean undercurrent in the Gulf of Cádiz. *Deep-Sea Res. Oceanogr. Abstr.*, 23(8):711–727. doi:10.1016/S0011-7471(76)80016-2
- Thouveny, N., Moreno, E., Delanghe, D., Candon, L., Lancelot, Y., and Shackleton, N.J., 2000. Rock magnetic detection of distal ice-rafted debris: clue for the identification of Heinrich layers on the Portuguese margin. *Earth Planet. Sci. Lett.*, 180(1–2):61–75. doi:10.1016/S0012-821X(00)00155-2

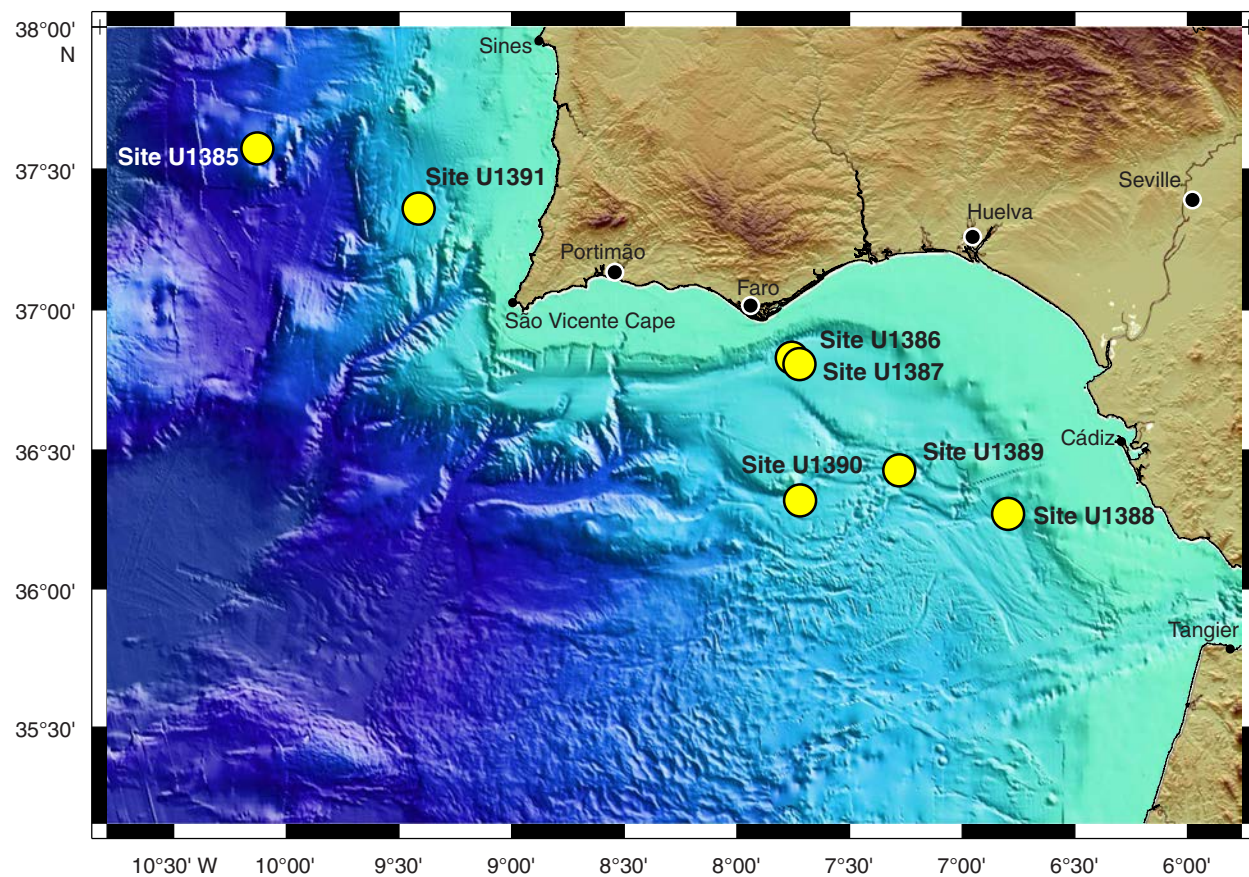


- van Aken, H.M., 2000. The hydrography of the mid-latitude Northeast Atlantic Ocean, II. The intermediate water masses. *Deep-Sea Res., Part I*, 47(5):789–824. doi:10.1016/S0967-0637(99)00112-0
- Voelker, A.H.L., and Lebreiro, S.M., 2010. Millennial-scale changes in deep water properties at the mid-depth western Iberian margin linked to Mediterranean Outflow Water activity. *Geo-Temas*, 11:85–186.
- Voelker, A.H.L., Lebreiro, S.M., Schönfeld, J., Cacho, I., Erlenkeuser, H., and Abrantes, F., 2006. Mediterranean Outflow strengthening during Northern Hemisphere coolings: a salt source for the glacial Atlantic? *Earth Planet. Sci. Lett.*, 245(1–2):39–55. doi:10.1016/j.epsl.2006.03.014
- Wilson, R.C.L., Sawyer, D.S., Whitmarsh, R.B., Zerong, J., and Carbonell, J., 1996. Seismic stratigraphy and tectonic history of the Iberia Abyssal Plain. In Whitmarsh, R.B., Sawyer, D.S., Klaus, A., and Masson, D.G. (Eds.), *Proc. ODP, Sci. Results*, 149: College Station, TX (Ocean Drilling Program), 617–633. doi:10.2973/odp.proc.sr.149.245.1996
- Zenk, W., 1975. On the Mediterranean Outflow west of Gibraltar. *“Meteor” Forschungsergeb., Reihe A*, 16:23–34.
- Zitellini, N., Gràcia, E., Matias, L., Terrinha, P., Abreu, M.A., DeAlteriis, G., Henriët, J.P., Daño-beitia, J.J., Masson, D.G., Mulder, T., Ramella, R., Somoza, L., and Diez, S., 2009. The quest for the Africa–Eurasia plate boundary west of the Strait of Gibraltar. *Earth Planet. Sci. Lett.*, 280(1–4):13–50. doi:10.1016/j.epsl.2008.12.005

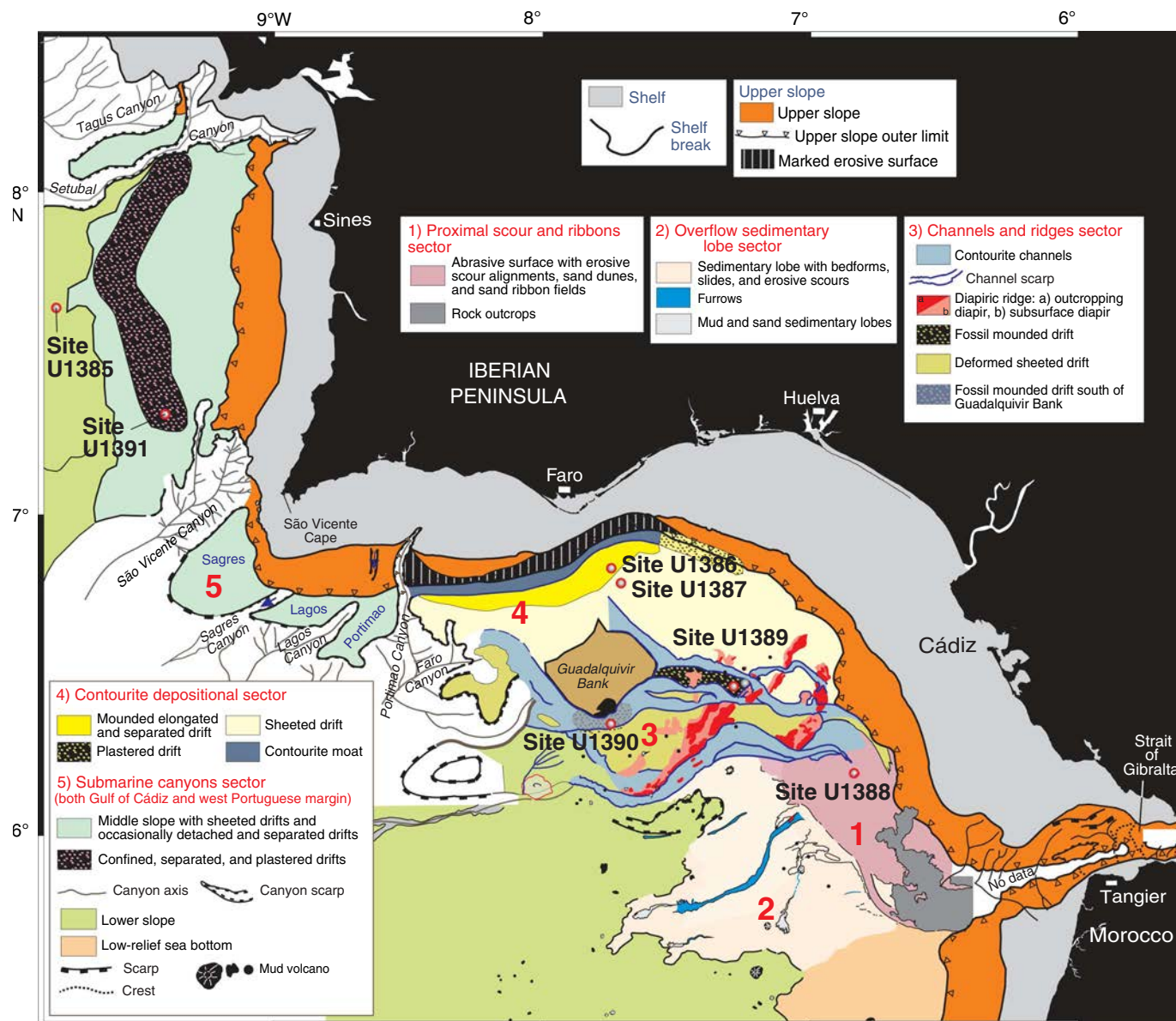
# Expedition 339 Preliminary Report

**Table T1. Coring summary, Expedition 339.**

Hole	Latitude	Longitude	Water depth (mbsl)	Cores (N)	Cored (m)	Recovered (m)	Recovered (%)	Drilled (m)	Penetration (m)	Time on hole (h)	Time on site (days)
U1385A	37°34.2894'N	10°7.5708'W	2586.7	17	151.5	155.87	102.9	0	151.5	40.5	
U1385B	37°34.2892'N	10°7.5561'W	2586.6	16	146.3	150.73	103.0	0	146.3	20.3	
U1385C	37°34.2892'N	10°7.5561'W	2586.6	1	9.5	9.87	103.9	0	9.5	1.8	
U1385D	37°34.2784'N	10°7.5559'W	2583.8	16	146.4	153.95	105.2	0	146.4	18.4	
U1385E	37°34.2785'N	10°7.5692'W	2588.7	17	148.7	151.32	101.8	0	148.7	26.3	
Site U1385 totals:				67	602.4	621.74	103.2	0	602.4	107.3	4.5
U1386A	36°49.6885'N	07°45.3309'W	560.4	39	349.3	347.04	99.4	0	349.3	50.1	
U1386B	36°49.688'N	07°45.3168'W	561.9	50	464.9	421.60	90.7	0	464.9	64.1	
U1386C	36°49.6773'N	07°45.3165'W	561.8	15	140.2	82.00	58.5	385.8	526.0	91.1	
Site U1386 totals:				104	954.4	850.64	89.1	385.8	1340.2	205.2	8.6
U1387A	36°48.3246'N	07°43.1408'W	559.1	38	352.4	347.84	98.7	0	352.4	34.8	
U1387B	36°48.3246'N	07°43.1278'W	558.2	36	338.3	327.61	96.8	0	338.3	29.8	
U1387C	36°48.3139'N	07°43.1277'W	558.4	61	580.0	409.50	70.6	290.0	870.0	157.4	
Site U1387 totals:				135	1270.7	1084.95	85.4	290.0	1560.7	222.0	9.3
U1388A	36°16.1378'N	06°47.6602'W	663.6	1	3.4	3.64	107.1	0	3.4	18.8	
U1388B	36°16.1383'N	06°47.6413'W	662.9	24	225.7	107.00	47.4	0	225.7	33.7	
U1388C	36°16.1495'N	06°47.6411'W	662.5	3	24.0	10.36	43.2	205.0	229.0	29.6	
Site U1388 totals:				28	253.1	121.00	47.8	205.0	458.1	82.0	3.4
U1389A	36°25.5183'N	07°16.6907'W	644.7	39	354.9	335.60	94.6	0	354.9	69.9	
U1389B	36°25.5199'N	07°16.6772'W	643.9	1	9.5	9.72	102.3	0	9.5	2.3	
U1389C	36°25.5199'N	07°16.6772'W	642.9	38	350.0	328.48	93.9	0	350.0	37.8	
U1389D	36°25.5092'N	07°16.6772'W	644.0	11	94.0	97.41	103.6	0	94.0	12.3	
U1389E	36°25.5084'N	07°16.6906'W	643.4	69	655.0	352.28	53.8	335.0	990.0	165.2	
Site U1389 totals:				158	1463.4	1123.49	76.8	335.0	1798.4	287.5	12.0
U1390A	36°19.0387'N	07°43.0812'W	993.4	38	350.0	326.26	93.2	0	350.0	62.2	
U1390B	36°19.1460'N	07°43.0815'W	990.7	21	194.1	189.93	97.9	0	194.1	33.4	
U1390C	36°19.1466'N	07°43.0674'W	992.4	19	175.4	170.08	97.0	0	175.4	29.2	
Site U1390 totals:				78	719.5	686.27	95.4	0	719.5	124.7	5.2
U1391A	37°21.5392'N	09°24.6601'W	1073.7	38	353.1	342.62	97.0	0	353.1	40.8	
U1391B	37°21.5288'N	09°24.6604'W	1073.3	38	353.5	346.93	98.1	0	353.5	37.5	
U1391C	37°21.5286'N	09°24.6468'W	1073.3	35	331.5	269.02	81.2	340.0	671.5	103.2	
Site U1391 totals:				111	1038.1	958.57	92.3	340.0	1378.1	181.5	
Expedition 339 totals:				681	6301.6	5446.66	86.4	1555.8	7857.4	1210.2	50.4

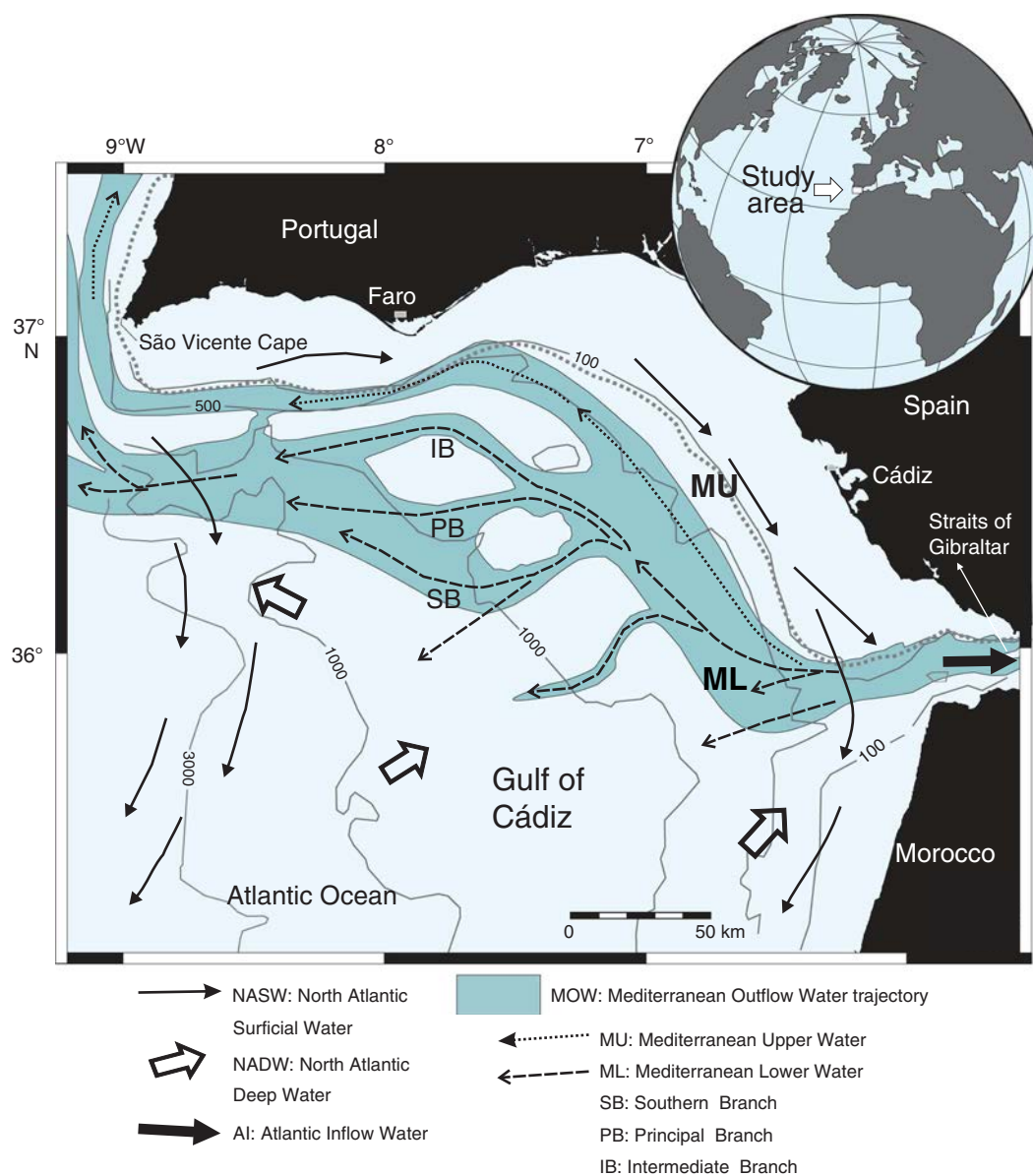
**Figure F1.** Expedition 339 sites in the Gulf of Cádiz and West Iberian margin.

**Figure F2.** Regional map of the contourite depositional system on the middle slope of the Gulf of Cádiz and West Iberian margin with Expedition 339 site locations. Morphosedimentary sectors (1–5) based on Hernández-Molina et al. (2003, 2006) and S. Lebreiro (pers. comm., 2006).

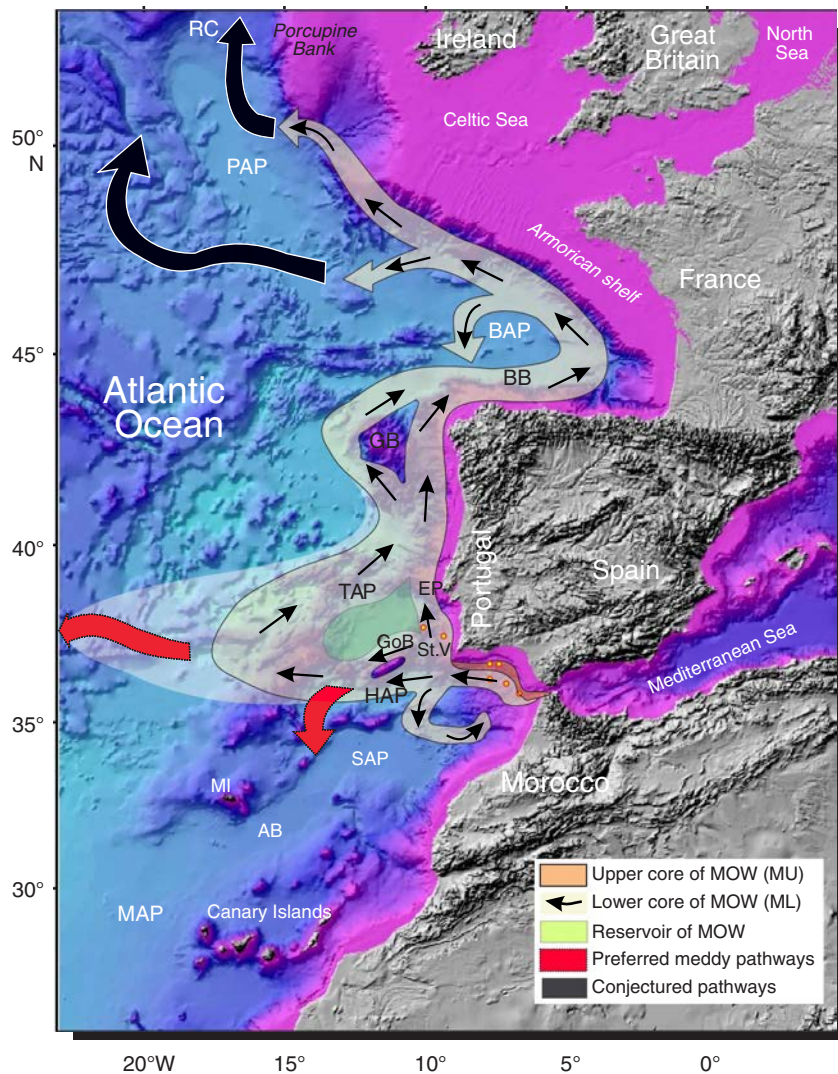




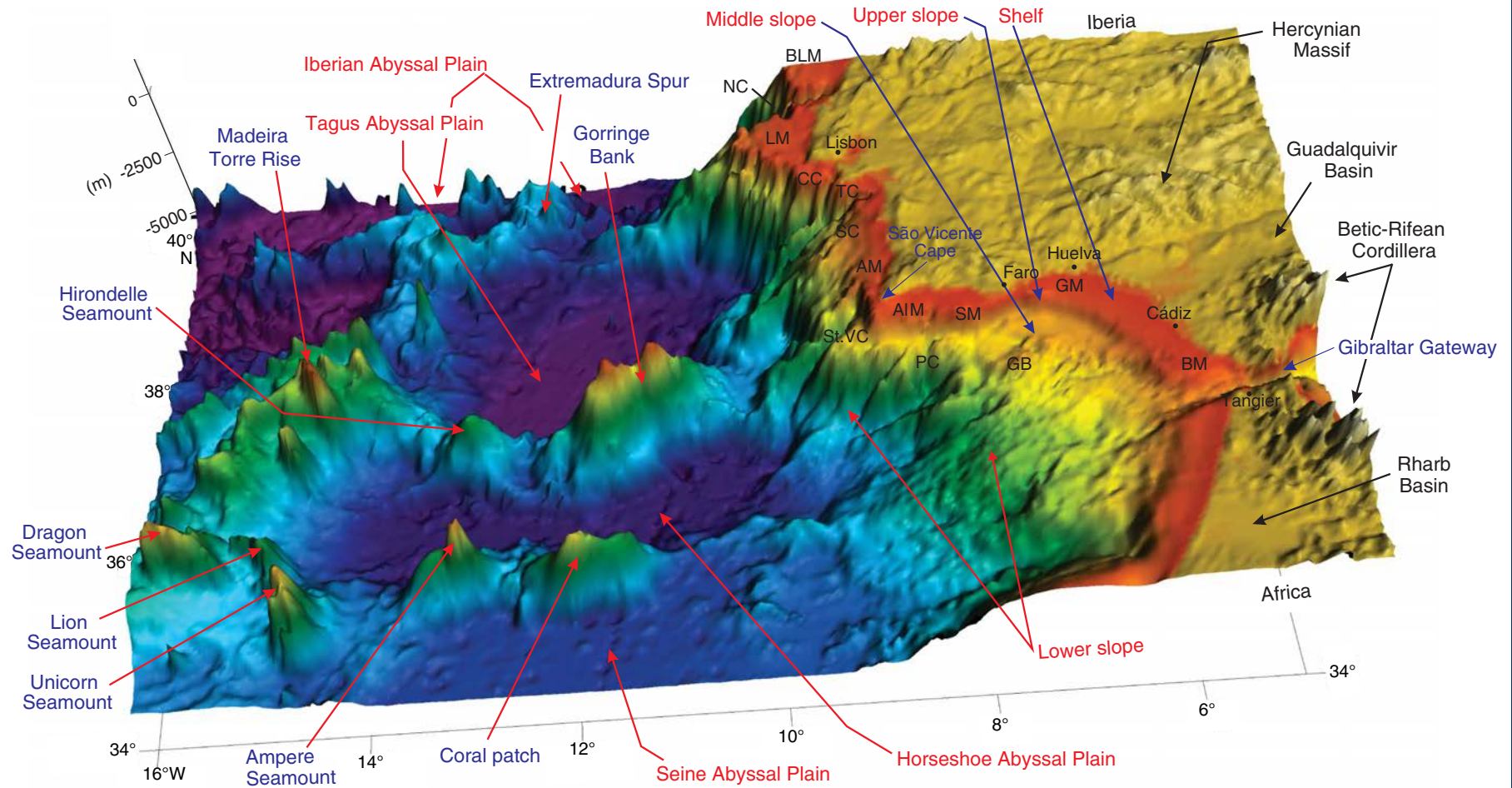
**Figure F3.** Location sketch with main water-mass circulation along the margin (modified from Hernández-Molina et al., 2006).



**Figure F4.** General circulation pattern of the Mediterranean Outflow Water (MOW) pathway in the North Atlantic (modified from Iorga and Lozier, 1999). Red circles filled with yellow indicate relative location of proposed sites. AB = Agadir Basin, BAP = Biscay Abyssal Plain, BB = Bay of Biscay, EP = Extremadura Promontory, GaB = Galicia Bank, GoB = Gorringe Bank, HAP = Horseshoe Abyssal Plain, MAP = Madeira Abyssal Plain, MI = Madeira Island, PAP = Porcupine Abyssal Plain, RC = Rockall Channel, SAP = Seine Abyssal Plain, St.V = Cape São Vicente, TAP = Tagus Abyssal Plain.

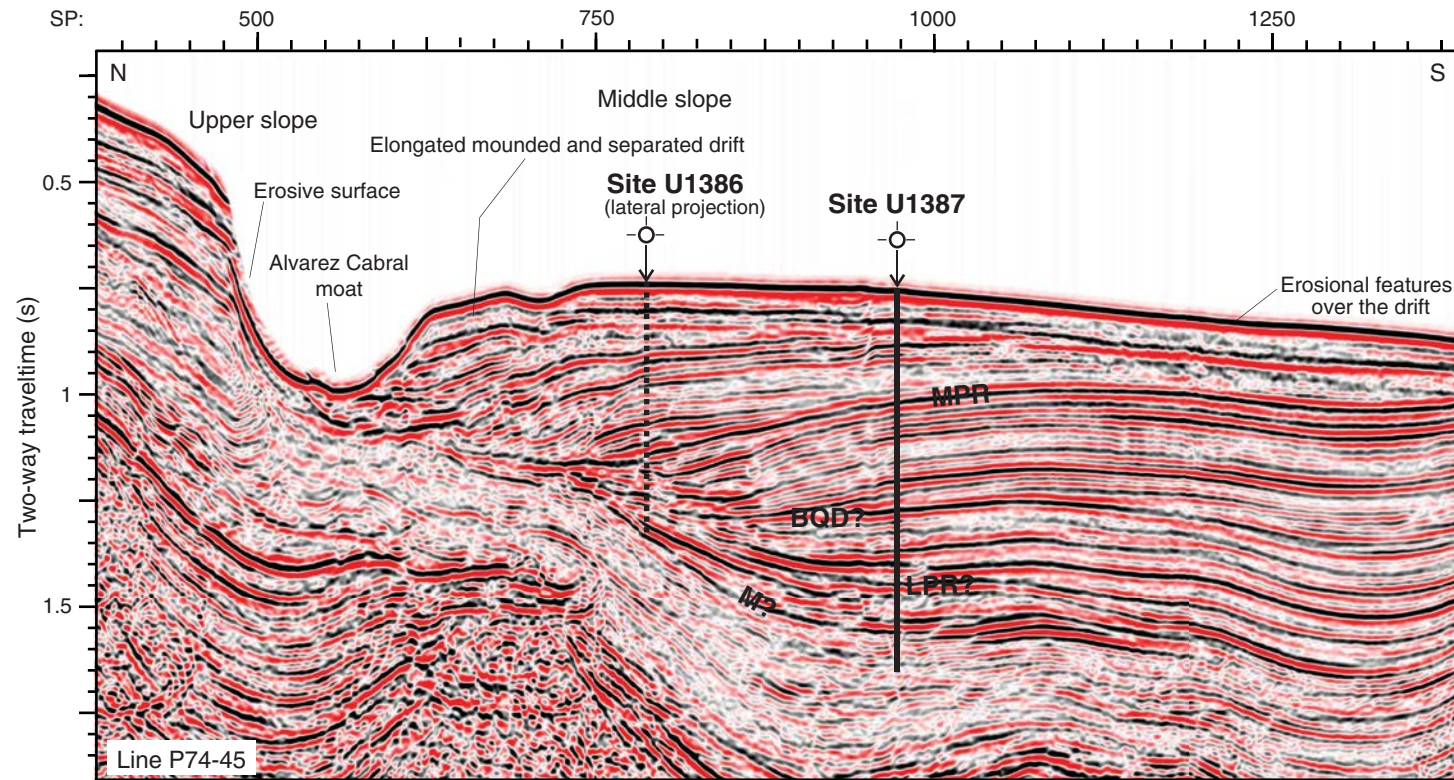


**Figure F5.** Three-dimensional regional bathymetric map of the Gulf of Cádiz (realized J.T. Vázquez [IEO] from satellite data from Smith and Sandwell, 1997). CC = Cascais Canyon, GB = Guadalquivir Bank, NC = Nazaré Canyon, PC = Portimao Canyon, St. VC = São Vicente Canyon, SC = Setúbal Canyon, TC = Tagus Canyon. AIM = Algarve margin; BLM = Beira litoral margin, BM = Betic domain margin, GM = Guadalquivir margin, LM = Lisbon margin, SM = Sudiberic margin.



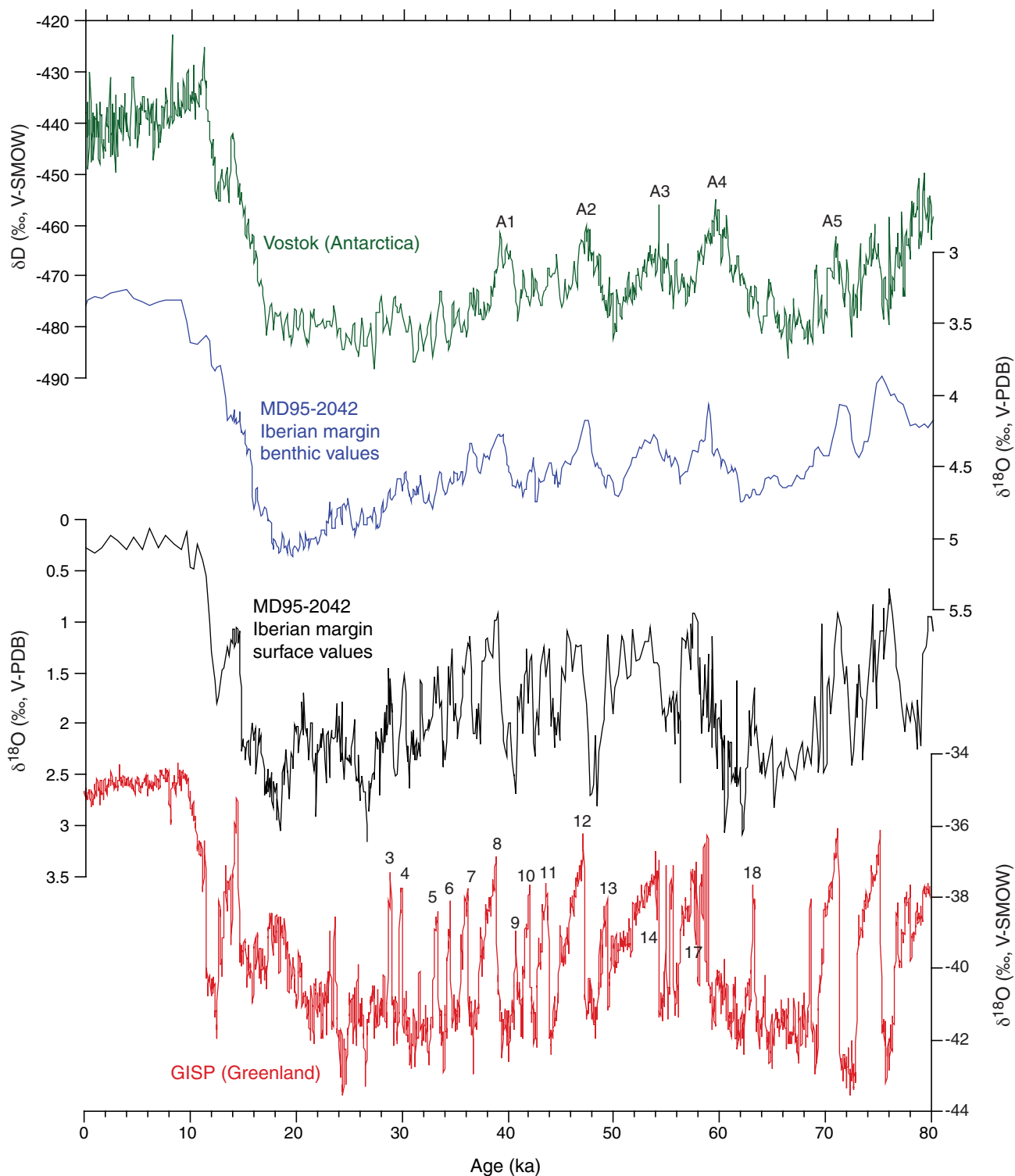


**Figure F6.** Multichannel seismic (MCS) reflection profile (Line P74-45) of Site U1387 on the Faro-Albufeira Drift (MCS lines provided by REPSOL Oil Company). SP = shotpoint. MPR = mid-Pleistocene revolution discontinuity, BQD = base Quaternary discontinuity, LPR = intra-lower Pliocene discontinuity, M = late Miocene discontinuity.

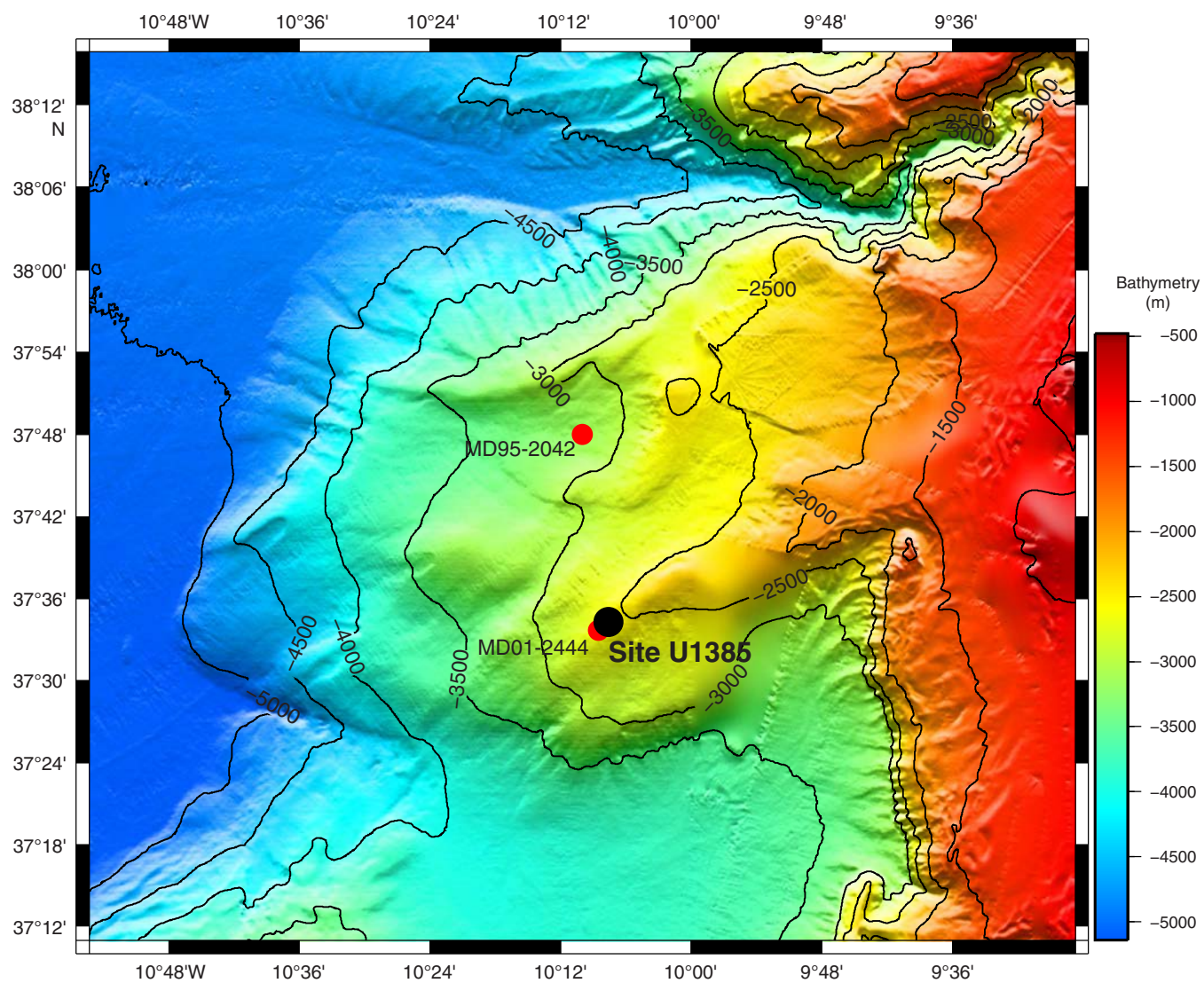




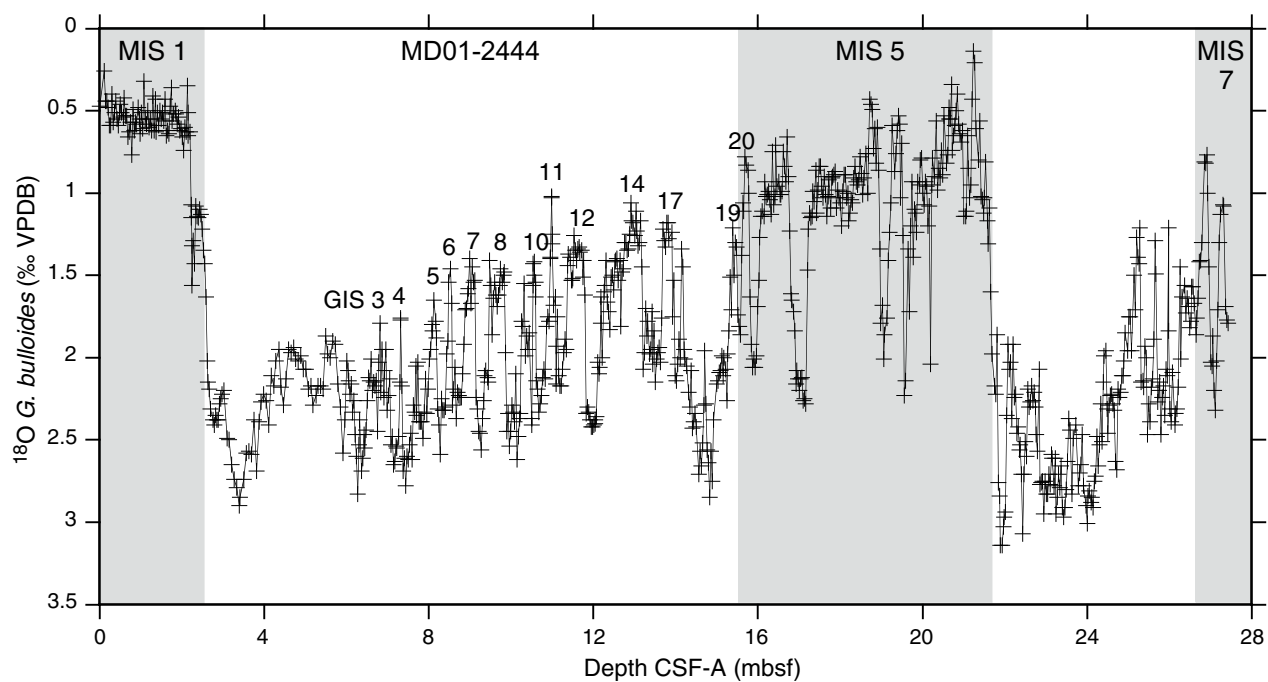
**Figure F7.** Correlation of  $\delta^{18}\text{O}$  record of GISP ice core (red line; 1–18 = marine isotope stages) to  $\delta^{18}\text{O}$  of *Globigerina bulloides* (black line) in Core MD95-2042. Resulting correlation of Vostok  $\delta\text{D}$  (green line; A1–A5 = oscillation events) and benthic  $\delta^{18}\text{O}$  of Core MD95-2042 (blue line) based on methane synchronization. V-PDB = Vienna Pee Dee belemnite, V-SMOW = Vienna standard mean ocean water. Age is from Shackleton et al. (2004).



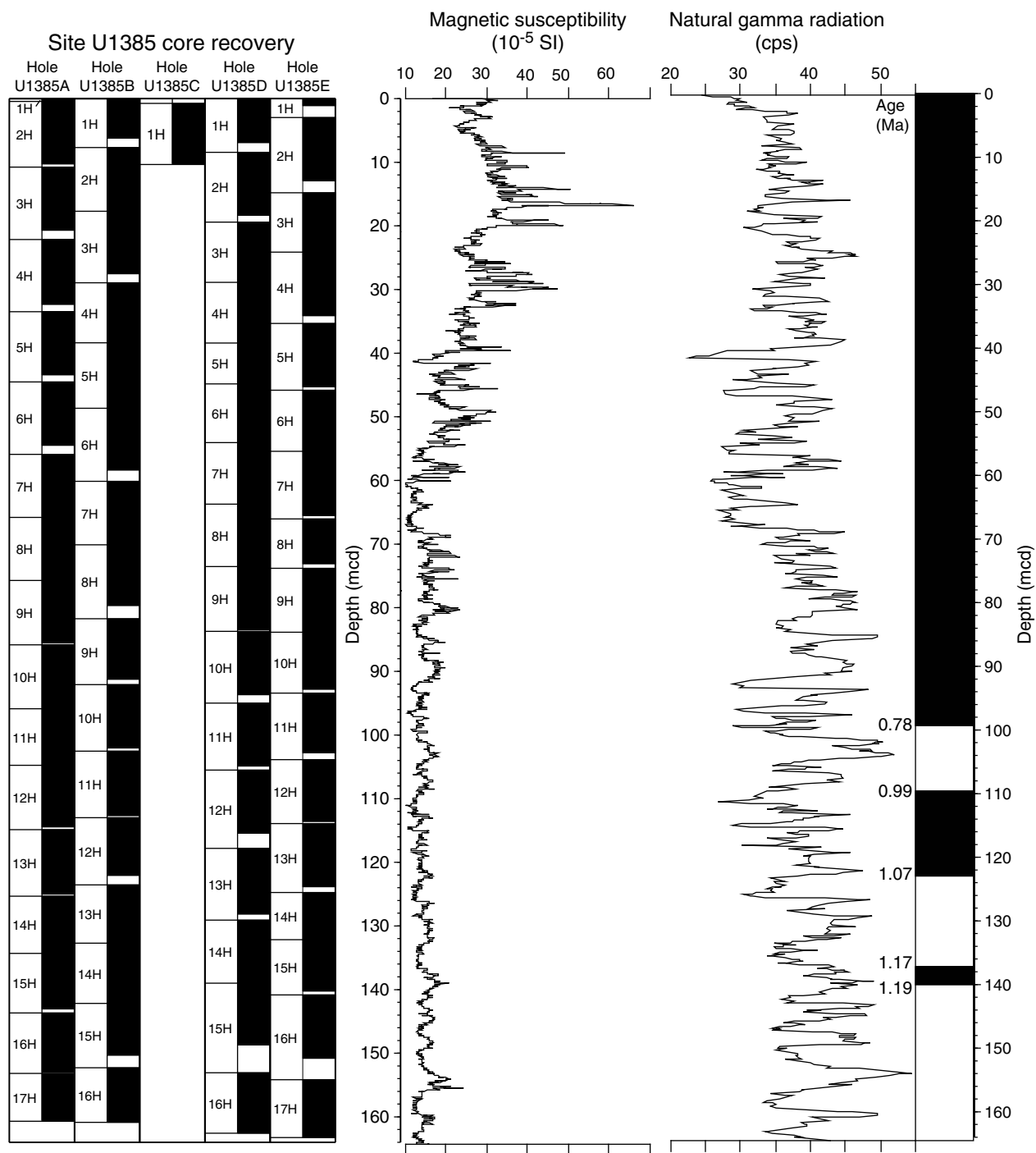
**Figure F8.** Bathymetric map of the southwestern Iberian margin showing the position of Site U1385 and nearby piston Cores MD01-2444 and MD95-2042.

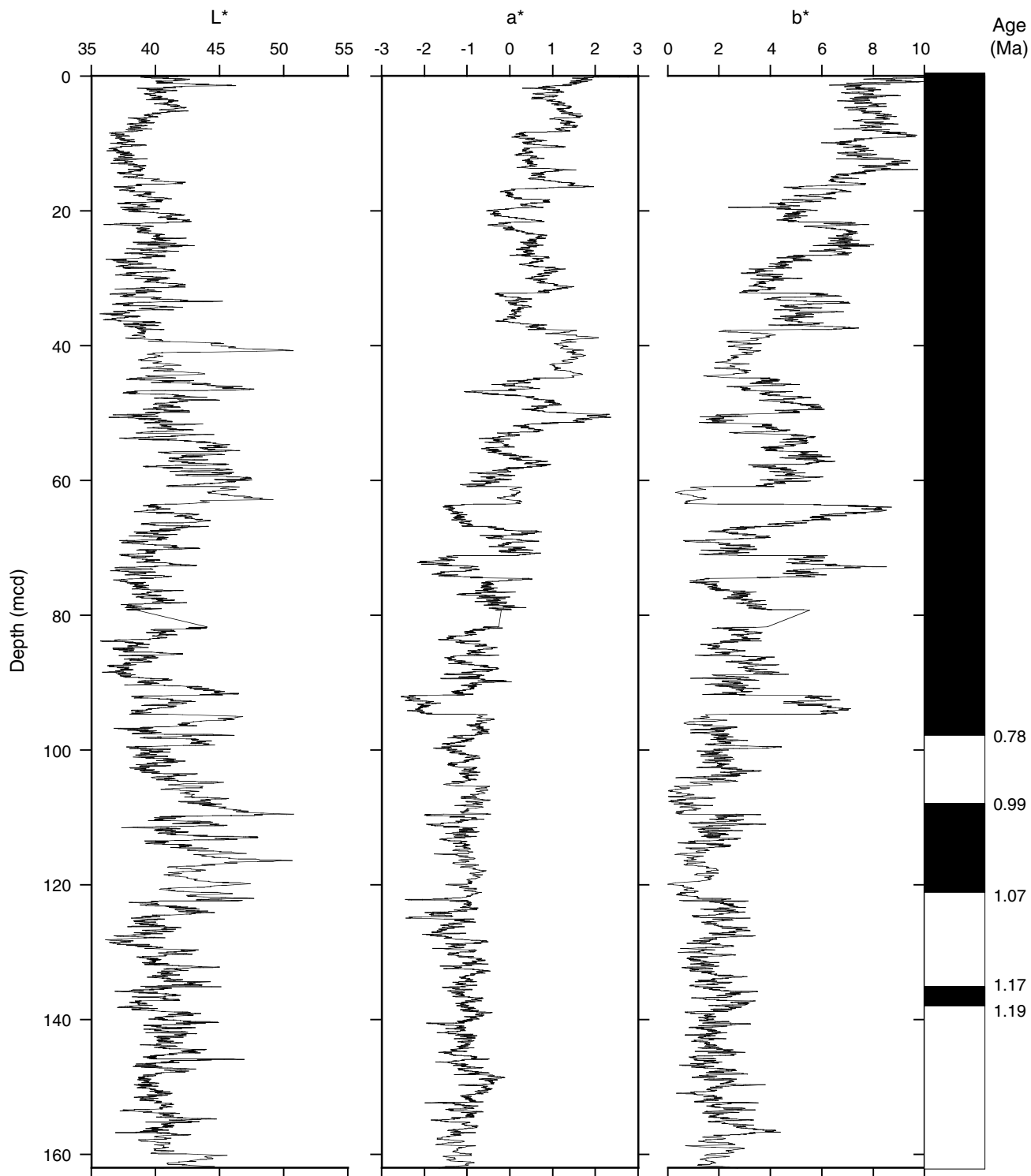


**Figure F9.** Oxygen isotope record of *Globigerina bulloides* from piston Core MD01-2444, located at approximately the same position as Site U1385. VPDB = Vienna PeeDee belemnite. MIS = marine isotope stage, GIS = Greenland interstadial stage.



**Figure F10.** Core recovery, magnetic susceptibility, natural gamma radiation, and polarity reversal boundaries for the spliced composite section, Site U1385.



**Figure F11.** Spliced color reflectance records and polarity reversal stratigraphy, Site U1385.



**Figure F12.** Sparker seismic reflection profile (Line FADO L-38) across the Faro Drift on the middle slope showing location of Site U1386. An important change in the overall architectural stacking of the mounded contourite deposits from a more aggrading depositional sequence to a clear progradational body is associated to the mid-Pleistocene revolution (MPR) discontinuity. BQD = base Quaternary discontinuity, LPR = intra-lower Pliocene discontinuity, M = late Miocene discontinuity.

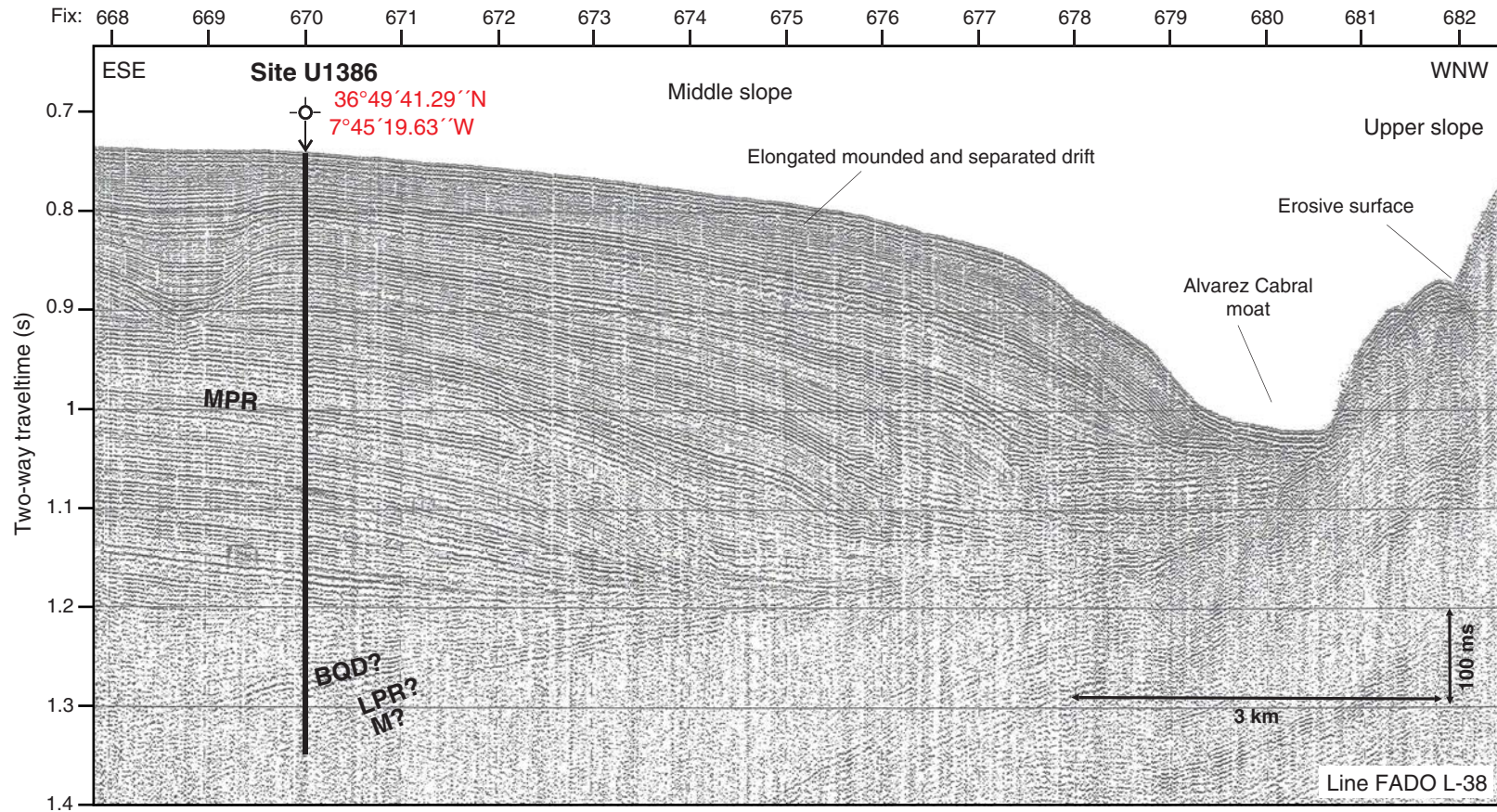


**Figure F13.** Lithologic summary, Site U1386. MOW = Mediterranean Outflow Water, MPR = mid-Pleistocene revolution discontinuity, BQD = base Quaternary discontinuity, LPR = intra-lower Pliocene discontinuity, M = late Miocene discontinuity

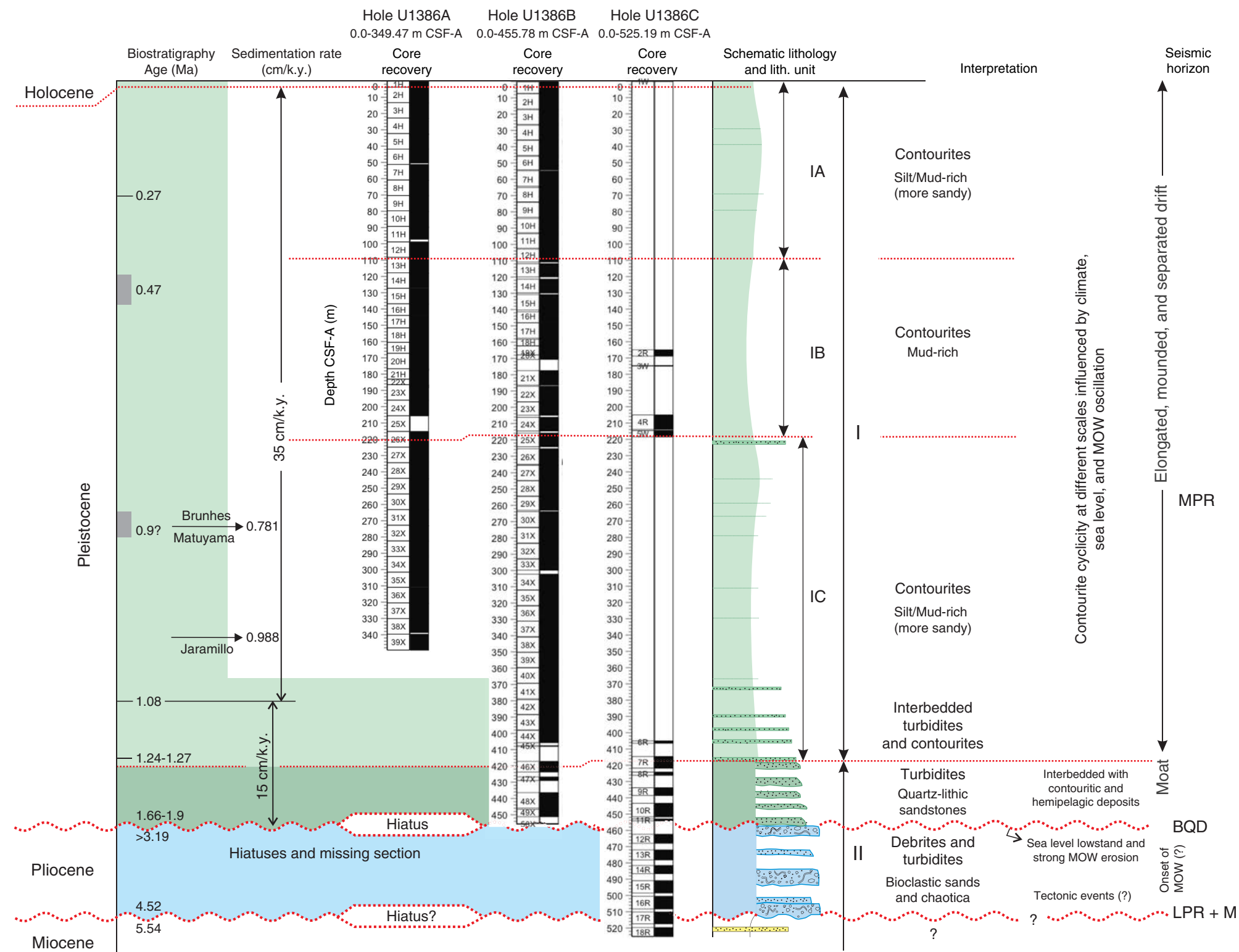


**Figure F14.** Lithologic summary, Site U1387. MOW = Mediterranean Outflow Water, MPR = mid-Pleistocene revolution discontinuity, BQD = base Quaternary discontinuity, LPR = intra-lower Pliocene discontinuity, M = late Miocene discontinuity.

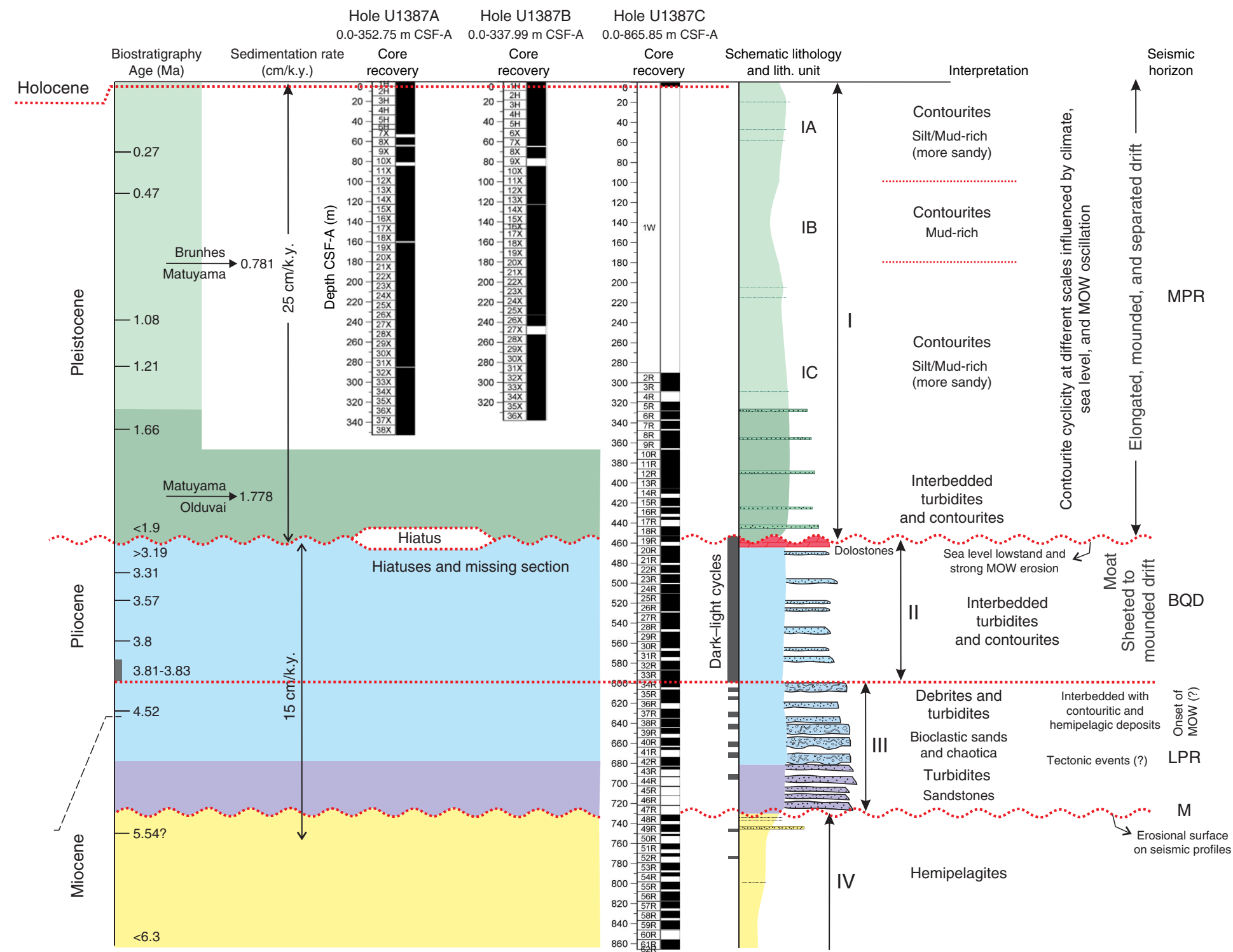




**Figure F15.** Multichannel seismic (MCS) reflection profile (Line S81A-16) of Site U1388 over the Cádiz Drift (MCS lines provided by REPSOL Oil Company). SP = shotpoint. MPR = mid-Pleistocene revolution discontinuity, BQD = base Quaternary discontinuity, LPR = intra-lower Pliocene discontinuity.

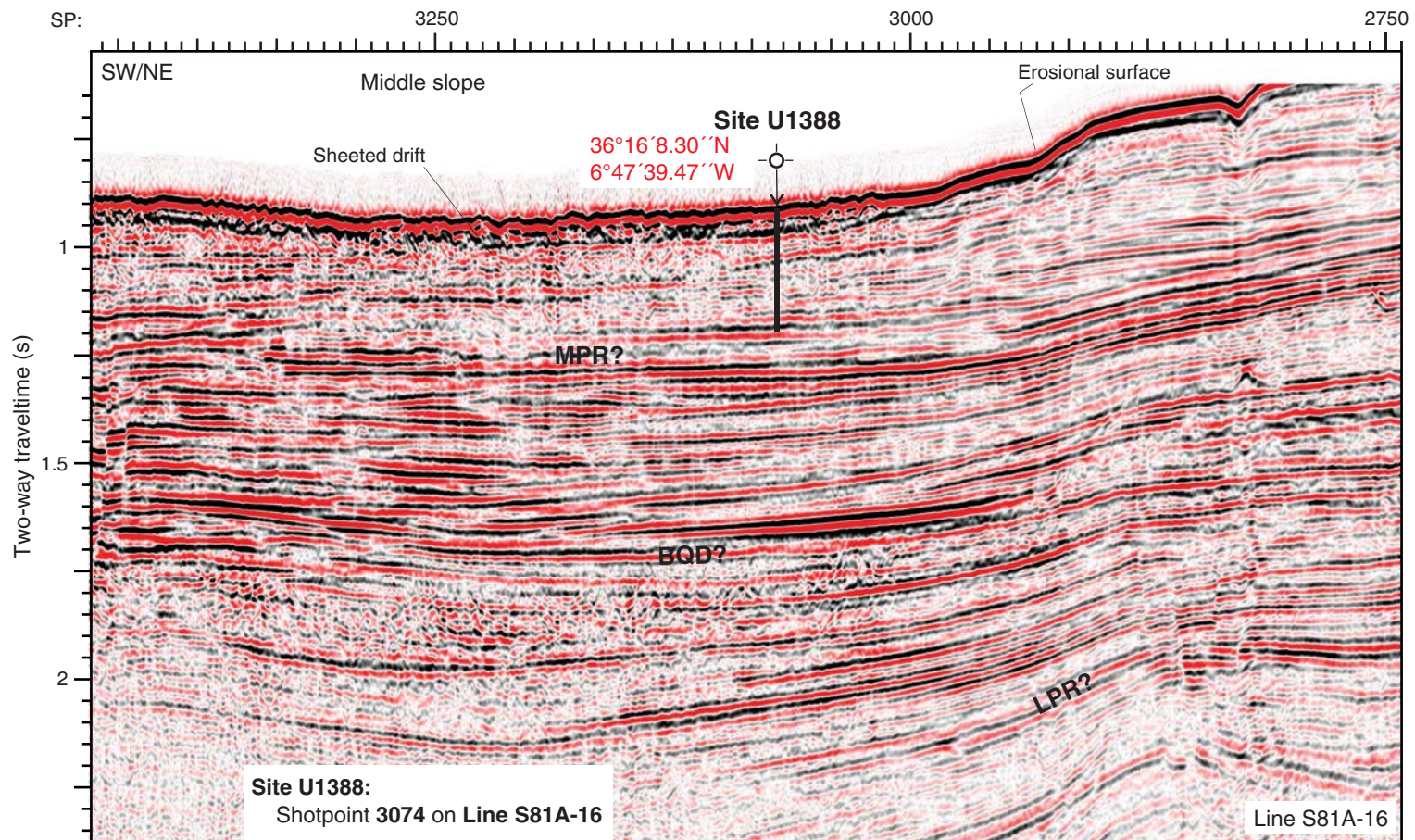


**Figure F16.** Lithologic summary, Site U1388. MPR = mid-Pleistocene revolution discontinuity.

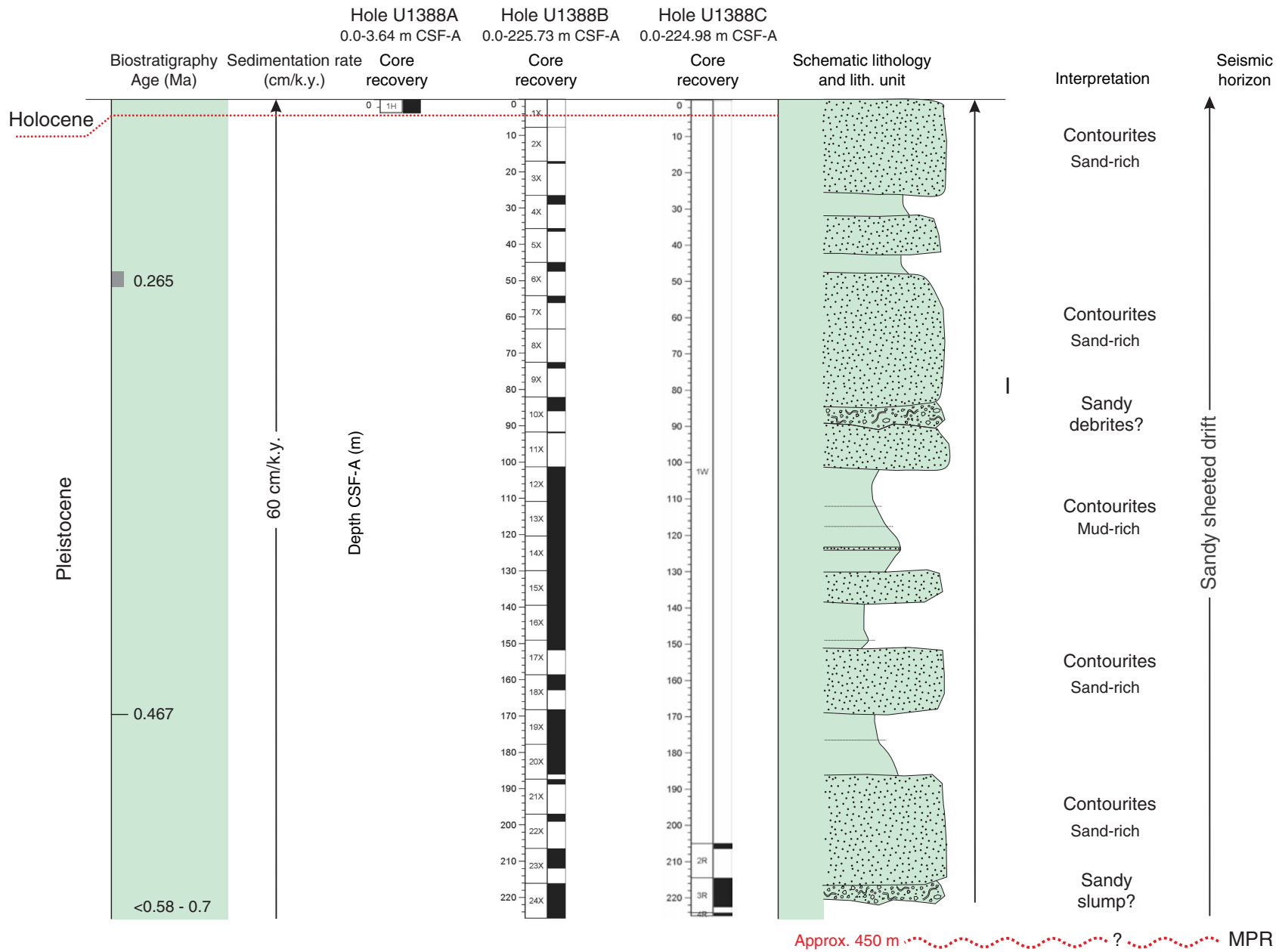




**Figure F17.** Multichannel seismic (MCS) reflection profile (Line HE91-20) of Site U1389 on the Huelva drift (MCS lines provided by REPSOL Oil Company). SP = shotpoint. MPR = mid-Pleistocene revolution discontinuity, BQD = base Quaternary discontinuity, LPR = intra-lower Pliocene discontinuity.

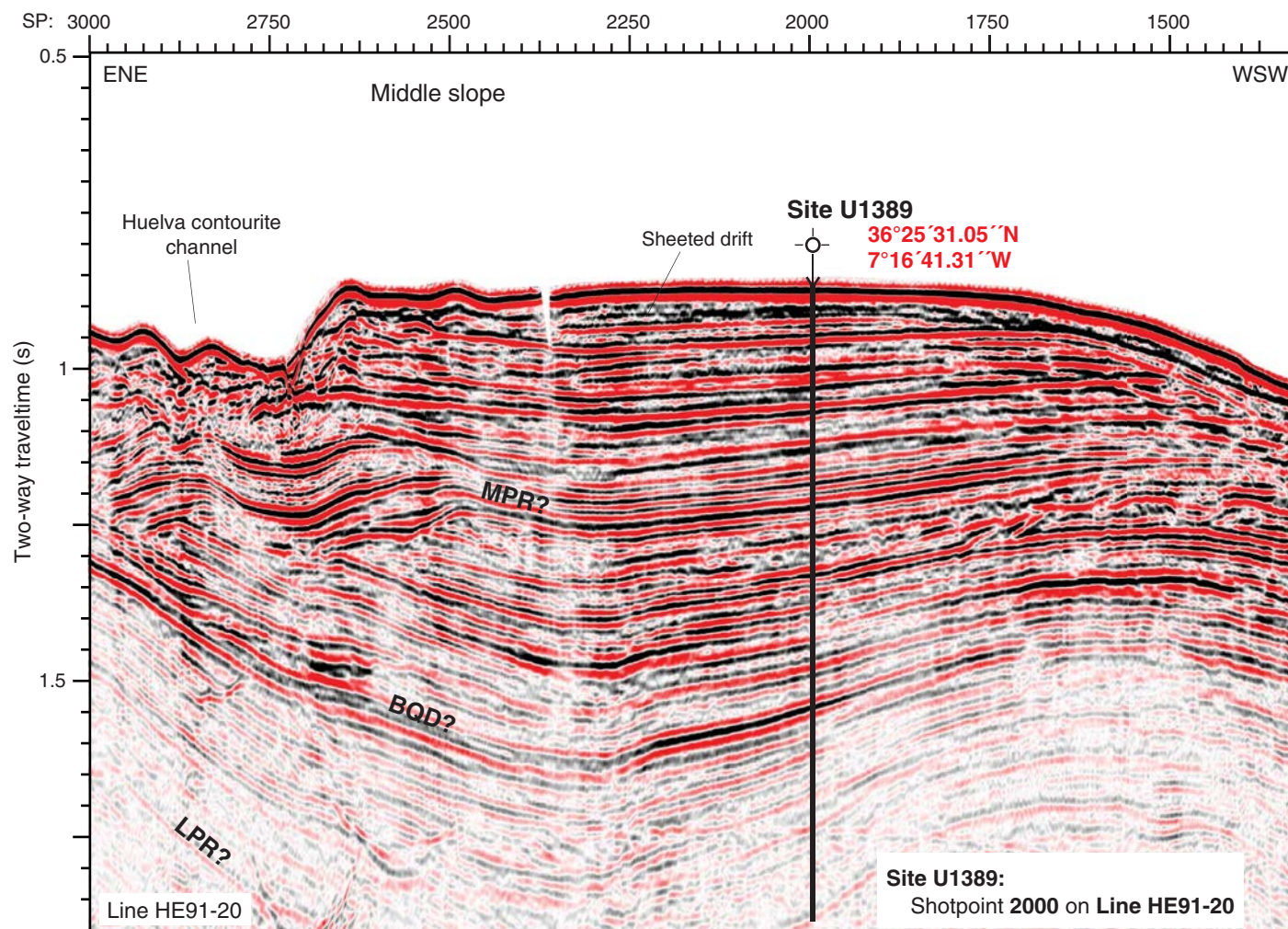
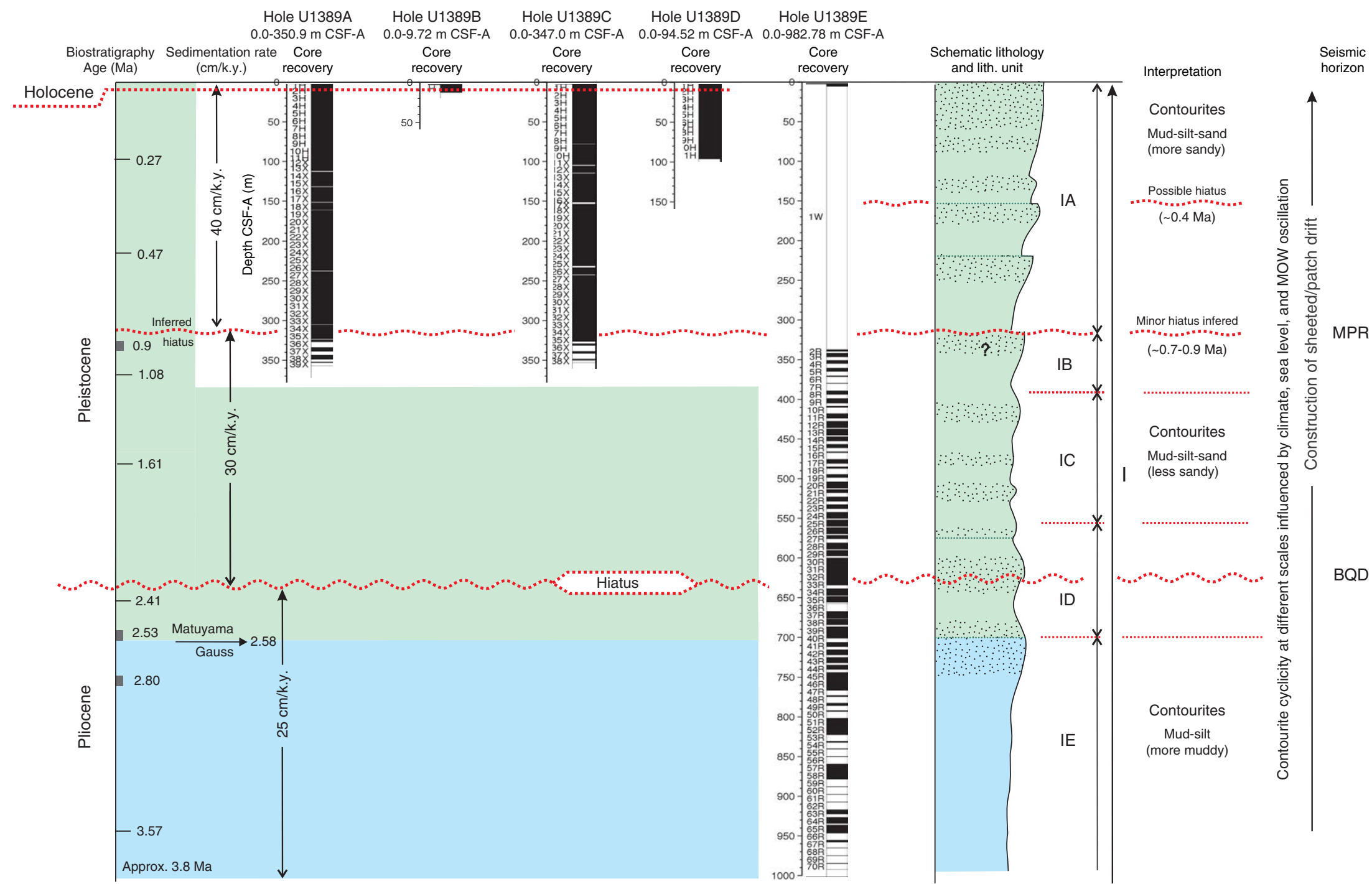
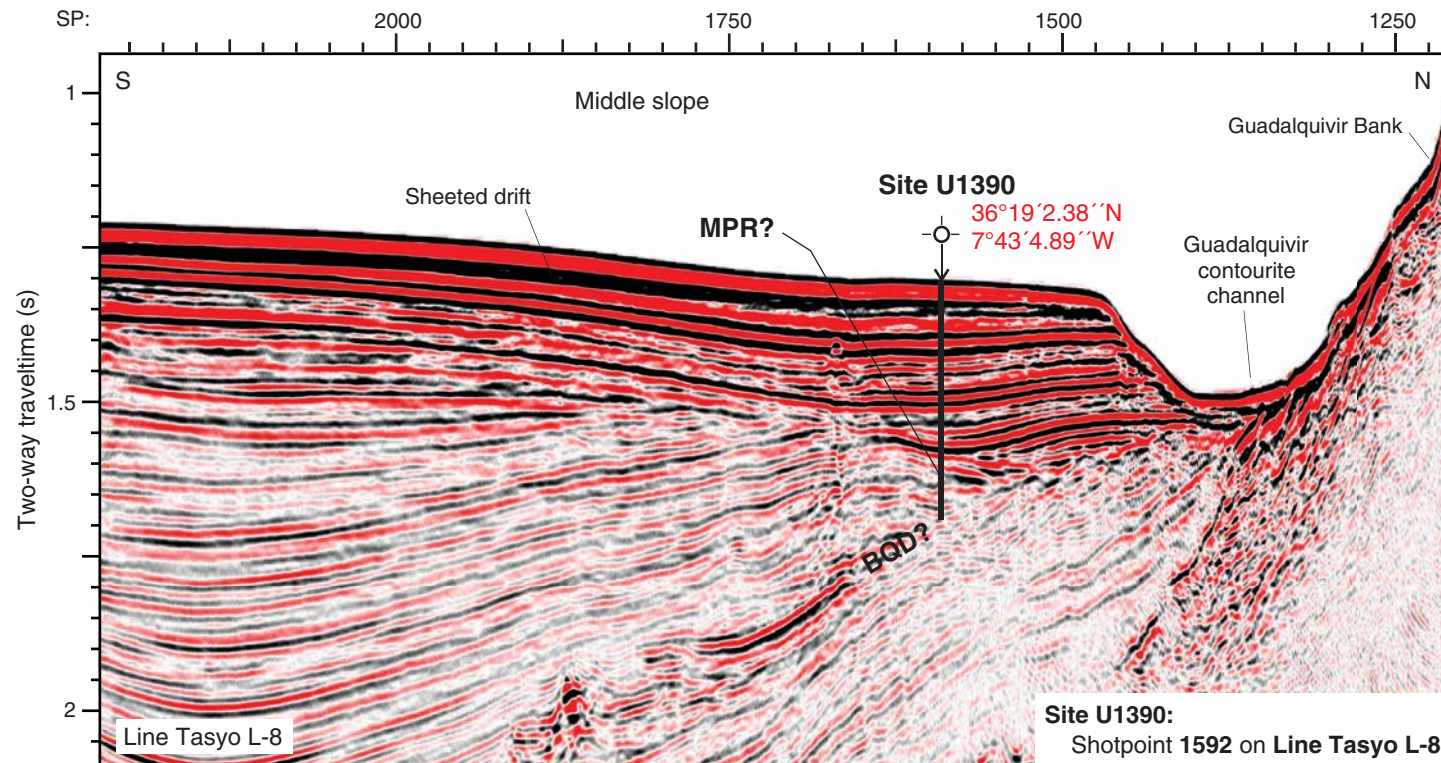


Figure F18. Lithologic summary, Site U1389. MOW = Mediterranean Outflow Water, MPR = mid-Pleistocene revolution discontinuity, BQD = base Quaternary discontinuity.



**Figure F19.** Multichannel seismic (MCS) reflection profile (Line Tasyo L-8) of Site U1390 on the Guadalquivir Drift. SP = shotpoint. MPR = mid-Pleistocene revolution discontinuity, BQD = base Quaternary discontinuity.





**Figure F20.** Lithologic summary, Site U1390. MOW = Mediterranean Outflow Water, MIS = marine isotope stage, MPR = mid-Pleistocene revolution discontinuity.

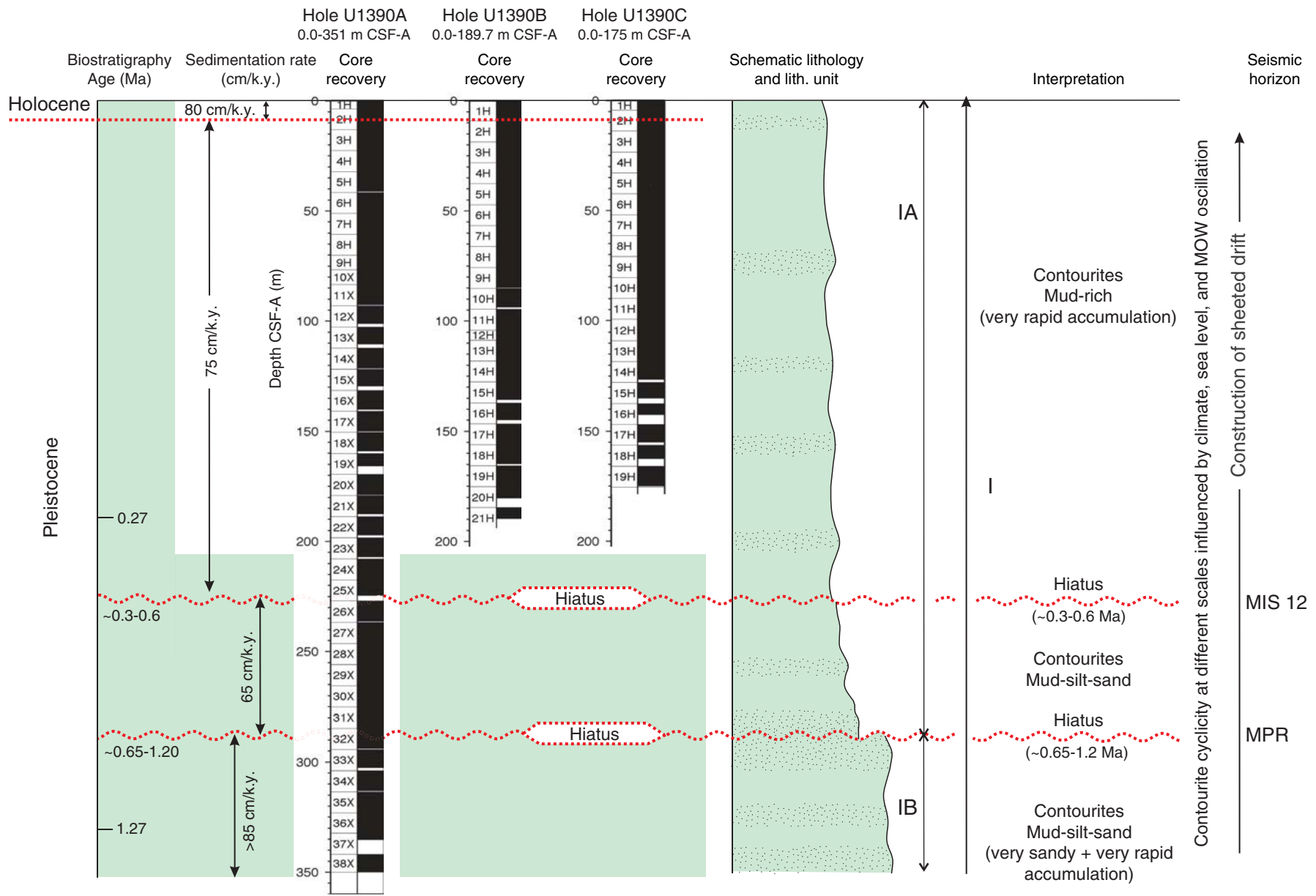


**Figure F21.** Multichannel seismic (MCS) reflection profile (Line PD00-522) of Site U1391 on the southwest Portuguese margin (MCS line TGS-NOPEC Geophysical Company ASA). SP = shotpoint. MPR = mid-Pleistocene revolution discontinuity, BQD = base Quaternary discontinuity, M = late Miocene discontinuity.

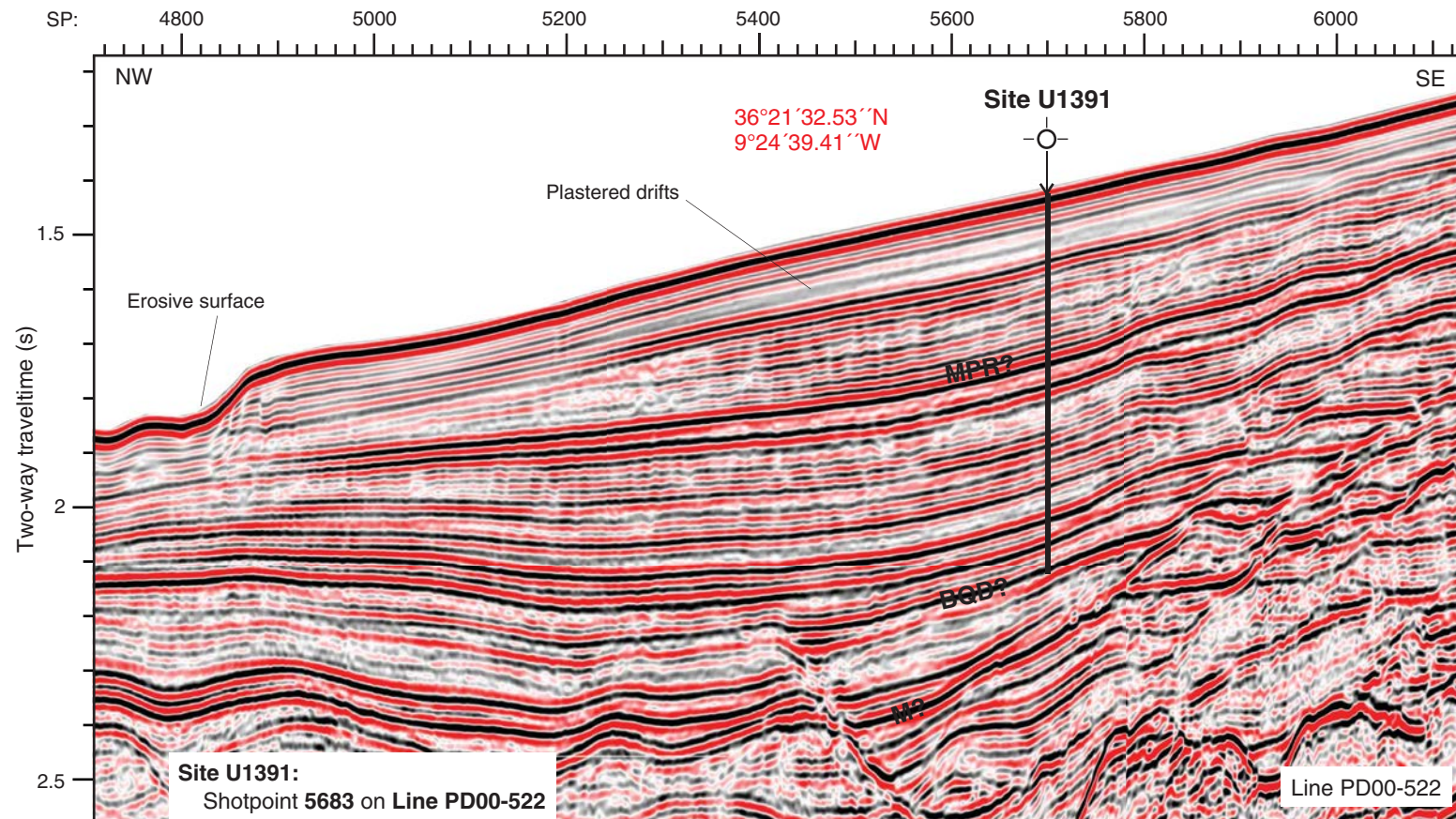


**Figure F22.** Lithologic summary, Site U1391. MOW = Mediterranean Outflow Water, MPR = mid-Pleistocene revolution discontinuity, BQD = base Quaternary discontinuity.

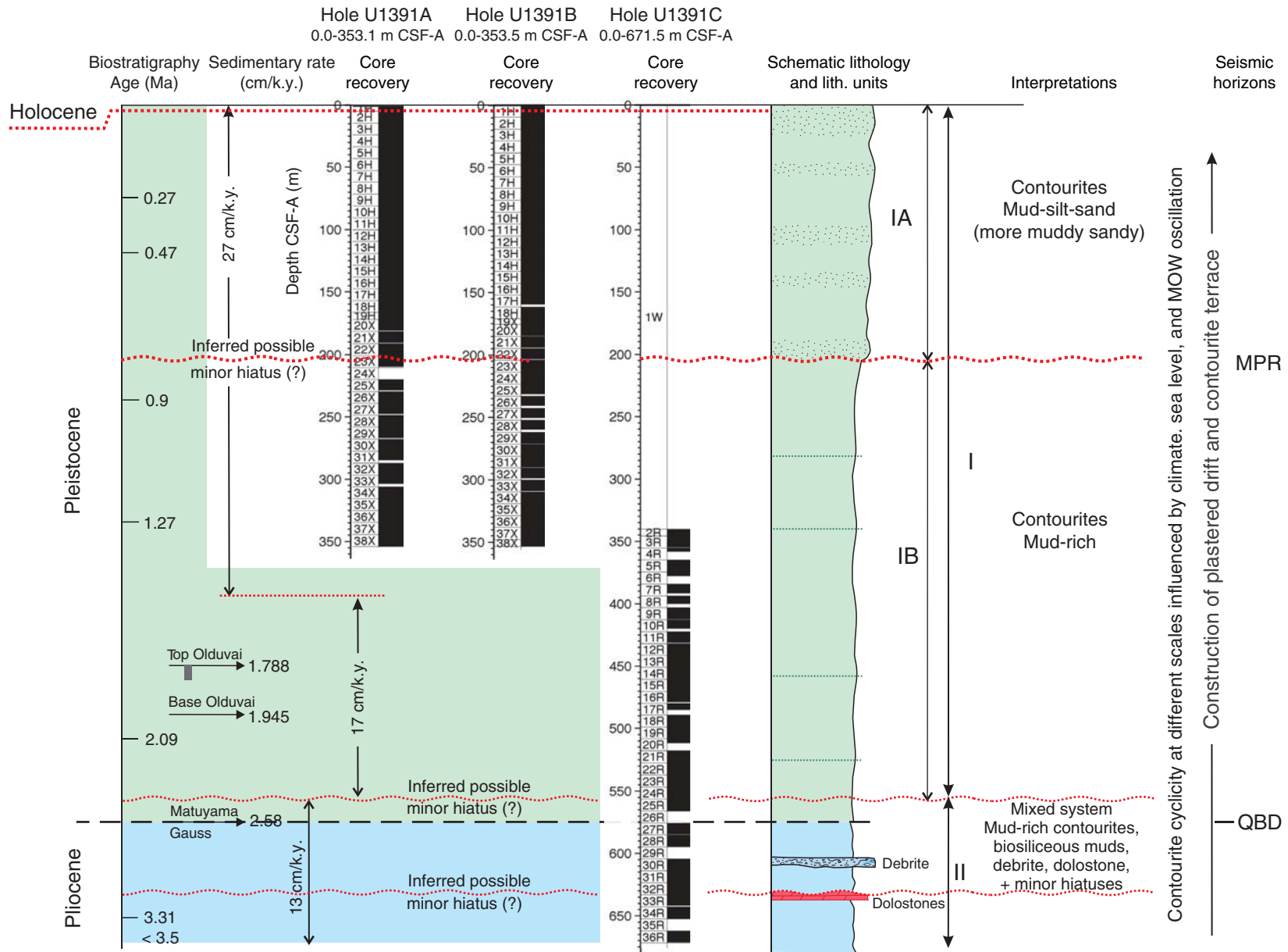




**Figure F23.** Lithologic summary for sites drilled during Expedition 339. Includes general preliminary interpretations from the proximal area close to the Strait of Gibraltar to the distal area west off Portugal.

